Forschungszentrum Jülich

Institut für Chemie und Dynamik der Geosphäre 3:
Atmosphärische Chemie

# *Mechanism for the Atmospheric Degradation of $NH_3$ in the Gas-Phase*

*Jörg-Peter Kohlmann* *Dirk Poppe*

Jül-3473

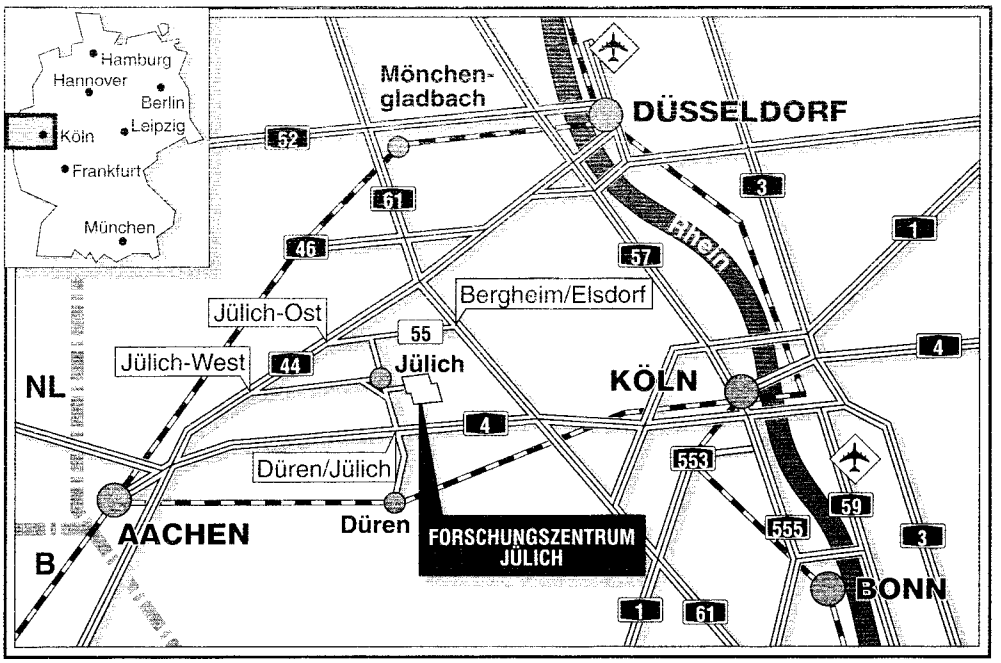


**Berichte des Forschungszentrums Jülich ; 3473**
ISSN 0944-2952
Institut für Chemie und Dynamik der Geosphäre 3:
Atmosphärische Chemie Jül-3473

Zu beziehen durch: Forschungszentrum Jülich GmbH · Zentralbibliothek
D-52425 Jülich · Bundesrepublik Deutschland
☎ 02461/61-6102 · Telefax: 02461/61-6103 · e-mail: zb-publikation@fz-juelich.de

# *Mechanism for the Atmospheric Degradation of $NH_3$ in the Gas-Phase*

*Jörg-Peter Kohlmann* *Dirk Poppe*

## Abstract

The most common alkaline trace gas in the earth's atmosphere is ammonia ($NH_3$). Most of the emitted $NH_3$ is removed from the atmosphere by heterogeneous reactions implying that the atmospheric budget of $NH_3$ is slightly affected by the gas-phase processes. However the global budgets of $NO_x$ and $N_2O$ are influenced by the gas-phase degradation of $NH_3$. It is likeley that up to 10 % of the antropogenic emision of these trace gases is due to the $NH_3$ degradation.

In this work, a simple box model is used for the model calculations. The gas-phase chemical mechanism of the Reginal Acid Deposition Model RADM2 is complemented by 27 reactions of $NH_3$ and the products of its initial reaction with OH. For the first time, the isomerization reaction of $NH_2O$ forming NHOH is used in a mechanism for the simulation of the gas-phase degradation of $NH_3$. It is shown that the value of the rate constant of this reaction influences substantial by the production of $N_2O$ from the $NH_3$ degradation.

Using the results of this work, a very simple estimation leads to a global source strength of $NO_x$ of (0.3 - 33) * $10^{12}$ g N $yr^{-1}$ from the degradation of $NH_3$. For $N_2O$ a value of (0.3 - 24) * $10^{11}$ g N $yr^{-1}$ is found. These results agree with data from the literature.

## Zusammenfassung

Das wichtigste alkalische Spurengas in der Erdatmosphäre ist Ammoniak ($NH_3$). Der größte Teil des emittierten $NH_3$ wird durch heterogene Prozesse aus der Atmosphäre entfernt, der Abbau in der Gasphase spielt für $NH_3$ nur eine untergeordnete Rolle. Allerdings wird die atmosphärische Bilanz der Stickoxide NO und $NO_2$ sowie von $N_2O$ durch den Abbau von $NH_3$ in Gasphasenreaktionen beeinflußt. Es wird geschätzt, daß jeweils bis zu 10 % der anthropogenen Quellen dieser Gase aus der Oxidation von $NH_3$ stammen.

Im Rahmen dieser Arbeit wird für die Simulationsrechnungen ein einfaches Boxmodell verwendet, in dem der Gasphasen Reaktionsmechanismus des Regional Acid Deposition Model (RADM2) um 27 Reaktionen des $NH_3$ und der Folgeprodukte seiner Reaktion mit OH erweitert wurde. Erstmals wird dabei die Isomerisierung von $NH_2O$ zu NHOH in einen Mechanismus zur Beschreibung des $NH_3$ Abbaus verwendet. Es kann gezeigt werden, daß diese Reaktion einen entscheidenden Einfluß auf die Bildung von $N_2O$ hat. Aus diesem Grund werden Sensitivitätsstudien durchgeführt, in denen die Größe der wichtigsten Geschwindigkeitskonstanten variiert wird. Weitere Sensitivitätsstudien wurden zur Reaktion von $NH_2$ mit $NO_2$ durchgeführt, in der $N_2O$ gebildet wird.

Aus einer sehr einfachen Abschätzung erhält man aus den Ergebnissen der Simulationsrechnungen eine globale $NO_x$-Quellstärke von (0.3 - 33) * $10^{12}$ g N $yr^{-1}$ aus der Oxidation von $NH_3$, für $N_2O$ ergibt sich ein Wert von (0.3 - 24) * $10^{11}$ g N $yr^{-1}$. Diese Ergebnisse stimmen mit Ergebnissen aus der Literatur überein.

# Contents

# 1 Introduction

Ammonia ($NH_3$) is most abundant alkaline trace gas in the earth´s atmosphere. Local measurements over Europe show $NH_3$ mixing ratios of 0.3 - 5 ppb [Han90, War88]. In Northern America 0.3 - 12 ppb [Lan92] $NH_3$ were found, in Africa about 4 ppb, in Asia 1 - 30 ppb and in Australia 2 ppb [Fer92], respectively. The average mixing ratio of $NH_3$ in the atmosphere has been estimated by model calculations to be in the range of 1 - 10 ppb [Log83] and 0.1 - 2 ppb [Den94], respectively. These calculations show substantial regional variations.

From a literature study Hardwiger-Fangmeier et al. [Har92] reported an annually mean concentration of $NH_3$ in Germany of about 2.5 $\mu g\ m^{-3}$ ( 3.6 ppb), for Europe they estimated rather low values of less than 0.2 $\mu g\ m^{-3}$ (< 0.3 ppb) in Norway and large burdens of more than 10 $\mu g\ m^{-3}$ (> 14 ppb) in the Netherlands. In their study $NH_3$ concentrations are also given near $NH_3$ sources, for example inside stables (67 ppm), in the immediate vicinity of stables (71 - 214 ppb), and near power plants equipped with removal of $NO_x$ by use of $NH_3$ (4.4 - 29 ppm).

The main sink of $NH_3$ in the atmosphere is the heterogenous reaction with sulfuric acid ($H_2SO_4$) aerosols yielding $NH_4HSO_4$ and $(NH_4)_2SO_4$. Another possible removal process is the reaction with nitric acid ($HNO_3$) forming $NH_4NO_3$ particle [Ste82] which is of minor importance in the atmosphere [Den94].

$NH_3$ is not only important for the neutralisation of acidic aerosols, but it also influences the chemistry inside the droplets since many rate constants for aqueous phase reactions depend on the pH-value.

The gas-phase degradation of $NH_3$ is initiated by the attack of OH radicals viz.

$$NH_3 + OH \rightarrow NH_2 + H_2O \qquad (R1)$$

This reaction is, however, only of minor importance for the atmospheric $NH_3$ budget, since most of the emitted $NH_3$ (about 96 % [Den94]) is removed by heterogeneous losses. Up to now there are only a few investigations about the role of $NH_3$ gas-phase chemistry in the atmosphere. Particularly the influence on the local atmospheric budget of $HO_x$, $NO_x$, and $N_2O$ is poorly known. Böttger et al. [Böt78] estimated that NO is the main relatively stable intermediate of the gas-phase degradation of $NH_3$. They determined a global NO source strength of

1.2 - 4.9 Tg N $yr^{-1}$ implying that 5 - 15 % of the nitrogen emitted as $NH_3$ is converted to NO and estimated a 25 % contribution of the gas-phase degradation to the global removal of $NH_3$. Recent investigations show that this fraction is much lower. Dentener and Crutzen [Den94] estimated that only about 4 % of the emitted $NH_3$ react with OH. Logan [Log83] assumed that the oxidation of $NH_3$ by OH is only a minor sink of $NH_3$, because of the small rate constant for the reaction of $NH_3$ with OH. Accordingly to Logan the oxidation of $NH_3$ is neither an important sink nor source of $NO_x$ in the atmosphere. She reported a maximal source strength of 1 - 10 Tg N $yr^{-1}$ $NO_x$ from the oxidation of $NH_3$. The work of Tyndall et al. [Tyn91] showed that the influence of $NH_3$ on the concentrations of $NO_x$ and radicals depends on the ratio of $NO_x$ and $O_3$. If $[O_3]$ exceeds 100 * $[NO_x]$, the oxidation of $NH_3$ is a source of $NO_x$ and of radicals, otherwise the oxidation is a sink for both types of compounds but a source of $N_2O$. Lee et al. [Lee97] estimated an $NO_x$ source strength of 0.9 Tg N $yr^{-1}$ from the oxidation of $NH_3$. Dentener and Crutzen [Den94] performed 3-D model studies about the cycle of $NH_3$ in the atmosphere using an emission model with a latidtudinal-longitudinal resolution of 10° x 10° that accounts for the sources and sinks of $NH_3$. They found that the main sink of $NH_3$ is the uptake by acidic aerosols, mostly of sulphuric acid. The oxidation of $NH_3$ in the gas-phase by attack of OH radicals was also included in the model used by Dentener and Crutzen with particularly emphasis on the global budget of $N_2O$.

The lifetime of $NH_3$ with respect to degradation in the gas-phase is of the order of 45 days (for $[OH] = 1.6 * 10^6$ $cm^{-3}$ and $k_1 = 1.6 * 10^{-13}$ $cm^3$ $s^{-1}$ [Atk92, DeM94]), which is large compared to the lifetime of several hours with respect to heterogenous loss of $NH_3$ [Den94]. Consequently the degradation in the gas-phase initiated by attack of OH radicals usually is only minor sink of $NH_3$. Nevertheless there might be an influence on the budget of $HO_x$, $NO_x$, $N_2O$ and $O_3$ at least in the vicinity of $NH_3$ sources.

It is the main objective of this paper to review the $NH_3$ gas-phase chemistry and to discuss the influence of recent kinetic data on the role of the $NH_3$ degradation within the tropospheric gas-phase chemistry. The regional acid deposition mechanism (RADM2) from Stockwell et al. [Sto90] supplemented by the gas-phase degradation of $NH_3$ was used. In contrast to previous work the chemistry of $NH_3$ and its degradation products was implemented in great detail by a relatively large mechanism with 26 reactions taking into account the most recent kinetic results from the literature.

In this work a mechanism for the atmospheric gas-phase-oxidation of $NH_3$ is presented and the rate constants as well as the branching ratios for reactions with several possible reaction pathways are discussed. First simulation runs and some implications of the gas-phase depletion of $NH_3$ on the budget of other trace gases will be given.

## 2 Gas-phase chemistry of $NH_3$

The oxidation of $NH_3$ in the gas-phase of the troposphere is initiated by abstraction of an H atom by an OH radical. This reaction and the subsequent chemical processes of the degradation products are summarized in table 1.
In the following a reaction is denoted by Ri, its rate by Fi and its rate constant by $k_i$. The numbers are also entered in tables 1, 10, and 11. The net gain of compound X is defined as the difference of the chemical production and destruction:

$$G(X) = P(X) - D(X) \qquad (1).$$

The relative yield Y(X) describes the net gain G(X) relative to the destruction rate of $NH_3$ by R1:

$$Y(X) = \frac{P(X) - D(X)}{D(NH_3)} = \frac{G(X)}{D(NH_3)} \qquad (2).$$

The relative yield of a single reaction i relative to the destruction rate of $NH_3$ by R1 is defined as $Y_i(X)$:

$$Y_i(X) = \frac{Fi}{D(NH_3)} \qquad (3).$$

The rate constant $k_1$ is well known. The temperature dependence follows an Arrhenius-law and was calculated by DeMore et al. [DeM94] using measured data from Zellner and Smith [Zel74], Diau et al. [Dia90] covering temperatures between 228 and 472 K, and 6 measurements at room temperature. The activation energy ($E_a/R$) is (710 ± 200) K [DeM94].

**Tab. 1:** Reactions of $NH_3$ and of the products of the H atom abstraction added to the RADM2 (T in units of K)

| No. | Reaction | k [$cm^3/s$],[$s^{-1}$] | k(283) | Ref. |
|---|---|---|---|---|
| 1 | $NH_3+OH \rightarrow NH_2+H_2O$ | $1.7*10^{-12}*\exp(-710/T)$ | $1.4*10^{-13}$ | a |
| 2 | $NH_2+O_3 \rightarrow NH_2O+O_2$ | $4.3*10^{-12}*\exp(-930/T)$ | $1.6*10^{-13}$ | a |
| 3 | $NH_2+HO_2 \rightarrow NH_2O+OH$ | $4.8*10^{-7}*T^{-1.32}*\exp(-628/T)$ | $3.0*10^{-11}$ | b |
| 4 | $NH_2+HO_2 \rightarrow H_2O+HNO$ | $9.4*10^{-9}*T^{-1.12}*\exp(-356/T)$ | $4.8*10^{-12}$ | b |
| 5 | $NH_2+HO_2 \rightarrow NH_3+O_2$ | $2.7*10^{-20}*T^{1.55}*\exp(-1020/T)$ | $4.6*10^{-18}$ | b |
| 6 | $NH_2+NO \rightarrow HO_2+OH+N_2$ | $1.92*10^{-12}*(T/298)^{-1.5}$ | $2.1*10^{-12}$ | c |
| 7 | $NH_2+NO \rightarrow H_2O+N_2$ | $1.41*10^{-11}*(T/298)^{-1.5}$ | $1.5*10^{-11}$ | c |
| 8 | $NH_2+NO_2 \rightarrow N_2O+H_2O$ | $1.2*10^{-11}*(T/298)^{-2.0}$ | $1.3*10^{-11}$ | d |
| 9 | $NH_2+NO_2 \rightarrow NH_2O+NO$ | $0.8*10^{-11}*(T/298)^{-2.0}$ | $8.9*10^{-12}$ | d |
| 10 | $NH_2+OH \rightarrow H_2O+NH$ | $7.7*10^{-13}*(T/298)^{1.5}*\exp(230/T)$ | $1.6*10^{-12}$ | e |
| 11 | $NH_2+OH \rightarrow NH_3+O_3$ | $3.3*10^{-13}*(T/298)^{0.4}*\exp(-250/T)$ | $1.3*10^{-13}$ | e |
| 12 | $NH_2O+O_3 \rightarrow NH_2+O_2$ | $1.2*10^{-14}$ | $1.2*10^{-14}$ | f |
| 13 | $NH_2O \rightarrow NHOH$ | $1.3*10^{3}$ | $1.3*10^{3}$ | f |
| 14 | $NH+O_2 \rightarrow NO+OH$ | $1.1*10^{-14*}(T/298)^{1.5}*\exp(-50/T)$ | $8.5*10^{-15}$ | g |
| 15 | $NH+NO \rightarrow OH+N_2$ | $4.9*10^{-11}$ | $4.9*10^{-11}$ | a |
| 16 | $HNO+OH \rightarrow NO+H_2O$ | $8*10^{-11}*\exp(-500/T)$ | $1.4*10^{-11}$ | h |
| 17 | $HNO+NHOH \rightarrow NH_2OH+NO$ | $1.66*10^{-12}*\exp(-1500/T)$ | $8.3*10^{-15}$ | i |
| 18 | $HNO+HNO \rightarrow N_2O+H_2O$ | $4.2*10^{-17*}(T/298)^{3.98}*\exp(-600/T)$ | $4.1*10^{-18}$ | i |
| 19 | $HNO+HNO \rightarrow H_2N_2O_2$ | $6.64*10^{-15}*\exp(-270/T)$ | $2.6*10^{-15}$ | i |
| 20 | $HNO+HNO \rightarrow H_2N_2O_2$ | $3.02*10^{-14*}(T/298)^{-2.4}*\exp(-590/T)$ | $4.3*10^{-15}$ | i |
| 21 | $H_2N_2O_2 \rightarrow N_2O+H_2O$ | $4.3*10^{11}*\exp(-8250/T)$ | $9.4*10^{-2}$ | i |
| 22 | $HNO+NO_2 \rightarrow HONO+NO$ | $1*10^{-12}*\exp(-1000/T)$ | $2.9*10^{-14}$ | h |

| | | | | |
|---|---|---|---|---|
| 23 | $NHOH+OH \rightarrow HNO+H_2O$ | $1.66*10^{-12}$ | $1.7*10^{-12}$ | i |
| 24 | $HONO+OH \rightarrow NO_2+H_2O$ | $1.8*10^{-11}*exp(-390/T)$ | $4.5*10^{-12}$ | c |
| 25 | $NH_2OH+OH \rightarrow NHOH+H_2O$ | $4.13*10^{-11}*exp(-2138/T)$ | $1.8*10^{-14}$ | j |
| 26 | $HNO+O_2 \rightarrow HO_2+NO$ | $3.65*10^{-14}*exp(-4600/T)$ | $3.2*10^{-21}$ | k |

a: [DeM94], b: [Sum96a], c: [Atk92], d:[Bul89, Meu96], e: [Coh91], f: [Bul80], g: [Mil92], h: [Tsa91], i: [Lin92], j: [Esp93], k: [Bry93]

The product of R1, the $NH_2$ radical, forms a very unstable adduct with oxygen

$$NH_2 + O_2 \rightarrow NH_2O_2.$$

This reaction is described by Jayanty et al. [Jay76] and Hack et al. [Hac82]. It can be neglected under atmospheric conditions, since $NH_2O_2$ is very unstable because of the small binding energy of the N-O bond in $NH_2O_2$, which has a value of < 4 kJ $mol^{-1}$ [Pag79]. While Michael et al. [Mic85] determined an upper limit of the rate constant for the reaction of $NH_2$ and $O_2$ of k(298) = 7.7 * $10^{-18}$ $cm^3$ $s^{-1}$, Tyndall et al. [Tyn91] estimated a much smaller upper limit of 6 * $10^{-21}$ $cm^3$ $s^{-1}$ from a numerical simulation of their experimental results. Patrick and Golden [Pat84] and DeMore et al. [DeM94] assumed that the yield of this reaction is negligibly small. In liquid $NH_3$ the formation of $NH_2O_2$ was observed by Giguere and Herman [Gig76]. Because of the higher density of the liquid phase compared to the gas phase, a similar reaction mechanism in the gas phase is very questionable. Consequently, the reaction of $NH_2$ with $O_2$ was neglected in this work.

In the presence of ozone $NH_2$ reats to form $NH_2O$ viz.

$$NH_2 + O_3 \rightarrow NH_2O + O_2 \qquad (R2)$$

The rate constant $k_2$ is very uncertain [DeM94] with relative differences among several authors up to a factor of about 5. The temperature dependence was taken from Pattrick and Golden [Pat84] and Hack et al. [Hac81] following the recommendation by DeMore et al.. The products of reaction R2 are better known. Bulatov et al. [Bul80] and Patrick and Golden [Pat84] showed that the formation of $NH_2O$ is the dominant product channel. The reaction is strongly exothermic with

$\Delta H = -147$ kJ $mol^{-1}$ [Pat84]. Two other product channels of the reaction of $NH_2$ and $O_3$ are also possible:

$$NH_2 + O_3 \rightarrow NHO_2 + OH \quad \text{(R2a)}$$
$$\rightarrow NH_2O_2 \quad \text{(R2b)}$$

Reaction R2a is unlikely to occur because of the large endothermicity of $\Delta H = 347$ kJ $mol^{-1}$ [Bul80]. Formation of $NH_2O_2$ can also be ruled out (see above). Thus, only the production of $NH_2O$ from the reaction of $NH_2$ with $O_3$ was incorporated in the mechanism.

$NH_2$ can also react with $HO_2$ in several ways:

$$NH_2 + HO_2 \rightarrow NH_2O + OH \quad \text{(R3)}$$
$$\rightarrow H_2O + HNO \quad \text{(R4)}$$
$$\rightarrow NH_3 + O_2 \quad \text{(R5)}$$

As shown by Baulch et al. [Bau92], the over all rate constant for the loss of $NH_2$ in the reaction with $HO_2$ is well known. In principle, there are many product channels possible for this reaction [Sum96a, Sum96b]. Although many of these channels are accessible from the thermodynamical point of view, most pathways have high activation energies. Thus only the three channels R3 - R5 above are potentially important under atmospheric conditions. Recent kinetic studies by Sumanthi et al. [Sum96a, Sum96b] indicate that $k_5$ is much smaller than $k_3$ and $k_4$ by at least six orders of magnitude and can therefore be neglected.

$NH_2$ reacts also with NO:

$$NH_2 + NO \rightarrow HO_2 + OH + N_2 \quad \text{(R6)}$$
$$\rightarrow H_2O + N_2 \quad \text{(R7)}$$

The measured values of $k_6$ and $k_7$ for the reactions are not well known (see [DeM94]). Two groups of experimental data can be distinguished according to the experimental technique, one using flash photolysis (eg. [Wol94]) and the other using a discharge flow system (eg. [Sil82]). The flash photolysis data are always higher

than the discharge flow data. A possible reason is the formation of a complex of $NH_2NO$, which may decompose or diffuse out of the probing volume giving rise to an apparently too large measured rate constant. The temperature dependence is derived from a weighted average of all literature data available [DeM94]. The rate constants of the different product channels were taken from Atkinson et al. [Atk92].
Reaction R6 is not an elementary reaction. It is assumed that it consists of three steps

$$NH_2 + NO \rightarrow HN_2 + OH$$
$$HN_2 \rightarrow H + N_2$$
$$H + O_2 \rightarrow HO_2$$

summarized by R6 with a relative yield of 10 - 11 % of the reaction of $NH_2$ and NO [Dia96, Par96, DeM94]. The primary produced $HN_2$ decomposes instantaneously into $N_2$ and an H atom. This assumption is only valid at temperatures around 1000 K and pressures around 1 bar [Par96]. The production of $HN_2$ is slightly endothermic, the decomposition of $HN_2$ yielding $N_2$ and H is weakly exothermic with a small activation energy [Wol94]. Measurements of Miller et al. [Mil90] and calculations of Walch [Wal93] confirm these findings. Calculations lead to $\Delta H°_{298}$ = -26.2 and -81.6 kJ $mol^{-1}$, respectively, for the decomposition of $HN_2$ [Gme93]. In recent publications it is generally accepted that the lifetime of $HN_2$ is small also at ambient temperatures as discussed by Wolf et al. [Wol97]. Implying that instantaneous decomposition of $HN_2$ is the most likely process in the atmosphere the simplification made in R6 in the model leads only to a minor error. In particular it is irrelevant, whether a decomposition of $HN_2$ is possible or a direct reaction of $O_2$ with $HN_2$ takes place. A decomposition has to have a rate constant of the order of $10^5$ $s^{-1}$ or larger to prevent cumulation of $HN_2$ and to make sure that the reaction of $NH_2$ with NO yields directly OH and $HO_2$. To allow for an equal production of OH and $HO_2$ a possible reaction of $HN_2$ with $O_2$ should have a rate constant of > $10^{-19}$ $cm^3$ $s^{-1}$. It is well known that rate constants for the abstraction of a H-atom can differ by orders of magnitude (for example $k(HCO + O_2) = 5.5 * 10^{-12}$ $cm^3$ $s^{-1}$ [Atk92], $k(CH_3O + O_2) = 1.9 * 10^{-15}$ $cm^3$ $s^{-1}$ [Atk92], $k(HNO + O_2) = 7.2 * 10^{-21}$ $cm^3$ $s^{-1}$ [Bry93]). On the time scale of hours the influence of both pathways on the product forming is the same.
$NH_2$ may also react with $NO_2$

$$NH_2 + NO_2 \rightarrow N_2O + H_2O \quad \text{(R8)}$$

$$\rightarrow NH_2O + NO \quad \text{(R9)}$$

The overall rate constant of R8 and R9 ($k_8 + k_9$) and the dependence of temperature is poorly known with an uncertainty factor of 2 - 3 [Tyn91, DeM94]. We adopt for ($k_8 + k_9$) an average over 4 values from the literature. The branching ratio between R8 and R9 was estimated using the data of Bulatov et al. [Bul89] and Meunier et al [Meu96]. The main pathway with a yield of > 95 % is the production of $N_2O$ and $H_2O$ (R8) [Hac79,Qua96]. The results from Meunier et al. [Meu96] and Park and Lin [Par96, Par97] show the great uncertainty of the product branching ratio. Park and Lin measureded a yield for $N_2O$ of about 19 %, which disagrees with the yield of 60 % as determined by Meunier et al. [Meu96] and Mebel et al. [Meb95]. The latter estimated that reaction R9 is the most probable channel. They also concluded that the production of $N_2$ and $H_2O_2$ is unimportant. In this work the product branching ratio from Meunier et al. [Meu96] was used. They determined a fraction of 40 % for the production of $NH_2O$ and NO.

Possible reactions for $NH_2O$ are the isomerization reaction

$$NH_2O \rightarrow NHOH \quad \text{(R12)}$$

and the reaction with $O_3$

$$NH_2O + O_3 \rightarrow NH_2 + 2\,O_2 \quad \text{(R13)}$$

which yields back to $NH_2$. Reaction R13 is strongly exothermic ($\Delta H$ = -128 kJ $mol^{-1}$ [Pat84]). The rate constant $k_{13}$ is nevertheless relatively small ($k_{13} < 5 * 10^{-14}$ $cm^3$ $s^{-1}$ [Pat84], $k_{13} = 1.2 * 10^{-14}$ $cm^3$ $s^{-1}$ [Bul80]). Another channel, the production of HNO and OH (R13a),

$$NH_2O + O_3 \rightarrow HNO + OH + O_2 \quad \text{(R13a)}$$

could not be observed in the experiments of Patrick and Golden [Pat84], although this reaction is strongly exothermic ($\Delta H$ = -182 kJ $mol^{-1}$). The reaction of $NH_2O$ with

hyponitric acid ($H_2N_2O_2$) forming $NH_2OH$, HNO, and NO (k(298) = 1.08 * $10^{-14}$ $cm^3$ $s^{-1}$) is described in the literature [Lin92]. Because of the expected small concentration of $H_2N_2O_2$ this reaction can be neglected. In a possible further reaction $NH_2O$ reacts with $O_2$ viz.

$$NH_2O + O_2 \rightarrow HNO + HO_2 \qquad \text{(R12a).}$$

It would compete with R12 and would occur under H atom abstraction yielding most likely HNO and $HO_2$. It is capable of changing the $HO_x$ budget, if the rate constant is large enough. A rate constant of $k_{12a}$ = $10^{-18}$ $cm^3$ $s^{-1}$ is required to yield equal rates for R12 and R12a. Since no measured data for $k_{12a}$ are available from the literature, this reaction is not incorporated in the mechanism presented here.
The only known reaction of the isomerization product NHOH is H atom abstraction by OH

$$NHOH + OH \rightarrow HNO + H_2O \qquad \text{(R23).}$$

A possible further reaction of NHOH is the H atom abstraction by $O_2$ viz.

$$NHOH + O_2 \rightarrow HNO + HO_2 \qquad \text{(R23a)}$$
$$\rightarrow NOH + HO_2 \qquad \text{(R23b)}$$

To compete with R23 the rates F23a or F23b have to have the same order of magnitude like F23. For a mean OH concentration of about $10^6$ $cm^{-3}$ in the troposphere, a NHOH concentration of about $10^{10}$ $cm^{-3}$ is needed to obtain a value of F23 in the order of $10^4$ $cm^{-3}$ $s^{-1}$. At this NHOH concentration a reaction with $O_2$ having a rate constant of about $10^{-21}$ $cm^3$ $s^{-1}$ would have a rate of more than F23. Since no evidence for this reaction can be found in the literature, this reactions R23a and R23b are not part of the RAD-NH3 mechanism.
The reaction of HNO with $O_2$ (R26) has theoretically two product channels:

$$HNO + O_2 \rightarrow HO_2 + NO \qquad \text{(R26)}$$
$$\rightarrow OH + NO_2 \qquad \text{(R26a)}$$

Experiments of Bryukov et al. [Bry93] with a very sensitive $NO_2$-detection system show no evidence for $NO_2$ formation ruling out R26a. Therefore, only reaction R26 is used for the model mechanism.
Only one further reaction of table 1 has to be discussed. Yamasaki et al. [Yam91] observed only the formation of OH and $N_2$ in the reaction of NH with NO:

$$NH + NO \rightarrow OH + N_2 \qquad (R15)$$

Other authors [Oka94, Qua95] concluded that $N_2O$ and $HO_2$ are the main product of this reaction. Under tropospheric conditions, the abundance of NH is so small that R15 can be safely neglected.

## 3 Model and simulation program

A simple box model accounting only for the gas-phase chemistry was used to study the temporal evolution of the concentrations. To that end the $NH_3$ chemistry compiled in table 1 was added to the gas phase chemistry RADM2 of the Regional Acid Deposition Model (Stockwell et al. [Sto90]). The RADM2 scheme is designed to model tropospheric gas-phase reactions under moderately polluted conditions. The new mechanism (hereafter called RAD-NH3) contains 183 reactions (26 reactions added) and 73 compounds (9 compounds added). The implementation of the RADM2 mechanism was performed by Poppe [Pop94].
No attempt was made to include heterogeneous losses of $NH_3$ though they are much more important than the gas phase reactions as mentioned in chapter 1. Thus the $NH_3$ concentrations should be considered as an external forcing to the chemistry. In the real atmosphere the $NH_3$ mixing ratio will be determined by emissions, transport and heterogeneous losses.
A computer program (Facsimile 3.0, AEA Technology) was used to perform the simulations. Input files and the subroutines called by the program are listed in appendices A and B.

# 4 Model calculations

The impact of $NH_3$ budget is studied in numerical simulations for different scenarios summarized in table 2. Case ST1 is a reference case with vanishing initial $NH_3$ mixing ratio. The case ST2, A, B, and C have the same initial conditions as ST1 however the initial mixing ratios of $NH_3$ are different (see table 2). According to the rather long of ammonia with respect to gas-phase degradation lifetime the $NH_3$ mixing ratio decreases by less than 35 % after an integration time t = 90 h (see table 2) for all scenarios. All simulations were performed at a temperature of 283 K and a pressure of 1000 mbar. The diurnal cycle of the photolysis was not considered. The photolysis frequencies were choosen for a solar zenith angle of 30° under clear sky conditions.

**Tab. 2:** Summary of the initial concentrations of the most important trace gases; scenario ST1, ST2, A, B, C: RAD-NH3 with different $NH_3$ mixing ratio; scenario D - F: RAD-NH3 with variation of k: D: $10^{-6} * k_{13}$; E: $1/3 * k_2$; F: $3 * k_2$

| scenario | ST1 | ST2 [2)] | A [2)] | B [2)] | C | D | E | F |
|---|---|---|---|---|---|---|---|---|
| $NH_3$ [ppb] | 0 | 1 | 40 | 100 | 400 | 100 | 100 | 100 |
| $\Delta[NH_3]$ (90 h) [1)] | - | 17 % | 22 % | 25 % | 15 % | 7 % | 18 % | 35 % |
| NO [ppb] [2)] | 1 | 1 | 1 | 1 | 1 | 1 | 1 | 1 |
| $NO_2$ [ppb] | 1 | 1 | 1 | 1 | 1 | 1 | 1 | 1 |
| $O_3$ [ppb] | 43 | 43 | 43 | 43 | 43 | 43 | 43 | 43 |
| CO [ppb] | 300 | 300 | 300 | 300 | 300 | 300 | 300 | 300 |
| $CH_4$ [ppm] | 1.71 | 1.71 | 1.71 | 1.71 | 1.71 | 1.71 | 1.71 | 1.71 |
| $N_2O$ [ppb] | 320 | 320 | 320 | 320 | 320 | 320 | 320 | 320 |
| $C_2H_6$ [ppb] | 5 | 5 | 5 | 5 | 5 | 5 | 5 | 5 |
| $CH_2O$ [ppb] | 0.1 | 0.1 | 0.1 | 0.1 | 0.1 | 0.1 | 0.1 | 0.1 |
| $CH_3CHO$ [ppb] | 0.1 | 0.1 | 0.1 | 0.1 | 0.1 | 0.1 | 0.1 | 0.1 |

[1)] Change of the $NH_3$ concentration after 90 h relatively to the initial condition
[2)] Primed scenarios (ST1', A', and B') refer to simulations with fixed $NO_2$ mixing ratios

The scenarios D, E, and F address the sensitivity of the results with respect to several rate constants (see chapter 5.2). The initial conditions for these sensitivity studies were taken from scenario B.

# 5 Results and discussion

## *5.1 Simulation*

Figure 1 visualizes the gas phase degradation of $NH_3$. Reaction rates (in units of $[cm^{-3}\ s^{-1}]$) and relative yields in case of branching reactions are also given. The rates are taken from scenario A at time t = 10 h. As expected, the radicals $NH_2$, $NH_2O$ and NH are in quasi-stationary state. Their lifetimes estimated from the inverse total destruction frequency are of the order of a few seconds. Also HNO and $H_2N_2O_2$ (the latter denoted by NAC in the mechanism) are in quasi-steady state, since their lifetimes are less than 1 min. This is an interesting observation, because both compounds are no radicals. On the other hand, the radical NHOH has a lifetime of more than 60 h under all scenarios of this work.

As can be seen from figure 1, the main products of the oxidation of $NH_3$ are NO and $HO_2$. The intermediates are $NH_2$, $NH_2O$, NHOH and HNO. The most important side reactions are the reactions of $NH_2$ with $NO_2$ (R8, R9) yielding $N_2O$ and $H_2O$ (60 %, R8) and $NH_2O$ and NO (40 %, R9), the reactions of $NH_2$ with $HO_2$ (R3, R4) forming $NH_2O$ and OH (86 %, R3) and HNO and $H_2O$ (14 %, R4), the reactions of $NH_2$ with NO (R6, R7) with $H_2O$ and $N_2$ (88 %, R7) as main products and OH, $HO_2$ and $N_2$ (12 %, R6) as byproducts and the reaction of HNO with NHOH (R17) yielding $NH_2OH$ and NO. $NH_2OH$ can react with OH to give NHOH back again.

Quasi-catalytic depletion of OH takes place in the reaction sequence R23, R17 and R25:

| | | | | |
|---|---|---|---|---|
| | $NHOH + OH$ | $\rightarrow$ | $HNO + H_2O$ | (R23) |
| | $HNO + NHOH$ | $\rightarrow$ | $NH_2OH + NO$ | (R17) |
| | $NH_2OH + OH$ | $\rightarrow$ | $NHOH + H_2O$ | (R25) |
| net | $NHOH + 2\ OH$ | $\rightarrow$ | $NO + 2\ H_2O$ | |

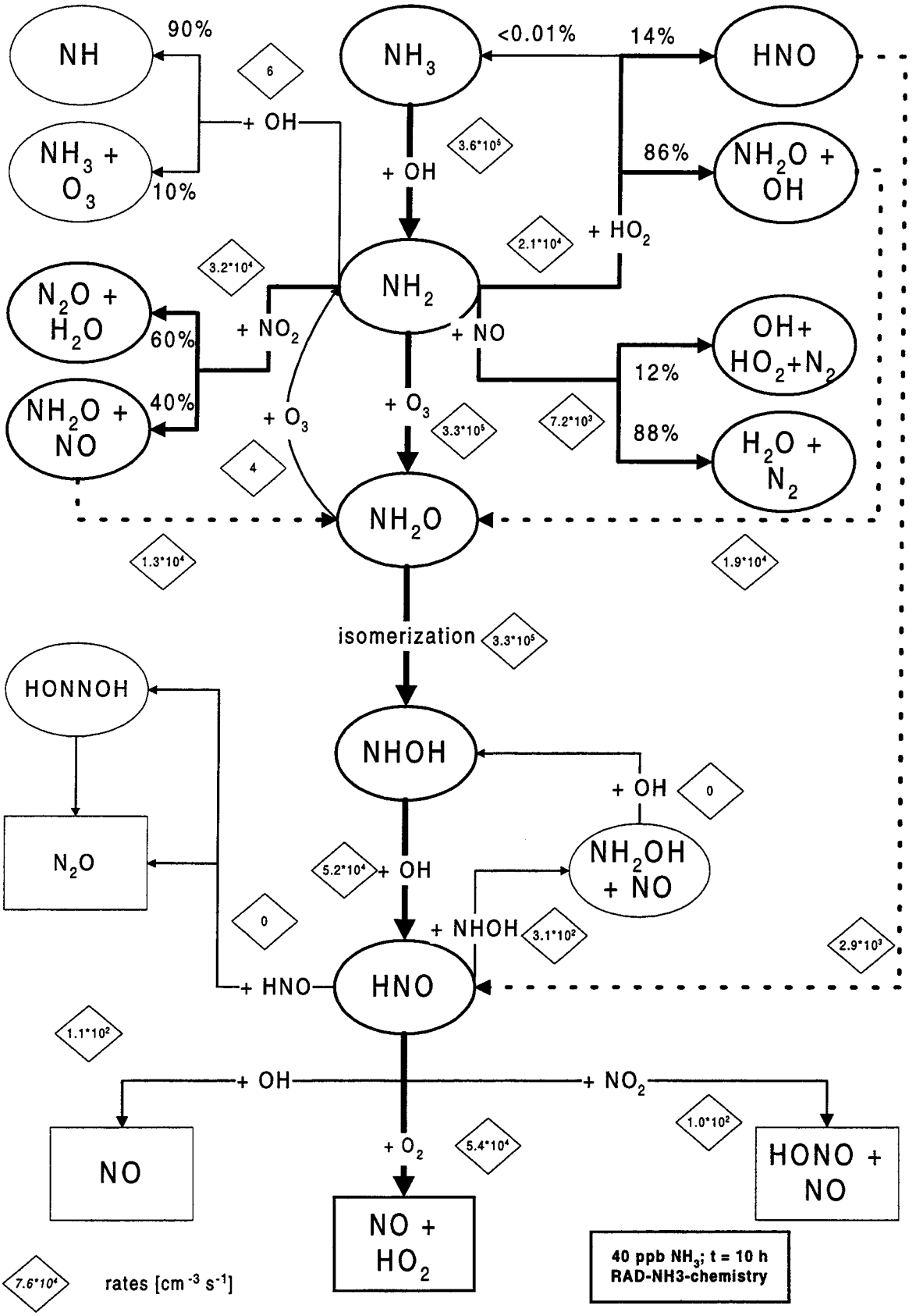


**Fig. 1:** Scheme of the degradation of $NH_3$ in the atmosphere; scenario A (40 ppb $NH_3$), t = 10 h, T = 283 K. The thickness of the arrows indicate schematically the importance of rates

However, the impact on the OH budget is very small. It was found that only 9 % of the $NH_3$ oxidized by OH in reaction R1 is processed in R17. The fraction of the rate of reaction R25 (F25) relativ to F1 is only 0.1 %. Relative to the primary production of OH from the reaction of $O(^1D)$ with $H_2O$ the maximum OH depletion via the catalytic cycle is also only 0.1 %. Thus the cycle is unimportant under atmospheric conditions. The $NH_3$ gas-phase degradation is also a source of $N_2O$ from two contributions. The self reaction of HNO (R18 - R20) is of minor importance since the HNO concentration is too small to yield appreciable reaction rates. As can be seen from figure 2, at t = 10 h and an initial $NH_3$ mixing ratio of 40 ppb no self reaction of HNO can be observed. The main contribution stems from the reaction of $NH_2$ with $NO_2$ (R8).

**Tab. 3:** Rates of the reactions in units of [$cm^{-3}$ $s^{-1}$] for different initial $NH_3$ mixing ratios; for reactions with different product channels the sum of all channels is given

| Scenario | ST2 | | A | | B | | C | |
|---|---|---|---|---|---|---|---|---|
| | 1 ppb | | 40 ppb | | 100 ppb | | 400 ppb | |
| Reaction | 10 h | 70 h | 10 h | 70 h | 10 h | 70 h | 10 h | 70 h |
| $NH_3$+OH | $9.6*10^3$ | $1.3*10^4$ | $3.6*10^5$ | $7.8*10^5$ | $8.2*10^5$ | $2.5*10^6$ | $2.2*10^6$ | $6.1*10^6$ |
| $NH_2$+$O_3$ | $8.0*10^3$ | $9.7*10^3$ | $3.0*10^5$ | $4.8*10^5$ | $6.8*10^5$ | $1.3*10^6$ | $1.9*10^6$ | $2.7*10^6$ |
| $NH_2O$[1)] | $8.8*10^3$ | $1.1*10^4$ | $3.3*10^5$ | $6.0*10^5$ | $7.5*10^5$ | $1.7*10^6$ | $2.0*10^6$ | $3.9*10^6$ |
| NHOH+OH | $1.5*10^3$ | $8.9*10^3$ | $5.2*10^4$ | $5.2*10^5$ | $1.1*10^5$ | $1.6*10^6$ | $2.0*10^5$ | $2.9*10^6$ |
| HNO+$O_2$ | $1.5*10^3$ | $9.0*10^3$ | $5.4*10^4$ | $5.1*10^5$ | $1.1*10^5$ | $1.5*10^6$ | $2.1*10^5$ | $2.4*10^6$ |
| $NH_2$+NO[2)] | $1.8*10^2$ | $4.5*10^2$ | $7.2*10^3$ | $5.0*10^4$ | $1.8*10^4$ | $2.0*10^5$ | $5.4*10^4$ | $7.2*10^5$ |
| $NH_2$+$NO_2$[3)] | $8.2*10^2$ | $1.7*10^3$ | $3.2*10^4$ | $2.0*10^5$ | $7.4*10^4$ | $8.8*10^5$ | $2.0*10^5$ | $2.5*10^6$ |
| $NH_2$+$HO_2$[4)] | $5.7*10^2$ | $1.1*10^3$ | $2.1*10^4$ | $4.8*10^4$ | $4.9*10^4$ | $1.0*10^5$ | $1.3*10^5$ | $1.7*10^5$ |
| HNO+NHOH | 0 | 6 | $3.1*10^2$ | $1.2*10^4$ | $1.5*10^3$ | $8.2*10^4$ | $7.6*10^3$ | $4.2*10^5$ |
| $NH_2OH$+OH | 0 | 0 | 0 | $1.3*10^2$ | 1 | $1.0*10^3$ | 4 | $3.3*10^3$ |
| HNO+OH | 3 | 29 | $1.1*10^2$ | $2.5*10^3$ | $2.1*10^2$ | $9.3*10^3$ | $2.7*10^2$ | $9.1*10^4$ |

[1)] Isomerization of $NH_2O$ yielding NHOH
[2)] Sum of F6 and F7
[3)] Sum of F8 and F9
[4)] Sum of F3, F4 and F5

In table 3 the rates of the important reactions for different initial $NH_3$ mixing ratios and after t = 10 h and t = 70 h are given. The rates F18 - F20 (selfreactions of HNO), F12 ($NH_2O + O_3$) and F10 - F11 ($NH_2 + OH$), which are not given in table 3, are always smaller than 230, 75 and 105 $cm^{-3}\ s^{-1}$, respectively.
The small values of F12 also imply that the catalytic destruction of $O_3$ through R2 and R12

| | | | | |
|---|---|---|---|---|
| | $NH_2 + O_3$ | $\rightarrow$ | $NH_2O + O_2$ | (R2) |
| | $NH_2O + O_3$ | $\rightarrow$ | $NH_2 + 2\ O_2$ | (R12) |
| net | $2\ O_3$ | $\rightarrow$ | $3\ O_2$ | |

is of no tropospheric significance. A possible impact on the stratospheric ozone can also be ruled out since $NH_3$ is completely destroyed in the troposphere.
The results presented in table 3 show that the reaction pattern presented in figure 1 applies by and large also to the scenarios ST2 and A - C. Some side reactions become more important if the initial $NH_3$ mixing ratio is increased. For example, the rates F6 and F7 relatively to F1 are only 4 % for scenario ST2, even for scenario C it is always less than 11 %. The reactions of $NH_2$ with $NO_2$ (R8, R9) become more important with increasing initial $NH_3$ mixing ratio. For scenario ST2 the amount of the ratio (F8 + F9)/F1 is 13 %, for scenario C it grows up to 41 %. This can also be observed for other reactions. The amount of the reaction of $NH_2$ with $O_3$ (R2) relatively to F1 is for scenario ST2 about 75 %, for scenario C only 44 %caused by the higher $NO_x$-concentration in scenario C (see below).
Table 4 shows the influence of the $NH_3$ degradation on the $HO_x$- and $NO_x$-concentrations for scenarios ST2, A, B, and C. In most cases, the degradation of $NH_3$ enhances the concentrations of OH, NO and $NO_2$. This effect is relatively small for low burdens of $NH_3$ (scenario ST2) where an increase of 2 % for OH, 5 % for NO, and 6 % for $NO_2$ is observed after t = 90 h. In scenario B the concentrations of OH, NO and $NO_2$ grow by a factor of 2, 4 and 7, respectively. Only the concentration of $HO_2$ decreases with increasing $NH_3$ concentration. While an enhancement of about 12 % after t = 90 h could be observed in scenario A relative to scenario ST2, at higher initial $NH_3$ burdens the $HO_2$ concentration decreases with a maximum in scenario A. At t < 50 h the increase of $HO_2$ can be observed up to 100 ppb initial

$NH_3$. Because most of $HO_x$ is $HO_2$, the degradation of $NH_3$ is a sink for $HO_x$ at high $NH_3$ concentration (t > 50 h) and a source of $NO_x$.

Obviously the shortlived OH and $HO_2$ as well as the peroxyradicals associated with the degradation of hydrocarbons are only weakly influenced directly by the $NH_3$ gas-phase chemistry. The more important impact is via the altered concentrations of $NO_x$ and to a smaller extend by the reactions R6 and R26 forming $HO_2$ or depleting $HO_2$ (R3 - R5).

The time dependence of $HO_x$ and $NO_x$ (figures 2 and 3) for scenario ST2 are very similar to those for scenario ST1. The OH concentration (figure 2a) increases with increasing $NH_3$ concentration at longer integration times up to an initial $NH_3$

**Tab. 4:** Influence of the oxidation of $NH_3$ on the $HO_x$ and $NO_x$ concentration

| t [h] | Scenario | $[NH_3]_0$ [ppb] | [OH] [$10^6$ $cm^{-3}$] | [$HO_2$] [$10^8$ $cm^{-3}$] | [NO] [$10^8$ $cm^{-3}$] | [$NO_2$] [$10^9 cm^{-3}$] | [$O_3$] [$10^{12} cm^{-3}$] |
|---|---|---|---|---|---|---|---|
| 10 | ST1 | 0 | 2.76 | 4.76 | 3.00 | 1.07 | 1.45 |
| | ST2 | 1 | 2.76 | 4.76 | 3.01 | 1.07 | 1.45 |
| | A | 40 | 2.59 | 4.67 | 3.16 | 1.09 | 1.42 |
| | B | 100 | 2.36 | 4.52 | 3.30 | 1.09 | 1.37 |
| | C | 400 | 1.60 | 3.88 | 3.31 | 0.94 | 1.22 |
| 50 | ST1 | 0 | 3.31 | 5.44 | 3.49 | 1.05 | 1.21 |
| | ST2 | 1 | 3.32 | 5.46 | 3.56 | 1.08 | 1.21 |
| | A | 40 | 3.79 | 5.82 | 6.87 | 2.03 | 1.26 |
| | B | 100 | 4.35 | 5.91 | 12.2 | 3.55 | 1.31 |
| | C | 400 | 2.99 | 4.52 | 18.2 | 4.30 | 1.13 |
| 90 | ST1 | 0 | 4.88 | 6.28 | 6.30 | 1.78 | 1.19 |
| | ST2 | 1 | 5.00 | 6.33 | 6.64 | 1.89 | 1.20 |
| | A | 40 | 8.71 | 7.10 | 17.6 | 6.52 | 1.81 |
| | B | 100 | 10.4 | 6.78 | 27.0 | 11.6 | 2.25 |
| | C | 400 | 5.94 | 3.79 | 46.2 | 14.9 | 1.82 |

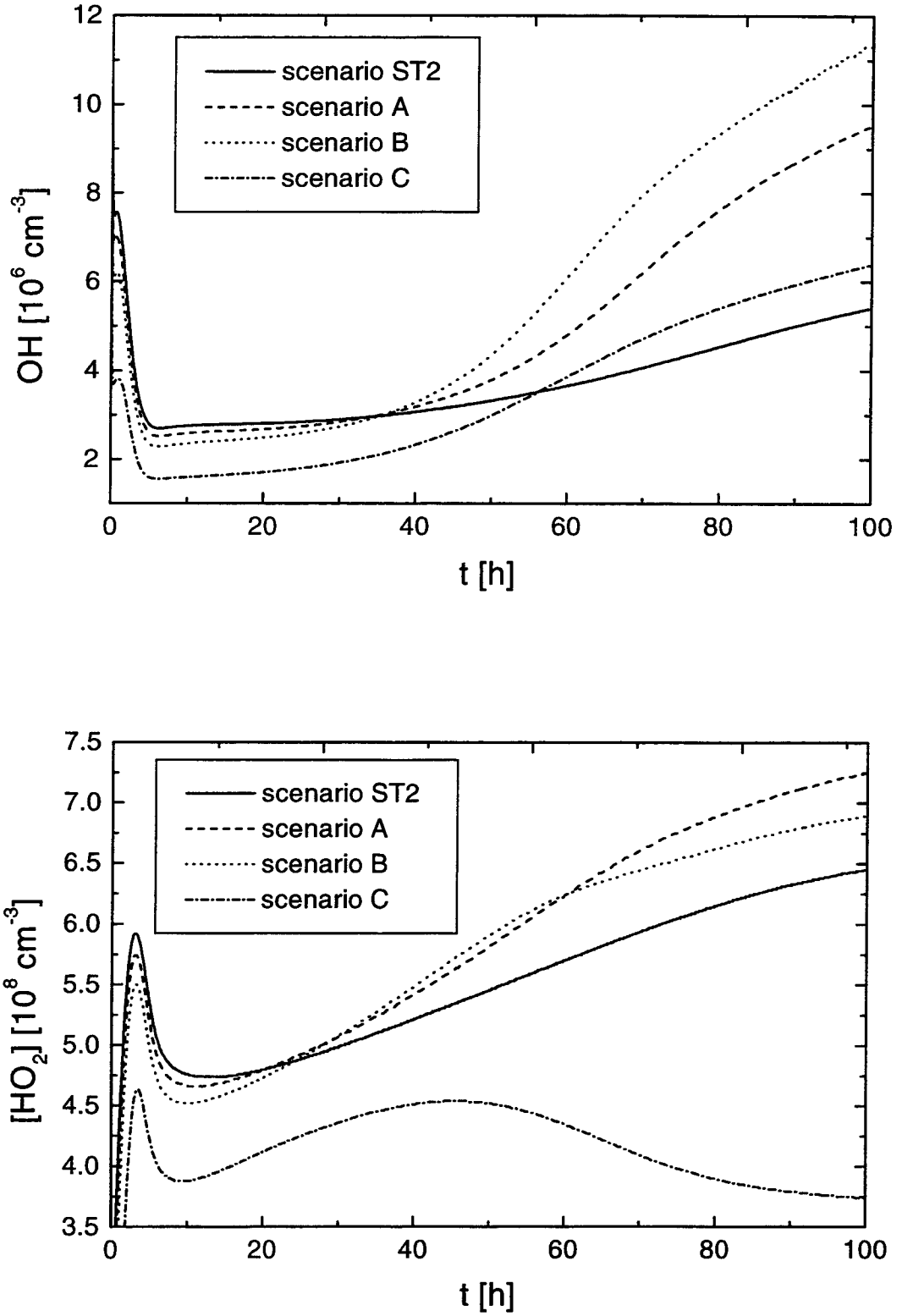


**Fig. 2:** Time dependence of the OH (top, figure 2a) und $HO_2$ (bottom, figure 2b) concentration for scenarios ST2, A, B, and C

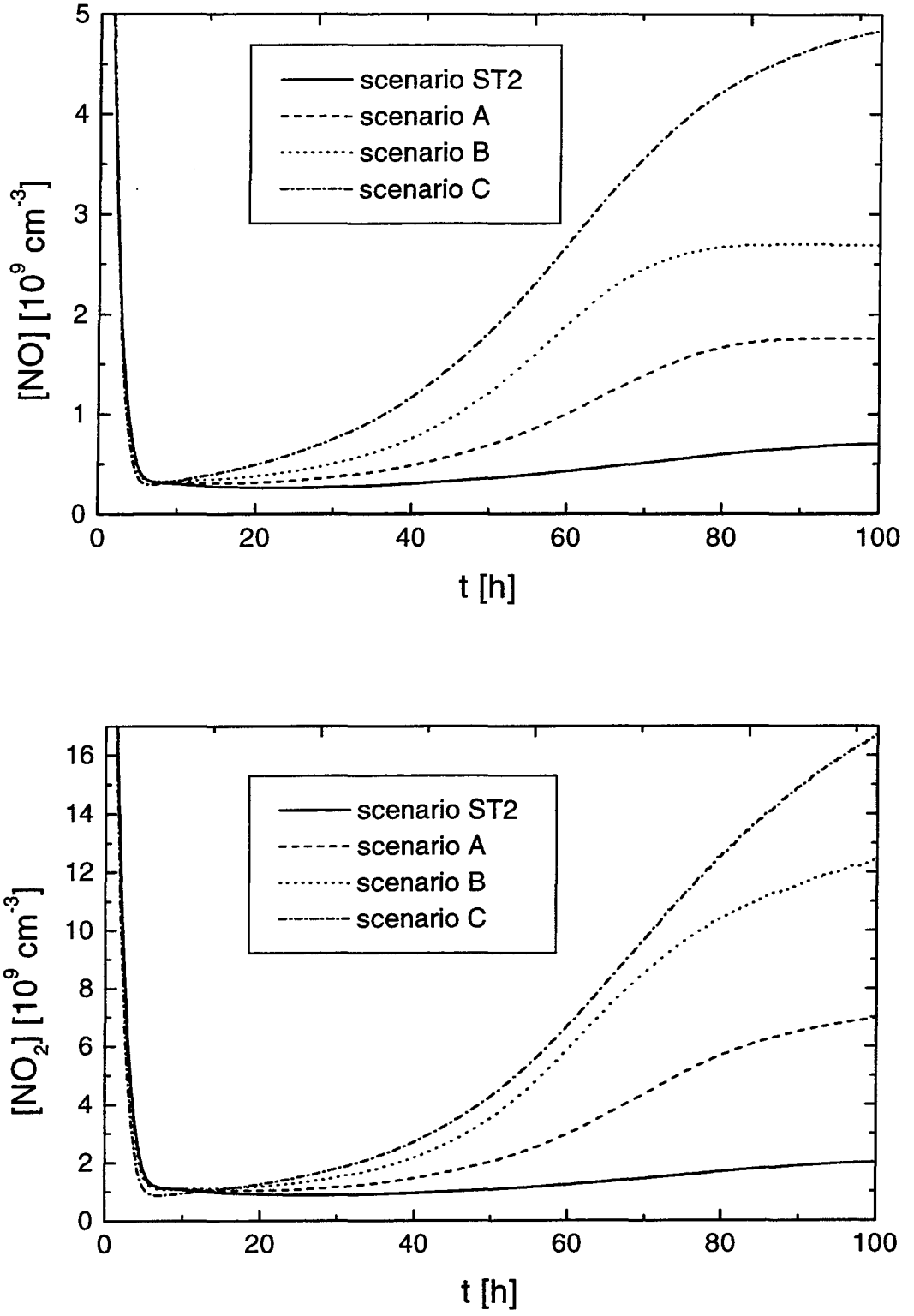


**Fig. 3:** Time dependence of the NO (top, figure 3a) und $NO_2$ (bottom, figure 3b) concentration for scenario ST2, A, B, and C

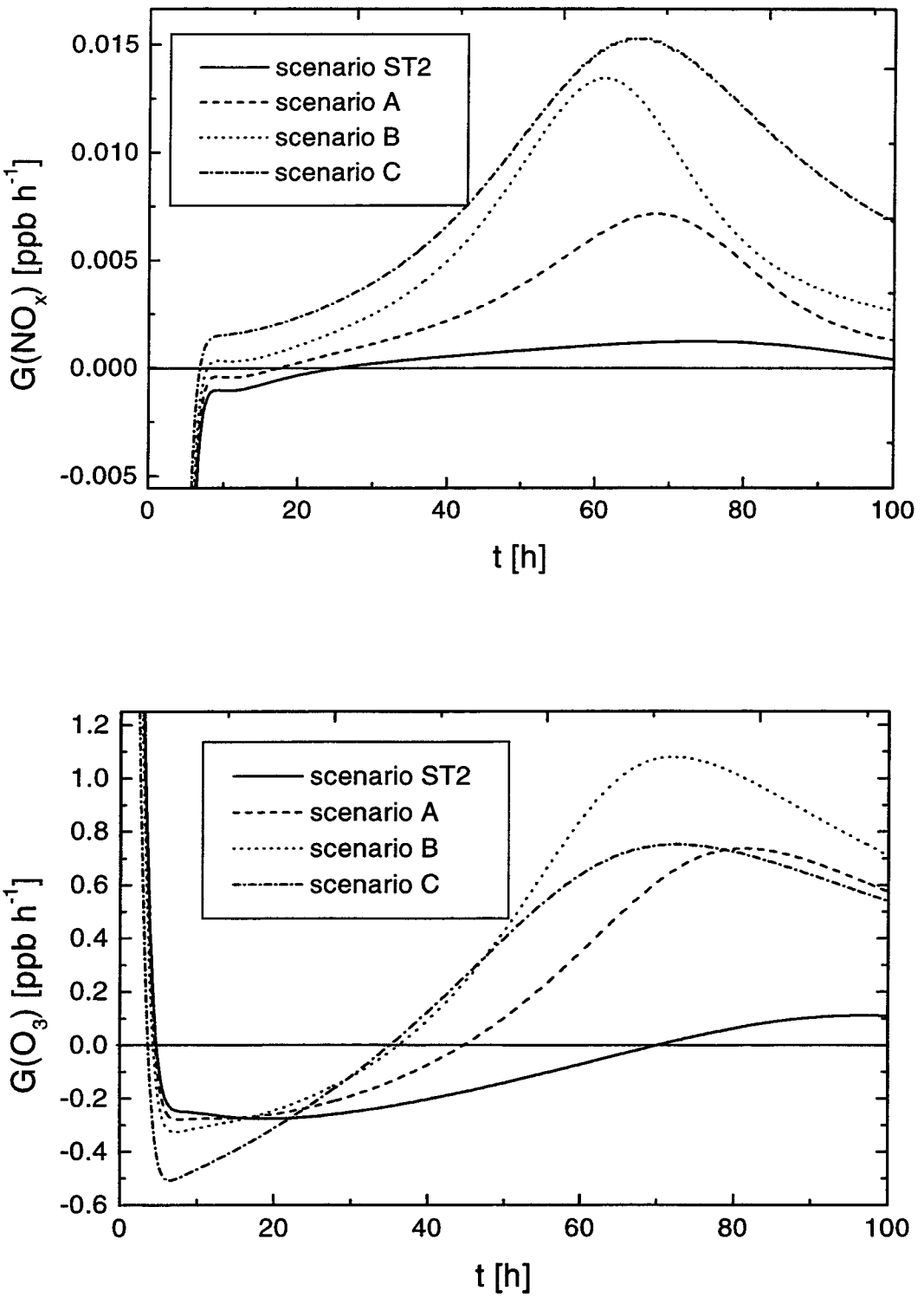


**Fig. 4:** Time dependence of the net production (equation (1)) of $NO_x$ (top, figure 4a) and $O_3$ (bottom, figure 4b) for scenario ST2, A, B, and C.

concentration of 100 ppb (scenario B). At higher initial $NH_3$ concentrations the OH concentration decreases. The $HO_2$ concentration in scenario C is lower than in all other scenarios. The response in the $HO_2$ concentration shows a similar behaviour (figure 2b). The maximum $HO_2$ concentration, however, is observed in scenario A. Furthermore the lower $HO_2$ concentration for the largest initial $NH_3$ concentration is a consequence of the increasing $NO_x$ concentration with increasing $NH_3$ concentration which leads to a higher NO concentration and hence to an increased conversion of $HO_2$ into OH. The mixing ratios of NO and $NO_2$ show a differenet time dependence, as can be seen from figures 3a and 3b. Obviously the $NO_x$ concentration increases with increasing $NH_3$ concentration. The maximum rate of NO production by the reaction of HNO with $O_2$ (R26) is 261 ppt/h for case B at t = 90 h, while the loss of $NO_x$ by the reactions $NH_2$ and NO (R6, R7) and $NH_2$ and $NO_2$ (R8) is 179 ppt/h resulting a maximal net $NO_x$ source of 82 ppt/h. The yield $Y_{26}(NO)$ as defined in equation (3) decreases with increasing $NH_3$ concentration. $Y_{26}(NO)$ is 79 % for scenario ST2 and 43 % for case C. To obtain the yield of $NO_x$ caused by the degradation of $NH_3$, the production of NO by reactions R14 - R17 and R26 as well as the loss of $NO_x$ by the reactions R6 - R8 have to be taken into account (defined by $Y^*(NO_x)$, equation (4), see below). The value of 68 % for $Y^*(NO_x)$ is slightly smaller than $Y_{26}(NO)$ for scenario ST1. For case C $Y^*(NO_x)$ is only 13 %. The time dependence of the net production of $NO_x$ $G(NO_x)$ is shown in figure 4a. A maximum of 15 ppt/h $NO_x$ production is observed at t = 70 h in scenario C. As can be seen from figure 4b, the time dependence of $G(O_3)$ differs greatly among scenarios ST2, A, B and C. The minimum at the beginning is a consequence of the fast transient initial decay of $NO_x$, which can be observed in all cases as mentioned in chapter 4. The maximum of $G(O_3)$ occurs in all scenarios after about 60 - 70 h. In scenario ST2 $G(O_3)$ is small and similar to $G(O_3)$ in scenario ST1. The maximum $G(O_3)$ increases with increasing $NH_3$ concentration. In scenarios B and C the largest $G(O_3)$ is about 1 ppb/h. The oxidation of $NH_3$ has a varying but not negligible influence on the $O_3$ concentration (table 4). While this influence is small in the case of scenario ST2, where a small increase of the $O_3$ concentration can be observed only at the end of the simulation, this influence increases with enhanced initial $NH_3$ concentration up to 100 ppb (scenario B). At higher concentration and longer integration times, the influence decreases again by a small amount (scenario C).

## *5.2 Sensitivity of product distribution with respect to selected rate constants*

Rate constants are varied in order to test the sensitivity of the product distribution to these parameters.

There are two reactions that appear to have a substantial influence on the product distribution of the $NH_3$ degradation, namely R13 and R2. The main reaction of $NH_2O$ is the isomerization reaction (R13). It is also this reaction by which the mechanism presented here differs conceptually from all other schemes in the literature. Another key reaction is R2, the rate constant of which has a large experimental uncertainty. Sensitivity studies were conducted to study the influence of both reactions.

### 5.2.1 Variation of the rate constant of the isomerization of $NH_2O$

Scenario D is identical to scenario B, however the isomerization R13 was suppressed by multiplying $k_{13}$ with $10^{-6}$ to account for possible non existence of this reaction.

The influence of this tremendous variation of $k_{13}$ on the rates of several reactions is surprisingly small related to the substantial variation, however there are some substantial differences compared to scenario B, as can be seen from table 5 and figure 5. F13 decreases by a factor of about 2 at t = 10 h, and by a factor of about 8 at t = 90 h. Scenario D shows reaction rates F3 - F5) that are larger by a factor of 2 than in scenario B. Simultaneously the rates of F6 - F9 are smaller than in case B. The reactions of $NH_2$ with $HO_2$ yield HNO (R3) and $NH_2O$ and OH (R4) which should lead to more pronounced influence of the variation of $k_{13}$ on the $HO_x$ than on the $NO_x$ concentration. As can be seen from figures 6 and 7 the relative influence on the $NO_x$ concentration is comparable to that on the $HO_x$ concentration. The concentrations increase only slightly, and at t = 100 h they are much lower than in scenario B. It should be mentioned that F1 for scenario D is smaller by a factor of about 6 than for scenario B as a consequence of the smaller OH concentration in scenario D.

The largest increase of rates relative to scenario B occurs for the reaction of $NH_2O$ with $O_3$ (R12), as it was expected, because the isomerization is the main sink of $NH_2O$ in scenario B. The increase of F12 ($NH_2O + O_3$) is due to the high $NH_2O$ concentration which can be observed in scenario D. Under these conditions

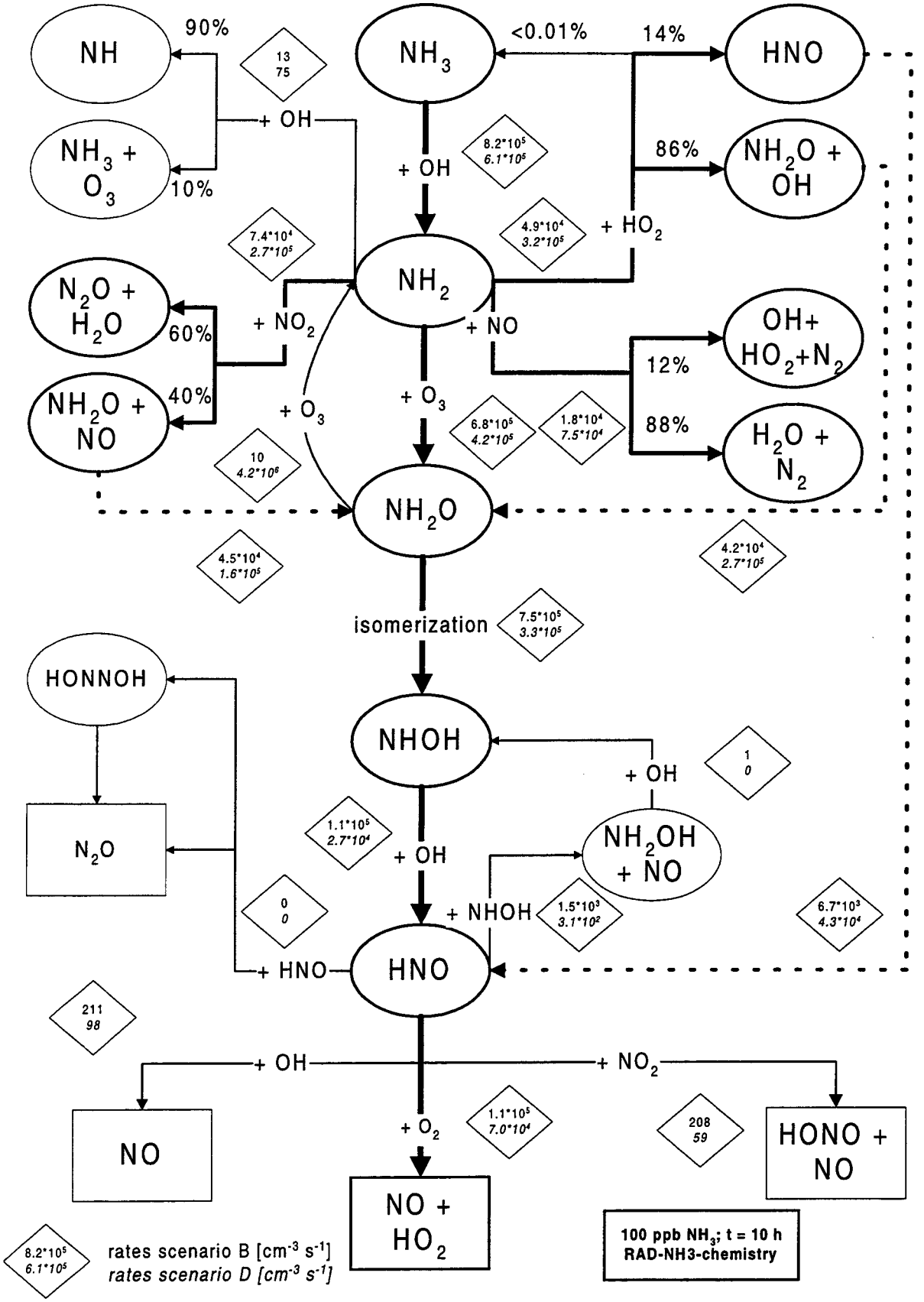


**Fig. 5:** Scheme of the degradation of $NH_3$ in the atmosphere; scenarios B and D (see tables 1 and 5), t = 10 h, T = 283 K. The thickness of the arrows indicate schematicaly the importance of rates

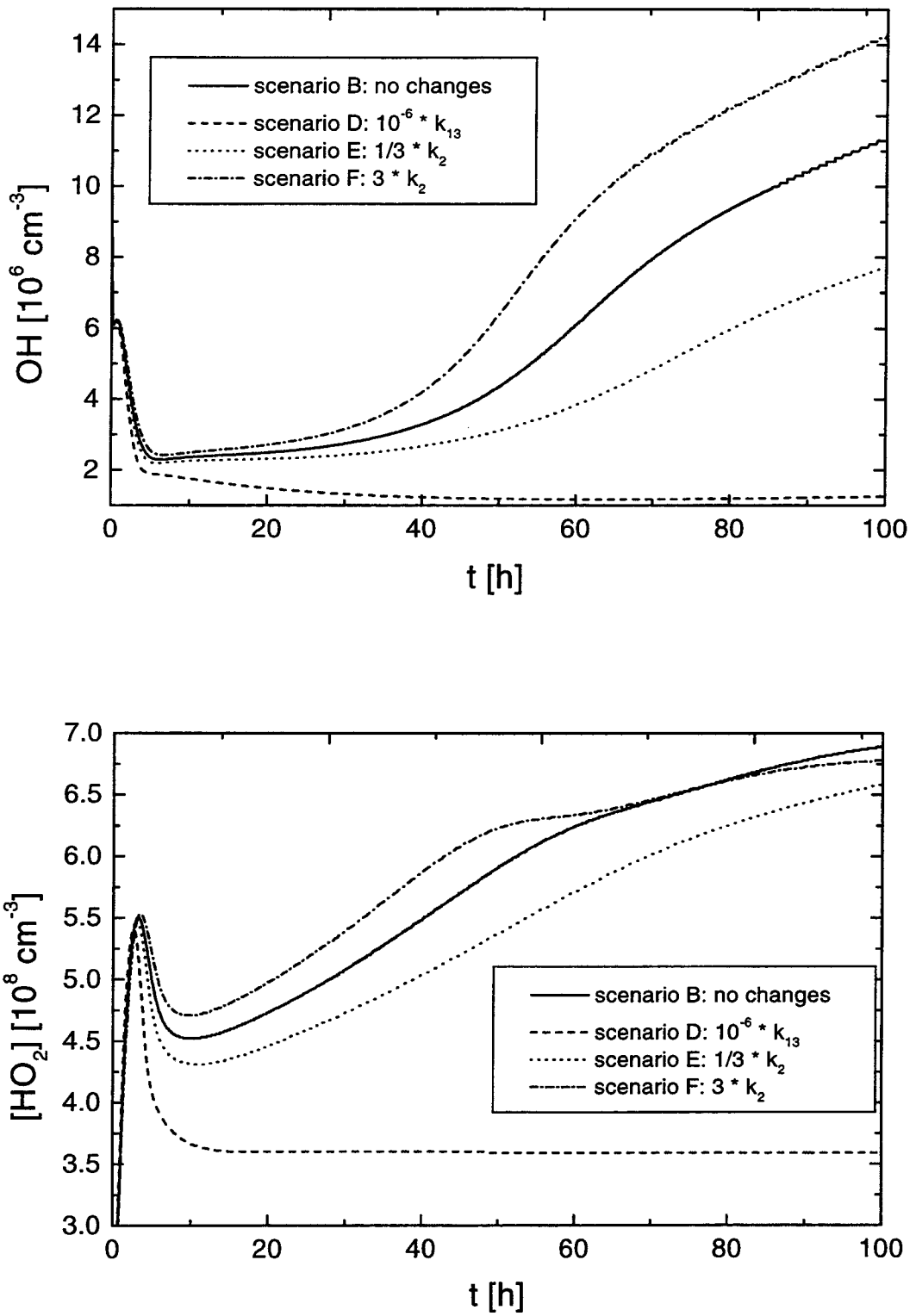


**Fig. 6:** Time dependence of the OH (top) and $HO_2$ (bottom) concentrations for scenario B, D ($10^{-6}$ $k_{13}$), E (1/3 * $k_2$), and F (3 * $k_2$)

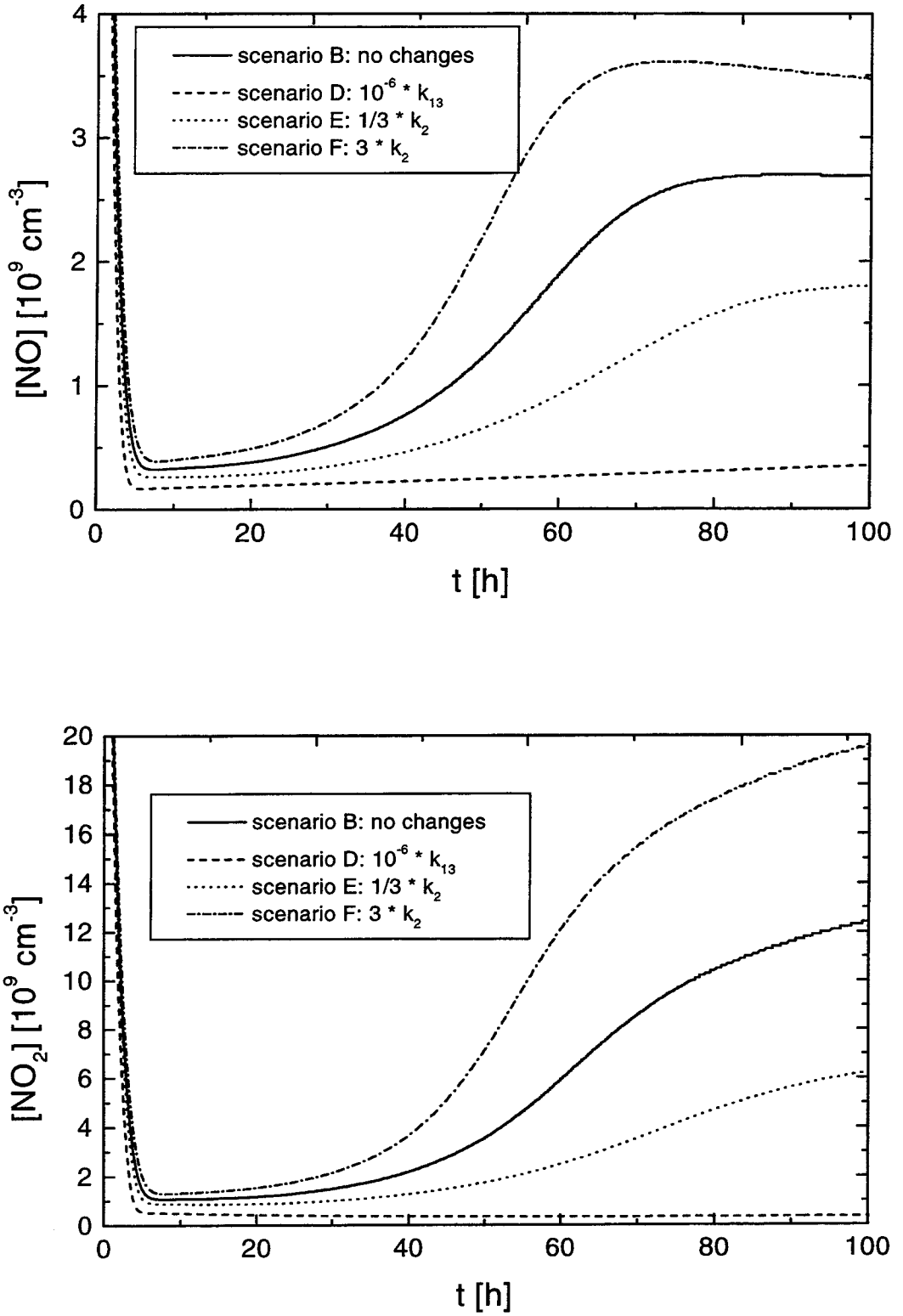


**Fig. 7:** Time dependence of the NO (top) and $NO_2$ (bottom) concentrations for scenario B, D ($10^{-6}$ $k_{13}$), E (1/3 * $k_2$), and F (3 * $k_2$)

catalytic destruction of ozone, as mentioned above, can occur. The maximal loss of $O_3$ by reactions R2 and R12 is about 1.2 ppb/h in scenario D. Because of the changed concentrations of $HO_x$ and $NO_x$ compared to scenario B the total loss of $O_3$ is about 1.8 ppb/h which is higher than in scenario B where the largest $O_3$ destruction rate is 0.3 ppb/h. At longer integration times a net production of $O_3$ of about 1 ppb/h occurs in scenario B (see chapter 5.1).

Further details of the influence of the variation of $k_{13}$ on the $NO_x$, $HO_x$ and $O_3$ concentration are given in table 6. The concentrations of all compounds decrease for the smaller value of $k_{13}$. At t = 90 h the $NO_2$ concentration is smaller by a factor of 32, the OH and $O_3$ concentrations are smaller by a factor of about 10.

**Tab. 5:** Rates of the reactions in units of [$cm^{-3}$ $s^{-1}$] for variation of selected rate constants for a $NH_3$ concentration of 100 ppb; for reactions with different product channels the summ of all channels is given; scenario B: see table 2, variation of k: D: $10^{-6}$ * $k_{13}$; E: 1/3 * $k_2$; F: 3 * $k_2$; for reactions with different product channels the sum of all channels is given

| Scenario | B | | D | | E | | F | |
|---|---|---|---|---|---|---|---|---|
| | no change | | $10^{-6}$ * $k_{13}$ | | 1/3 * $k_2$ | | 3 * $k_2$ | |
| Reaction | 10 h | 90 h | 10 h | 90 h | 10 h | 90 h | 10 h | 90 h |
| $NH_3$+OH | $8.2*10^5$ | $2.5*10^6$ | $6.1*10^5$ | $4.1*10^5$ | $7.9*10^5$ | $2.1*10^6$ | $8.7*10^5$ | $3.5*10^6$ |
| $NH_2$+$O_3$ | $6.8*10^5$ | $1.3*10^6$ | $4.2*10^6$ | $6.8*10^5$ | $5.1*10^5$ | $6.7*10^5$ | $8.0*10^5$ | $2.6*10^6$ |
| $NH_2O$[1)] | $7.5*10^5$ | $1.7*10^6$ | $3.3*10^5$ | $2.2*10^5$ | $6.6*10^5$ | $1.2*10^6$ | $8.3*10^5$ | $2.9*10^6$ |
| NHOH+OH | $1.1*10^5$ | $1.6*10^6$ | $2.7*10^4$ | $1.1*10^5$ | $8.5*10^4$ | $1.2*10^6$ | $1.4*10^5$ | $2.8*10^6$ |
| HNO+$O_2$ | $1.1*10^5$ | $1.5*10^6$ | $7.0*10^4$ | $1.4*10^5$ | $9.8*10^4$ | $1.1*10^6$ | $1.4*10^5$ | $2.6*10^6$ |
| $NH_2$+NO[2)] | $1.8*10^4$ | $2.0*10^5$ | $7.5*10^4$ | $9.0*10^4$ | $3.2*10^4$ | $2.4*10^5$ | $8.2*10^3$ | $1.1*10^5$ |
| $NH_2$+$NO_2$[3)] | $7.4*10^4$ | $8.8*10^5$ | $2.7*10^5$ | $1.2*10^5$ | $1.4*10^5$ | $1.0*10^6$ | $3.5*10^4$ | $7.6*10^5$ |
| $NH_2$+$HO_2$[4)] | $4.9*10^4$ | $1.0*10^5$ | $3.2*10^5$ | $2.0*10^5$ | $1.1*10^5$ | $1.8*10^5$ | $2.0*10^4$ | $4.3*10^4$ |
| $NH_2O$+$O_3$ | 10 | 43 | $4.2*10^6$ | $6.9*10^5$ | 8 | 18 | 11 | 78 |

[1)] Isomerization of $NH_2O$ yielding NHOH (R13)
[2)] Sum of F6 and F7
[3)] Sum of F8 and F9
[4)] Sum of F3, F4 and F5

**Tab. 6** Influence of the oxidation of $NH_3$ on the $HO_x$, $NO_x$ und $O_3$ concentrations for variation of selected rate constants; scenario B: see table 2, D: $k_{13} * 10^{-6}$, E: $k_2/3$; F: $k_2 * 3$

| t [h] | Scenario | [OH] [$10^6$ $cm^{-3}$] | [$HO_2$] [$10^8$ $cm^{-3}$] | [NO] [$10^8$ $cm^{-3}$] | [$NO_2$] [$10^9 cm^{-3}$] | [$O_3$] [$10^{12} cm^{-3}$] |
|---|---|---|---|---|---|---|
| 10 | B | 2.36 | 4.52 | 3.30 | 1.09 | 1.37 |
| | D | 1.75 | 3.67 | 1.76 | 0.49 | 1.06 |
| | E | 2.25 | 4.31 | 2.64 | 0.87 | 1.36 |
| | F | 2.49 | 4.71 | 3.99 | 1.32 | 1.40 |
| 50 | B | 4.35 | 5.91 | 12.2 | 3.55 | 1.31 |
| | D | 1.19 | 3.59 | 2.45 | 0.35 | 0.40 |
| | E | 3.12 | 5.38 | 6.50 | 1.75 | 1.15 |
| | F | 6.42 | 6.23 | 22.1 | 7.18 | 1.56 |
| 90 | B | 10.4 | 6.78 | 27.0 | 11.6 | 2.25 |
| | D | 1.22 | 3.59 | 3.28 | 0.35 | 0.27 |
| | E | 6.95 | 6.44 | 17.5 | 5.63 | 1.57 |
| | F | 13.3 | 6.73 | 36.3 | 18.7 | 2.89 |

In summary, neglecting the isomerization of $NH_2O$ has a remarkably small effect on the $HO_x$ and $NO_x$ budget.

There is, however, a substantial influence on the temporal evolution of the system. Since the isomerization product, NHOH, has a rather long lifetime, because it is only slowly depleted by OH, it can build up substantial concentrations in the atmosphere. The calculations indicate stationary concentrations of $0.14 * 10^{10}$, $5.2 * 10^{10}$, $11.7 * 10^{10}$, and $38.5 * 10^{10}$ $cm^{-3}$ in scenario ST1, A, B, and C, respectively. As mentioned in chapter 2, there are no additional degradation reactions of NHOH reported in the literature. But it is very likely that NHOH reacts with molecular oxygen to form in one or two steps $HO_2$ and NO. Since both compounds are also the main products of the degradation of NHOH with OH, inclusion of a $O_2$ reaction would only change the timescale but not substantially the balance of $NO_x$ and $HO_x$.

### 5.2.2 Variation of the rate constant of the reaction of $NH_2$ with $O_3$

To explore the influence of the experimental uncertainty of $k_2$ mentioned in chapter 2 the value of $k_2$ was varied by a factor of 1/3 (scenario E, table 5) and 3 (scenario F, table 5), respectively.

The rate F2 at t = 10 h decreases slightly for scenario E. At t = 90 h F2 is only half of the value in case B. The simultaneous increase of F9 and F3 compensates that loss, such that the yield of NHOH from R13 remaining nearly unchanged compared to scenario B. This should lead to an influence on the $HO_x$ and $NO_x$ concentrations. Indeed, the OH and $NO_2$ concentrations decrease obviously at longer integration times (figures 6 and 7). The relative influence on the $HO_2$ and NO concentration is lower (table 6). The largest decrease of the $NO_x$ concentration is found after 50 h to half its value in scenario B. After 90 h the concentration of $HO_x$ is decreased only by a small amount while the $NO_x$ concentration reaches only 50 % of the value in scenario B.

Table 5 shows that the influence of an increased $k_2$ is higher. The rate F2 is doubled. The rates of the reactions of $NH_2$ with $HO_2$ (R3 - R5) and NO (R6, R7) are smaller by a factor of about 2. For the reactions with $NO_2$ (R8, R9) the influence is smaller. As a consequence of the increased F2 value the rates in the main degradation pathway increase by a factor of about 50 %. One would expect that this behaviour would substantially affect the $HO_x$ and $NO_x$ concentrations. However, the $HO_2$ concentration is only slightly smaller, as shown in figure 6b. In contrast the OH and $NO_x$ concentrations increase clearly (figures 6a, 7, see also table 6). The largest difference between scenario F and B to be found occurs at t = 90 h. The $NO_x$ concentration increases by a factor of about 2 at this point. The OH concentration is also larger at t = 90 h in scenario F. Only the $HO_2$ concentration decreases compared to scenario B.

### 5.2.3 Discussion of the effect of the variation of $k_2$ and $k_{13}$

The sensitivity calculations with respect to the experimental uncertainties of $k_2$ and $k_{13}$ show that the results of this work have to be taken with some care.

The pathway of the degradation of $NH_3$ presented at the beginning of this chapter (figure 1) seems to be the dominant pathway under all conditions, but the product distribution is uncertain to the extend shown by the calculations in 5.2.1 and 5.2.2. The $NH_3$ concentrations in the atmosphere are normally lower so that the sensitivity

tests provide a worstcase scenario. Within the range of variation the effect of the reaction of $NH_2$ with $O_3$ (R2) on the rates of the oxidation of $NH_3$ is larger than the impact of the isomerization reaction of $NH_2O$ (R13).

From a global point of view the discussed experimental uncertainties are likely to have a small influence because of the small fraction of $NH_3$ that is removed by gas-phase processes (see chapter 1). However, near strong sources of $NH_3$ e.g. $NO_x$ removal by $NH_3$ in the exhaust of power plants with high $NH_3$ and $O_3$ concentration a strong influence on the product distribution is possible. Under these conditions an increase of the reaction rate R8 ($NH_2$ with $NO_2$) enhances the yield of $N_2O$.

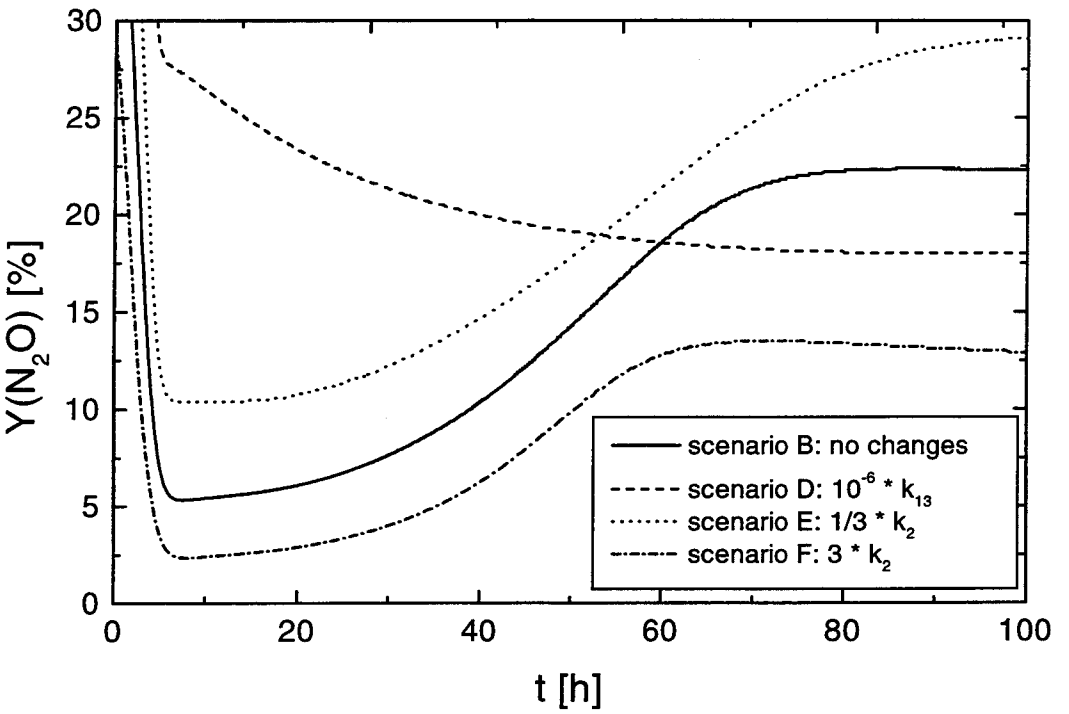


**Fig. 8:** Time dependence of $Y(N_2O)$ (equation (2)) for scenario B (no change), scenario D ($10^{-6}$ * $k_{13}$), scenario E (1/3 * $k_2$) and scenario F (3 * $k_2$); $[NH_3]$ = 100 ppb

The influence of the variation of the values of $k_2$ and $k_{13}$ on the relative $N_2O$ yield $Y(N_2O)$ defined in equation (2) is shown in figure 8. The small $Y(N_2O)$ at $t < 10$ h are caused by the transient initial decay of the $HO_x$ and $NO_x$ concentration. While in scenario B, E, and F the production is lower at 10 h $< t <$ 30 h than at longer integration times, only a small decrease is calculated in scenario D for $t >$ 10 h. The maximum of the $N_2O$ production shown in figure 8 is 83 ppt/h for scenario E after 90 h.

### *5.3 Comparison with results from the literature*

In this chapter the results for RAD-NH3 are compared with the findings for other reaction schemes. First the reaction schemes used by other groups were compared to the RAD-NH3 followed by a comparison of the results.

*Quotschalla* [Quo94] has used a simplified mechanism with only 7 reactions for the $NH_3$ degradation which were added to RADM2 (denoted here by QU-NH3). The differences are summarized as follows:

1. Use of the reaction of $NH_2$ with $O_2$ with a rate constant of $1 * 10^{-18}$ $cm^3$ $s^{-1}$ taken from Patrick and Golden [Pat84], in RAD-NH3 this process was neclected.
2. No reaction of HNO with $O_2$ (R26)
3. No isomerization of $NH_2O$ (R13)
4. Higher values of $k_{16}$ ($k = 4.96 * 10^{-12}$ $cm^3$ $s^{-1}$ after [Sot91], HNO + OH) and $k_{18}$ ($k = 1.0 * 10^{-14}$ $cm^3$ $s^{-1}$ after [Sar84], HNO + HNO $\rightarrow$ $N_2O$ + $H_2O$) than in this work

As a consequence the main fraction of the $NH_2$ radicals reacts with $O_2$. Because the reaction of HNO with $O_2$ (R26) is excluded in QU-NH3, only reaction with OH and the self reaction occur. This leads to differences in the concentration of $NO_x$ and $HO_x$. They are caused by the fact, that both reactions yield NO, but in the first reaction one $HO_x$ radical is destroyed (as OH), while in the latter reaction one $HO_x$ radical is produced (as $HO_2$). Using the results of Quotschalla 1/3 of the OH destruction within the $NH_3$ degradation chemistry is caused by the reaction of HNO with OH. Therefore, the influence of the oxidation of $NH_3$ on the OH concentration is underpredicted by QU-NH3. It should be mentioned that for a $NH_3$ concentration of 10 ppb and t = 100 h Quotschalla [Quo94] determined an increase of the concentration of OH by 30 %, of NO by 65 % and of $NO_2$ by 83 % relative to RADM2. This agrees qualitively with the results from this work.

*Dentener and Crutzen* [Den94] used also a less detailed mechanism for the degradation of $NH_3$ than RAD-NH3. The main differences are:

1. Higher value for $k_8$ ($NH_2$ + $NO_2$ $\rightarrow$ $N_2O$ + $H_2O$) by about 50 % (based on JPL 92 [DeM92])
2. Smaller value of $k_2$ ($NH_2$ + $O_3$ $\rightarrow$ $NH_2O$ + $O_2$) by about 20 % (based on JPL 92 [DeM92])
3. No reaction of HNO with $O_2$ (R26)
4. No isomerization of $NH_2O$ (R13)

The part of the reaction of $NH_2$ with $NO_2$ yielding $N_2O$ is overpredicted by Dentener and Crutzen, because of the simpler chemical mechanism and the different value of $k_8$.

*Logan* [Log83] and *Lee et al.* [Lee97] implemented in their model a mechanism that is similar to that of Dentener and Crutzen. The rate constant for the reaction of $NH_2$ with $O_3$ is smaller by a factor of 3 compared to this work, while the rate constant for the reaction of $NH_2$ with $NO_2$ is 20 % higher. Therefore, the $NO_x$ production from $NH_3$ degradation is underestimated, because the reaction of $NH_2$ with $O_3$ yields NO and $HO_2$ as main products. In addition the reaction of $NH_2$ with $NO_2$ increases the $NO_x$ losses. The mechanism of Lee et al. [Lee97] is the same as of Logan, but updated rate constants were used. Similar to Logan [Log83] and Dentener and Crutzen [Den94] Lee et al. neglected the isomerization of $NH_2O$ to yield NHOH (R13). This leads to a different estimate of the $NO_x$ source strength from the oxidation of $NH_3$ by these authors.

*Böttger et al.* [Böt78] used a less detailed mechanism for the degradation of $NH_3$ than the RAD-NH3. The differences are summarized as follows:

1. Use of the reaction of $NH_2$ with $O_2$ with a rate constant of $2.7 * 10^{-18}$ $cm^3$ $s^{-1}$ taken from Halstead and Jenkins [Hal68], in RAD-NH3 this process was neclected.
2. No isomerization of $NH_2O$ (R13)
3. Higher value of $k_7$ ($NH_2 + NO \rightarrow N_2 + H_2O$) by a factor of about 2 from Gordon et al. [Gor71]
4. Smaller value of the sum of $k_{10}$ and $k_{11}$ ($NH_2 + OH$) by a factor of $10^4$ from Garvin et al. [Gar74]

As mentioned, inclusion of the reaction of $NH_2$ with $O_2$ leads to an larger $HO_x$ concentration. The higher value of $k_7$ predicts smaller NO concentrations. On the other hand, the $NH_2$ concentration is smaller caused by reaction of $NH_2$ with $O_2$. As a consequence, the contribution of R7 to the $NH_2$ degradation is smaller. Despite the large difference between the values for ($k_{10} + k_{11}$), the product distribution of the $NH_3$ degradation is similar as expected, because the rates F10 and F11 are negligible.

Tyndall et al. [Tyn91] state that the $NH_3$ oxidation should be a source of $NO_x$ and radicals, if the concentration ratio of the $O_3$ and $NO_x$ exceeds 100. This is confirmed by this work. Their observation, that the $NH_3$ oxidation should be a sink for $NO_x$ and radicals for a ratio of $[O_3] < 100$ $[NO_x]$ and a source of $N_2O$, was not found in this work, because the corresponding range of concentrations are not accessible in the scenarios discussed.

## *5.4 Influence of the degradation of $NH_3$ on the chemistry of the atmosphere*

The $NH_3$ degradation influences the concentration of $NO_x$, $HO_x$, $N_2O$ and $O_3$. A summary of the results is given here. Relative yields of $NO_x$ and $N_2O$ from the $NH_3$ oxidation as well as a nitrogen balance of $NH_3$ degradation are presented. Finally, a very rough estimate of the global $NO_x$ and $N_2O$ source strength from the gas phase oxidation of $NH_3$ is given.

### 5.4.1 Influence of the $NH_3$ degradation on the concentration of $HO_2$, $NO_x$, $N_2O$ and $O_3$

Although the gas phase degradation of $NH_3$ is of minor importance for the global $NH_3$ budget (see chapter 1), there is some influence on the concentration of NO, $NO_2$, $N_2O$ and $O_3$. In table 7 the values of G(X) as defined in equation (1) for X = NO, $NO_2$, $N_2O$, and $O_3$ at different integration times for all scenarios are given.

The impact on the $NO_x$ concentration is quite substantial. While in scenario C a maximum production of NO of 3.0 ppt/h can be observed, in scenario ST1 only a value of 0.2 ppt/h is found. A maximum production of $NO_2$ of 0.6 ppt/h in scenario ST1 after 90 h is compared to a $NO_2$ production of 7.9 ppt/h in scenario C after the same time. The oxidation of $NH_3$ is a $NO_x$ source under most conditions. The largest differences can be observed for $O_3$. While in scenario ST1 a net destruction of $O_3$ of 0.25 ppb/h occurs after 10 h, in scenario D 1.4 ppb/h of $O_3$ is destroyed at this time. After 50 h a destruction of $O_3$ of 0.14 ppb/h in scenario ST1 and a production of 1.1 ppb/h in scenario F can be observed.

Since in the RADM2 (scenario ST1) does not include $N_2O$ chemistry, a comparison of $N_2O$ production in presence or absence of $NH_3$ is not possible. The entries in table 7 show large variability of the $N_2O$ production for the other scenarios. While less than 0.2 ppt/h of $N_2O$ is formed in scenario ST1, this rate increases to 280 ppt/h in scenario C. The reason for this observation is the higher $NO_2$ concentration in scenario C compared to scenario ST2 which leads to an increase of the rate of the reaction of $NH_2$ with $NO_2$ (R8, R9). The $N_2O$ yield from these reaction is about 60%.

**Tab. 7** Influence of the oxidation of $NH_3$ on G(X) = P(X) - D(X) for X = $NO_x$, $N_2O$ and $O_3$ for different scenarios; T = 283 K

| t [h] | Scenario | $[NH_3]_0$ [ppb] | G(NO)[1)] | $G(NO_2)$[1)] | $G(N_2O)$[1)] | $G(O_3)$[1)] |
|---|---|---|---|---|---|---|
| 10 | ST1 | 0 | -0.2 | -0.9 | - | -253 |
| | ST2 | 1 | -0.2 | -0.8 | 0.07 | -254 |
| | A | 40 | -0.06 | -0.4 | 2.6 | -276 |
| | B | 100 | 0.1 | 0.2 | 6.2 | -311 |
| | C | 400 | 0.5 | 1.0 | 16.3 | -467 |
| | D | 100 | 0.06 | -0.4 | 22.5 | -1416 |
| | E | 100 | 0.02 | -0.2 | 11.3 | -350 |
| | F | 100 | 0.3 | 0.6 | 2.9 | -268 |
| 50 | ST1 | 0 | 0.2 | 0.5 | - | -147 |
| | ST2 | 1 | 0.2 | 0.6 | 0.09 | -142 |
| | A | 40 | 1.0 | 2.9 | 6.7 | 103 |
| | B | 100 | 2.3 | 7.2 | 28.3 | 432 |
| | C | 400 | 3.0 | 7.7 | 98.3 | 401 |
| | D | 100 | 0.07 | -0.04 | 10.7 | -246 |
| | E | 100 | 0.9 | 2.3 | 25.5 | 49.0 |
| | F | 100 | 4.7 | 18.2 | 28.5 | 1052 |
| 90 | ST1 | 0 | 0.2 | 0.6 | - | 79.8 |
| | ST2 | 1 | 0.2 | 0.7 | 0.2 | 103 |
| | A | 40 | 0.07 | 2.3 | 24.7 | 689 |
| | B | 100 | -0.01 | 3.7 | 91.2 | 862 |
| | C | 400 | 1.1 | 7.9 | 280 | 637 |
| | D | 100 | 0.08 | 0.03 | 10.1 | -54.0 |
| | E | 100 | 0.4 | 2.9 | 83.0 | 605 |
| | F | 100 | -0.3 | 4.0 | 63.6 | 939 |

[1)] G in units of [ppt/h]

### 5.4.2 Relative yields of $N_2O$ and $NO_x$ from the $NH_3$ oxidation

To get further insight in the importance of the $NH_3$ degradation in the atmosphere, simulations were done using fixed $NO_2$ mixing ratios to simulate the effect of nitrogen oxides emissions in the atmosphere that tend to maintain a certain $NO_x$ burden. These scenarios are denoted as ST2', A', and B' because the initial conditions are otherwise the same as in the unprimed cases. The yield of $N_2O$ per $NH_3$ molecule consumed is shown in figures 9a - 9c. For fixed $NO_2$ concentrations of 1 and 10 ppb the relative yield $Y(N_2O)$ reaches a constant value of 23 % - 26 % (1 ppb $NO_2$) and 42% (10 ppb $NO_2$), respectively, at t = 70 h. While in the case of 1 ppb $NO_2$ this value is effected slightly by the $NH_3$ concentration, this dependence is not observed for 10 ppb $NO_2$. At a $NO_2$ concentration of 40 ppb a constant value of $Y(N_2O)$ of about 52 % occurs at t = 30 h. In this case $Y(N_2O)$ is also influenced by the initial $NH_3$ concentration. In case $Y(N_2O)$ does not depend on the $NH_3$ concentration, the $N_2O$ production is determined by the $NO_x$ concentration. The $NO_x$ concentration

a)

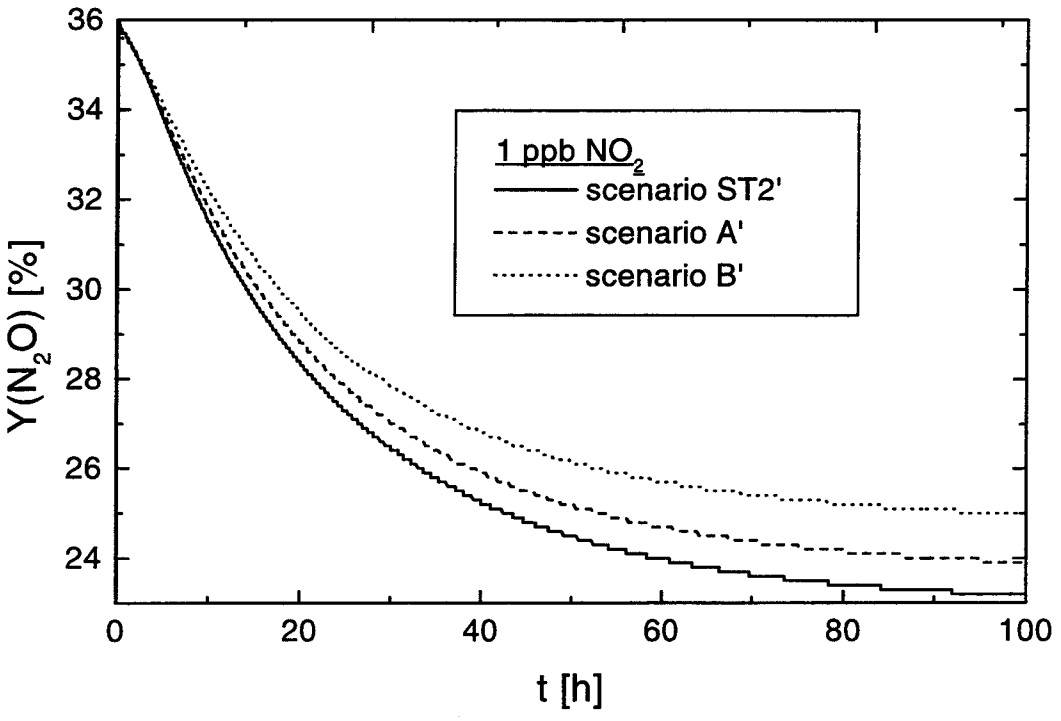


**Fig. 9:** Time dependence of $Y(N_2O)$ (equation (2)) for an $NO_2$ concentration of a) 1 ppb and scenarios ST2', A', and B' (T = 283 K)

b)

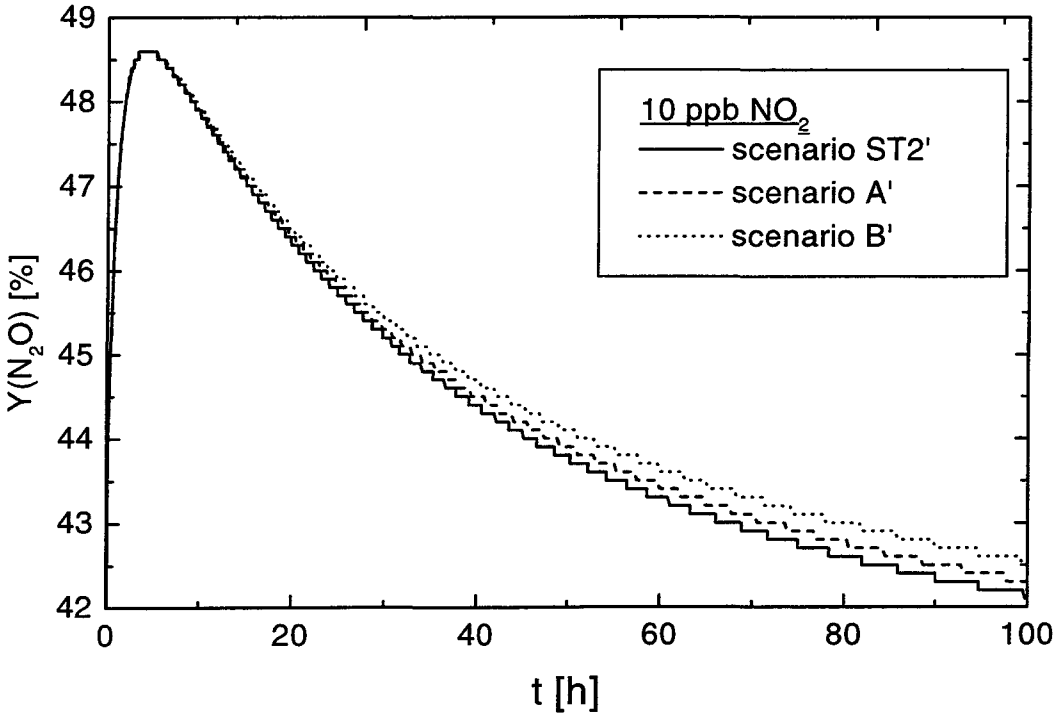


c)

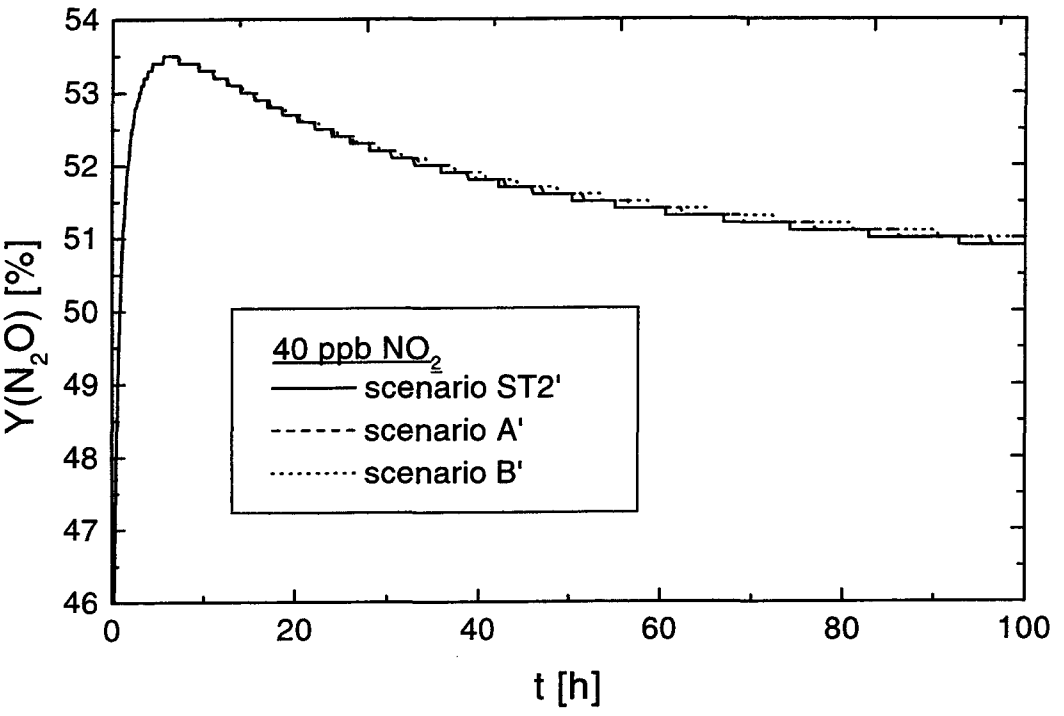


**Fig. 9:** Time dependence of $Y(N_2O)$ (equation (2)) for an $NO_2$ concentration of b) 10 ppb and c) 40 ppb and scenarios ST2', A', and B' (T = 283 K)

**Tab. 8:** Influence of the degradation of $NH_3$ on the concentrations of $NH_2$, HNO, $NO_x$ as well as the ratios $[NH_2]/[NO_x]$ und $[NH_2]/[HNO]$

| Szenario | | $[NH_2]$ $[10^5\ cm^{-3}]$ | $[HNO]$ $[10^6\ cm^{-3}]$ | $[NO_x]$ $[10^9\ cm^{-3}]$ | $[NH_2]/[NO_x]$ $[10^{-5}]$ | $[NH_2]/[HNO]$ |
|---|---|---|---|---|---|---|
| ST2 | 10 h | 0.34 | 0.09 | 1.4 | 2.4 | 0.38 |
| | 90 h | 0.56 | 0.70 | 2.6 | 2.2 | 0.08 |
| A | 10 h | 13.1 | 3.2 | 1.4 | 93.6 | 0.41 |
| | 90 h | 20.6 | 42.6 | 8.3 | 24.8 | 0.05 |
| B | 10 h | 30.8 | 6.5 | 1.4 | 220 | 0.47 |
| | 90 h | 42.6 | 110 | 14.3 | 29.8 | 0.04 |
| C | 10 h | 94.3 | 12.2 | 1.3 | 725 | 0.77 |
| | 90 h | 101 | 184 | 19.5 | 51.8 | 0.55 |

controls both the $N_2O$ production in reaction R8 from $NH_2$ with $NO_2$ as well as the destruction of $NH_3$ driven by OH (R1) with its influence on the $HO_x$ concentration.
The relative yield of $NO_x$ is more complicated to describe. In this work, only the direct influence of the $NH_3$ degradation on the $NO_x$ production from reactions R6 - R8, R14 - R17 and R26 was examined. $Y^*(NO_x)$ is defined by

$$Y^*(NO_x) = \frac{(F26 + F14 + F15 + F16 + F17) - (F6 + F7 + F8)}{F1} \qquad (4)$$

and shown in figure 10. As can be seen, $Y^*(NO_x)$ varies strongly with the $NH_3$ concentration. While a maximum $NO_x$ yield of 70 % occurs at 1 ppb $NH_3$ concentration, $Y^*(NO_x)$ decreases to less than 17 % at 400 ppb $NH_3$. The loss is caused by the increase of the ratio of $NH_2$ and $NO_x$, as can be seen from table 8. The ratio increases from scenario ST2 (1 ppb $NH_3$) to scenario C (400 ppb $NH_3$) by a factor of 300 after 10 h integration time, after 90 h this factor is 24. This ratio controls the $NO_x$ destruction from the oxidation of $NH_3$, because the reactions R6 - R9 are the main sinks of $NO_x$. Contrary, the ratio of $NH_2$ to HNO increases from scenario ST2 to C only by a factor of 2.0 after 10 h and after 90 h by a factor of 6. Compared to the ratio $[NH_2]/[NO_x]$ this increase is very small. The ratio $[NH_2]/[HNO]$ represents the

ratio of the main source to the main sink of $NO_x$ from the $NH_3$ degradation. The $NO_x$ production depends on the $NH_3$ concentration because the $NH_2$ concentration increases with enhanced $NH_3$, while the ratio of $NH_2$ and HNO remains unchanged.

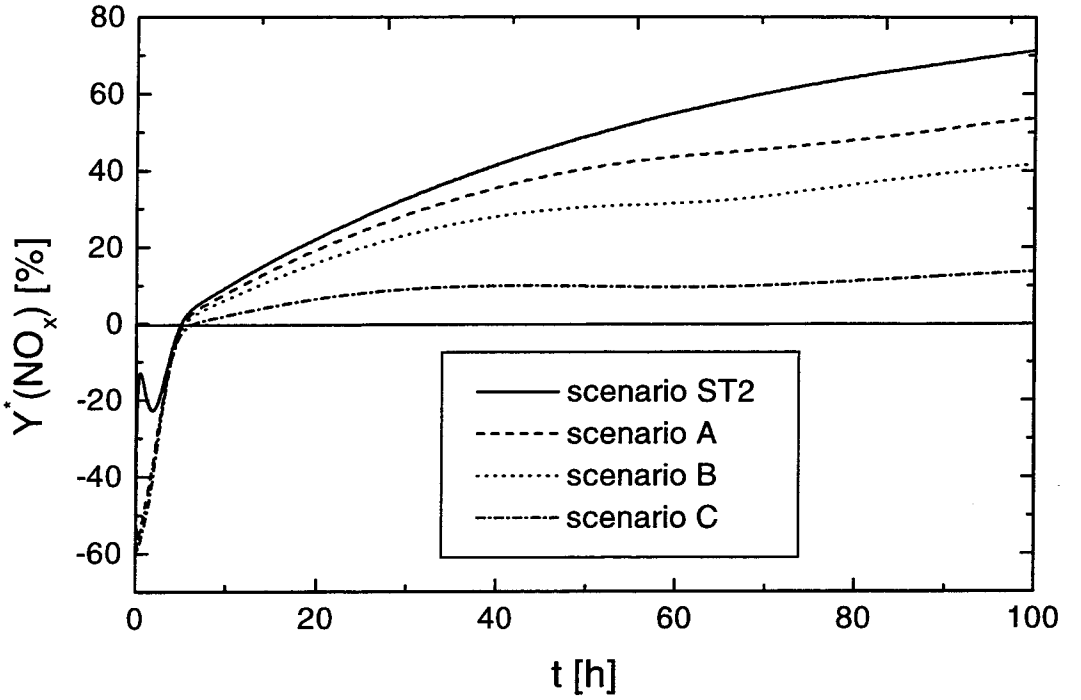


**Fig. 10:** Time dependence of $Y^*(NO_x)$ (equation (4)) for scenarios ST2, A, B, and C; (T = 283 K)

### 5.4.3 Nitrogen balance for the oxidation of $NH_3$

In this chapter a nitrogen balance for the gas-phase oxidation of $NH_3$ is presented. To that end the relative yields Y(X) (see equation (2)) of all reactions, in which reactive nitrogen containing compounds take part, were taken, like it is shown in figure 10 for $N_2O$. The net production of $NO_x$ and HONO from the $NH_3$ degradation, $P^*(NO_x)$ and $P^*(HONO)$, are defined as:

$$P^*(NO_x) = F26 + F14 + F15 + F16 + F17$$
$$P^*(HONO) = F22$$

In addition other nitrogen containing substances were formed like molecular nitrogen in reactions R6, R7 and R15, and NHOH, HNO and $NH_2OH$. Note that the yield of $NH_2OH$ has to be taken twice, because R17 is a reaction of two molecules formed from the $NH_3$ oxidation. The results of this balance is shown in table 9, where the values are entered for t = 90 h.

**Tab. 9:** Relative yields (equation (2)) for determination of the nitrogen balance; t = 90 h; Y($NH_2OH$) has to be taken twice (see text); scenario ST2: 1 ppb $NH_3$; scenario C: 400 ppb $NH_3$

| Scenario | ST2 | C |
|---|---|---|
| $P^*(NO_x)/D(NH_3)$ | 80 % | 43 % |
| $P^*(HONO)/D(NH_3)$ | 0 % | 1 % |
| $Y(N_2O)$ | 10 % | 28 % |
| $Y(NH_2OH)$ (* 2) | 0 % | 8 % |
| Y(NHOH) | 6 % | 1 % |
| Y(HNO) | 0 % | 0 % |
| $Y(N_2)$ | 4 % | 11 % |
| Σ | 100 % | 100 % |

### 5.4.4 Estimate of the global $N_2O$ and $NO_x$ source strength from $NH_3$ oxidation

Dentener and Crutzen [Den94] calculated the contribution to the global source strength of $N_2O$ from their degradation scheme of $NH_3$ in the gas phase to be 0.9 Tg $N_2O$ $yr^{-1}$ ($0.6 * 10^{12}$ g N $yr^{-1}$). This is 5 % of the total global $N_2O$ emission and 10 % of the global anthropogenic $N_2O$ production. One third of the $N_2O$ production from $NH_3$ is result of biomass burning with high $NO_2$ and $NH_3$ concentration, the remainder is mainly produced in the tropics at high OH, $NO_x$ and $NH_3$ concentrations [Den94]. Therefore, the gas phase degradation of $NH_3$ is important for the $N_2O$ budget. A $N_2O$ source of $3 * 10^{12}$ g N $yr^{-1}$ from industrial burning is given by Prather [Pra85], which is 25 % of the global $N_2O$ emission. Cicerone [Cic89] estimated from global budget consideration a source of $N_2O$ of $19 * 10^{12}$ g N $yr^{-1}$.

A crude estimate of the global $N_2O$ and $NO_x$ source strength from the oxidation of $NH_3$ in the gas phase is given here. It is assumed that $NH_3$ is mixed homogeneously in the planetary boundary layer with a thickness of 1000 m. Only in this layer the degradation of $NH_3$ takes place. The mixing ratio of 0.1 - 2 ppb is used according to Dentener and Crutzen [Den94]. The area of the earth was calculated to be $5.1 * 10^{14}$ $m^2$. A mean OH concentration of $1.6 * 10^6$ $cm^{-3}$ and a temperature of 283 K are used. For $N_2O$ the yields for the scenarios presented in this work vary between 8 and 25 % after t = 70 h. The yield of $NO_x$ is 64 % for 1 ppb $NH_3$ and 10 % for 400 ppb $NH_3$. For the estimate of the range of the source strengths the lower and upper limits of Y(X) were taken. The source strengths estimated are $(0.03 - 2.4) * 10^{12}$ g N $yr^{-1}$ for $N_2O$ and $(0.3 - 33) * 10^{12}$ g N $yr^{-1}$ for $NO_2$, respectively. The range for the $N_2O$ source strength encloses the value of $0.6 * 10^{12}$ g N $yr^{-1}$ reported by Dentener and Crutzen [Den94]. It should be mentioned again that the estimate presented in this work is a very crude. Compared to the over all source strength for $N_2O$ of $19 * 10^{12}$ g N $yr^{-1}$ as given by Cicerone [Cic89], the oxidation of $NH_3$ has no importance for the global production of $N_2O$.

Böttger et al. [Böt78] calculated a $NO_x$ source strength from the $NH_3$ oxidation of $(1.2 - 4.9) * 10^{12}$ g N $yr^{-1}$ which is consistent with the value estimated in this work. The value of $0.9 * 10^{12}$ g N $yr^{-1}$ from Lee et al. [Lee97] is also in agreement with the value presented here. They estimated a contribution of 2 % of the global $NO_x$ emision from the $NH_3$ gas-phase degradation.

## *5.5 Influence of other reactions*

There are several reaction, not discussed here, that are of potential importance for the degradation of $NH_3$. They are summarized in table 10.

The reaction

$$NH_2 + HNO \rightarrow NH_3 + HNO \qquad (R27)$$

was proposed by Mebel et al. [Meb96]. They determined a temperature dependent rate constant of this reaction of $k = 6.02 * 10^{-17} * T^{1.63} * \exp(630\ K/T)$ $cm^3$ $s^{-1}$ [Meb96] yielding $k_{27}(283) = 5.53 * 10^{-13}$ $cm^3$ $s^{-1}$. Because of the small calculated concentrations of $NH_2$ and HNO, the rate F27 is always smaller than $1 * 10^3$ $cm^{-3}$ $s^{-1}$

**Tab. 10:** Additional reactions of $NH_3$ and its degradation products not entered in RAD-NH3 (T in units of K)

| No. | Reaction | k [$cm^3/s$],[$s^{-1}$] | k(283) | Ref. |
|---|---|---|---|---|
| 27 | $NH_2+HNO \rightarrow NH_3+NO$ | $6.02*10^{-17}*T^{1.63}*exp(630/T)$ | $5.5*10^{-12}$ | l |
| 28 | $NH_3+O(^1D) \rightarrow NH_2+OH$ | $1.5*10^{-10}$ | $1.5*10^{-10}$ | a |
| 29 | $NH_3+O(^3P) \rightarrow NH_2+OH$ | $2.9*10^{-13}*(T/298)^{2.1}*exp(-2620/T)$ | $2.5*10^{-17}$ | e |
| 30 | $NH_2+O(^3P) \rightarrow H_2+NO$ | $8.30*10^{-12}$ | $8.3*10^{-12}$ | e |
| 31 | $NH_2+O(^3P) \rightarrow NH+OH$ | $1.16*10^{-11}$ | $1.2*10^{-11}$ | e |
| 32 | $NH_2+O(^3P) \rightarrow HNO+ H$ | $7.47*10^{-11}$ | $7.5*10^{-11}$ | e |
| 33 | $NH_2+CH_4 \rightarrow NH_3+CH_3$ | $7.80*10^{-12}*exp(-4679/T)$ | $5.1*10^{-19}$ | m |
| 34 | $HNO+O(^3P) \rightarrow OH+NO$ | $6.0*10^{-11}$ | $6.0*10^{-11}$ | h |
| 35 | $HNO+2NO \rightarrow NO_2+HN=NH$ | $1.7*10^{-38}$ *) | $1.7*10^{-38}$ | i |
| 36 | $NH_2+SO_2 \rightarrow NH_2SO_2$ | $1.5*10^{-13}*(T/298)^{1.3}$ | $1.4*10^{-13}$ | n |

*) in units of $cm^6\ s^{-1}$
a: [DeM94], e: [Coh91], h: [Tsa91], i: [Lin92], l: [Meb96], m: [Möl84], n: [Iof89]

for all scenarios, typical rates are in the range of 0.1 - 10 $cm^{-3}\ s^{-1}$. Therefore, R27 has been neglected for the reaction mechanism.

Instead of starting the oxidation of $NH_3$ by attack of OH, the reaction of $NH_3$ with O atoms is also possible (R28, R29). In the literature values for the rate constants of both the reaction of $NH_3$ with $O(^1D)$ (R28) and with $O(^3P)$ (R29) are reported. Although the reaction R28 is very fast, the concentration of $O(^1D)$ in the troposphere is so small that this reaction is unimportant for the degradation of $NH_3$ in the atmosphere. Similar arguments hold for the reactions involving $O(^3P)$.

Cohen and Westberg [Coh91] proposed three possible product channels for the reaction of $NH_2$ and $O(^3P)$ with rate constants independent of temperature:

$$NH_2 + O(^3P) \rightarrow H_2 + NO \quad k(298\text{-}3000) = 8.30 * 10^{-12}\ cm^3\ s^{-1} \qquad (R30)$$

$$\rightarrow NH + OH \quad k(298\text{-}3000) = 1.16 * 10^{-11}\ cm^3\ s^{-1} \qquad (R31)$$

$$\rightarrow HNO + H \quad k(298\text{-}3000) = 7.47 * 10^{-11}\ cm^3\ s^{-1} \qquad (R32)$$

Although all these reactions are fast, they can be excluded because of the small concentrations of $O(^3P)$ and $NH_2$.
Möller and Wagner [Möl84] proposed a reaction of $NH_2$ with $CH_4$:

$$NH_2 + CH_4 \rightarrow NH_3 + CH_3 \qquad \text{(R33)}.$$

Because $k_{33}$ is small under atmospheric conditions as consequence of the low temperatures, R33 is negligible for the degradation of $NH_3$, dispite the atmospheric concentration of $CH_4$.
For the reaction of HNO with $O(^3P)$ yielding OH and NO (R34) a rate constant of $k_{34}(300 - 2500) = 6.0 * 10^{-11}$ $cm^3$ $s^{-1}$ is given by Tsang and Herron [Tsa91]. Due to the small concentration of both HNO as well as $O(^3P)$ in the atmosphere, this reaction can be neglected.
For the termolecular reaction of HNO with NO

$$HNO + 2\ NO \rightarrow NO_2 + HN{=}NH \qquad \text{(R35)},$$

Lin et al. [Lin92] determined a rate constant of $1.7 * 10^{-38}$ $cm^6$ $s^{-1}$. Because of the small concentration of HNO F35 is in general less than $10^{-10}$ $cm^{-3}$ $s^{-1}$ for a $NH_3$ concentration of 100 ppb. Therefore, the reaction R35 is unimportant under atmospheric conditions.
The reaction of $NH_2$ and $SO_2$ yielding the adduct $NH_2SO_2$

$$NH_2 + SO_2 \rightarrow NH_2SO_2 \qquad \text{(R36)}$$

is of interest under particular conditions in the atmosphere. The high pressure limit of $k_{36}$ was determined by Ioffe et al. [Iof89] to be $k(T) = 1.5 * 10^{-13} * (T/298\ K)^{1.3}$ $cm^3$ $s^{-1}$. The maximum rate for the $SO_2$ mixing ratios of < 0.1 ppb assumed in this work leads to a value of 100 $cm^{-3}$ $s^{-1}$ at 100 ppb $NH_3$. If the $SO_2$ concentration is higher like it is in plumes of biomass burning, reaction R36 is of importance for the conversion of $NH_2$. Under those conditions this reaction must not be neglected. Calculations probing a wide range of $NH_3$, $NO_2$, and $SO_2$ concentrations show that for low $NO_2$ burden the relative rate F36/F1 is 29 % [Koh97]. For high $NO_2$ concentrations a value of about 3 % is found. The further reactions of $NH_2SO_2$ are unknown to our knowledge. Both the decay of $NH_2SO_2$ in so far unknown products and the uptake

into aerosols could be possible. In the second case, a transformation into $NH_3HSO_3$ occurs.

### *5.6 Mechanism of $NH_3$ degradation for use in chemical models*

**Tab. 11:** Reactions of $NH_3$ and of the products of the H atom abstraction which should be added to the RADM2; reaction numbers are the same as in table 1 and 10, respectively (T in units of K)

| No. | Reaction | k [$cm^3/s$],[$s^{-1}$] | Ref. |
|---|---|---|---|
| 1 | $NH_3+OH \rightarrow NH_2+H_2O$ | $1.7*10^{-12}*\exp(-710/T)$ | [DeM94] |
| 2 | $NH_2+O_3 \rightarrow NH_2O+O_2$ | $4.3*10^{-12}*\exp(-930/T)$ | [DeM94] |
| 3 | $NH_2+HO_2 \rightarrow NH_2O+OH$ | $4.8*10^{-7}*T^{-1.32}*\exp(-628/T)$ | [Sum96a] |
| 4 | $NH_2+HO_2 \rightarrow H_2O+HNO$ | $9.4*10^{-9}*T^{-1.12}*\exp(-356/T)$ | [Sum96a] |
| 6 | $NH_2+NO \rightarrow HO_2+OH + N_2$ | $1.92*10^{-12}*(T/298)^{-1.5}$ | [Atk92] |
| 7 | $NH_2+NO \rightarrow H_2O + N_2$ | $1.41*10^{-11}*(T/298)^{-1.5}$ | [Atk92] |
| 8 | $NH_2+NO_2 \rightarrow N_2O+H_2O$ | $1.2*10^{-11}*(T/298)^{-2.0}$ | [Bul89,Meu96] |
| 9 | $NH_2+NO_2 \rightarrow NH_2O + NO$ | $0.8*10^{-11}*(T/298)^{-2.0}$ | [Bul89,Meu96] |
| 12 | $NH_2O+O_3 \rightarrow NH_2+O_2$ | $1.2*10^{-14}$ | [Bul80] |
| 13 | $NH_2O \rightarrow NHOH$ | $1.3*10^{3}$ | [Bul80] |
| 16 | $HNO+OH \rightarrow NO+H_2O$ | $8*10^{-11}*\exp(-500/T)$ | [Tsa91] |
| 17 | $HNO+NHOH \rightarrow NH_2OH+NO$ | $1.66*10^{-12}*\exp(-1500/T)$ | [Lin92] |
| 22 | $HNO+NO_2 \rightarrow HONO+NO$ | $1*10^{-12}*\exp(-1000/T)$ | [Tsa91] |
| 23 | $NHOH+OH \rightarrow HNO+H_2O$ | $1.66*10^{-12}$ | [Lin92] |
| 24 | $HONO+OH \rightarrow NO_2+H_2O$ | $1.8*10^{-11}*\exp(-390/T)$ | [Atk92] |
| 25 | $NH_2OH+OH \rightarrow NHOH+H_2O$ | $4.13*10^{-11}*\exp(-2138/T)$ | [Esp93] |
| 26 | $HNO+O_2 \rightarrow HO_2+NO$ | $3.65*10^{-14}*\exp(-4600/T)$ | [Bry93] |
| 36 | $NH_2+SO_2 \rightarrow NH_2SO_2$ | $1.5*10^{-13}*(T/298)^{1.3}$ | [Iof89] |

Finally an attempt is made to reduce the scheme in table 1 to a minimum set in order to improve computational performance in a numerical model without lossing accuracy of the computed results. As shown in chapter 5.1, the reactions of HNO and HNO (R18 - R20) and of $NH_2$ with OH (R10, R11) have rates of less than $10^3$ $cm^{-3}$ $s^{-1}$. These reactions can be removed from the gas-phase mechanism for regional modelling of chemistry and transport. Since reaction R10 is the only source of NH radicals, all reactions of NH (R14, R15) can also be abandoned from the mechanism. The decay of $HON_2OH$ yielding $N_2O$ and $H_2O$ (R21) can also be neglected. Furthermore, the production of $NH_3$ from the reaction of $NH_2$ and $HO_2$ (R5) is unimportant.

The only reaction having a small rate, which must not be removed from the mechanism, is the reaction of $NH_2O$ and $O_3$ (R12), because the rate constant of the isomerization reaction (R13) is uncertain. If reaction R13 does not exist, reaction R12 would be the only sink of $NH_2O$.

In case of scenarios with high $SO_2$ concentrations, the reaction of $NH_2$ + $SO_2$ (R36) is included.

Table 11 summarizes all relevant reactions for use in atmospheric chemical models.

# 6 Summary

In this work numerical simulations are presented concerning the gas-phase degradation of $NH_3$ under atmospheric conditions using a simple box model. The RADM2 mechanism from Stockwell et al. [Sto90], that does not treat the $NH_3$ chemistry, was taken, and 26 reactions of $NH_3$ and its degradation products were added. The new mechanism was named RAD-NH3. Since no feature specific for the RADM2 mechanism was used in the added 26 reactions for the $NH_3$ chemistry, the use of other gas-phase models should lead to similar results.

The main degradation pathway of $NH_3$ in the gas-phase of the earth's atmosphere is the initial H atom abstraction by OH, the reaction of the formed $NH_2$ with $O_3$ yielding $NH_2O$ followed by the isomerization of $NH_2O$ under production of NHOH. NHOH then reacts with OH yielding HNO, which forms $HO_2$ and NO in the reaction with $O_2$. The most important side reactions are the reaction of $NH_2$ with $HO_2$, NO and $NO_2$, respectively, and the reaction of HNO with NHOH. Based on the present study $NH_3$ is mainly degraded in the atmosphere by the following reaction sequence:

$$NH_3 \xrightarrow[+O_3]{+OH} NH_2O \xrightarrow{\text{isomerization}} NHOH \xrightarrow[+O_2]{+OH} HO_2 + NO$$

This main degradation pathway is different to the mechanisms discussed so far in the literature [Böt78, Log83, Den94, Quo95, Lee97]. The far-reaching difference is the isomerization of $NH_2O$ forming NHOH (R13) in the present work. This reaction is neglected in the mechanisms reported in the literature so far. The only possible reactions of the $NH_2$ radical are the reaction with $HO_2$, NO and $NO_2$, respectively. Therefore, these mechanisms lead to different findings with respect to the impact of the gas-phase oxidation of $NH_3$ on the concentrations of other trace gases in atmosphere. For example, all other schemes exhibit a larger production of $N_2O$ by the $NH_3$ degradation.

The oxidation of $NH_3$ leads to a remarkable increase of the OH, $O_3$ and $NO_x$ concentrations under all conditions used. The influence on the $HO_2$ concentration is in general very small, only at high $NH_3$ concentration and long integration times an influence can be observed which is mainly caused by the change of the $NO_x$ concentration. A maximum $N_2O$ production of 280 ppt/h was found at an $NH_3$ mixing ratio of 400 ppb. The $N_2O$ production rate depends non-linearly on the $NH_3$ concentration. At a $NH_3$ mixing ratio of 1 ppb an $N_2O$ production of only about 0.2 ppt/h is observed. It corresponds with a yield of 11 % relatively to the reaction rate of $NH_3$ with OH. Dentener and Crutzen [Den94] found that up to 32 % of the $NH_3$ is converted into $N_2O$. It is possible that the formation of the $N_2O$ from the reaction of $NH_2$ with $NO_2$ is overpredicted by the less detailed chemical mechanism used by Dentener and Crutzen [Den94].

Based on the results of the present work a $N_2O$ source strength of (0.3 - 24) * $10^{11}$ g N $yr^{-1}$ was estimated using a very simple box model. Furthermore, investigations of the influence of the $NH_3$ oxidation on the $N_2O$ production were made using fixed $NO_2$ concentrations. While the yield of $N_2O$ depends slightly on the $NH_3$ mixing ratio at 1 ppb $NO_2$, this dependence can not be observed at $NO_2$ mixing ratios higher than 10 ppb. The relative yield of $N_2O$ reaches a constant value of 52 % after 30 h integration time at 40 ppb $NO_2$. At lower $NO_2$ concentrations a constant $N_2O$ yield is reached after 70 h. These results are very sensitive to the rate constant for the reaction of $NH_2$ with $NO_2$ which quite uncertain.

The influence of the $NH_3$ degradation on the $NO_x$ concentration differs for the scenarios discussed. For example, a maximum production of NO from the reaction of HNO with $O_2$ of 261 ppt/h was found after t = 90 h at a $NH_3$ mixing ratio of 100 ppb. Under the same conditions an $NO_x$ loss of 179 ppt/h can be observed caused by the reactions of $NH_2$ with NO and $NO_2$, respectively. It results in a total $NO_x$ formation rate of 82 ppt/h. Relative to the rate in the reaction of $NH_3$ with OH the NO yield from the reaction of HNO and $O_2$ decreases from 79 % at 1 ppb $NH_3$ to 43 % at 400 ppb. The real $NO_x$ yield can be determined, if both the production of NO from the reaction of HNO and $O_2$ as well as the destruction of $NO_x$ by the reactions of $NH_2$ with NO and $NO_2$, respectively, are considered leading to an $NO_x$ yield of 68 % at 1 ppb $NH_3$ and of 13 % at 400 ppb $NH_3$. The dependence of $Y(NO_x)$ on the $NH_3$ concentration is caused by the increasing $NH_2$ concentration with increasing $NH_3$ concentration. The reactions of $NH_2$ with NO and $NO_2$, respectively, are the main sinks of $NO_x$ due to the $NH_3$ degradation, while the reaction of HNO with $O_2$ is the main source of $NO_x$. The decrease of the $NO_x$ yield is caused by the constant ratio of the concentrations of HNO to $NH_2$ for increasing $NH_3$ concentration. Because of the altered $O_3$ and $HO_x$ concentration, the total $NO_x$ source strength is smaller. A maximum $NO_x$ production of 15 ppt/h was found after 70 h at a $NH_3$ mixing ratio of 400 ppb. A simple estimate of the global $NO_x$ source strength from the $NH_3$ degradation in the gas-phase of the atmosphere leads to a value of $(0.3 - 33) * 10^{12}$ g N $yr^{-1}$.

The influence of the $NH_3$ oxidation on the $O_3$ concentration should be small, because the catalytic destruction of $O_3$ in the reactions $NH_2 + O_3 \rightarrow NH_2O$ (R2), $NH_2O + O_3 \rightarrow NH_2 + 2\ O_2$ (R12) is less important due to the fast isomerization of $NH_2O$ forming NHOH. In many cases an enhanced production of $O_3$ can be observed caused by the higher $NO_x$ and $HO_x$ concentrations from the $NH_3$ degradation. A maximum $O_3$ destruction of 180 ppt/h in the reaction of $NH_2$ and $O_3$ was found at 100 ppb $NH_3$. The overall production of $O_3$ was found to be 862 ppt/h under these conditions. If the rate constant of the isomerization of $NH_2O$ is decreased by 6 orders of magnitude, a maximum $O_3$ destruction in reactions R2 and R12 of about 1.2 ppb/h is calculated which is the main contribution to the $O_3$ destruction after 10 h integration time. The influence of the rate constant for the reaction of $NH_2$ and $O_3$ is of great importance on the $O_3$ concentration. An increase of this rate constant leads to $O_3$ production with a maximum of 1.5 ppb/h. Furthermore, the $NH_3$ degradation is an $O_3$ sink at integration times less than 10 h.

In contrast to the oxidation of hydrocarbons, the oxidation of $NH_3$ produces both $HO_2$ and NO. Therefore, a potential $O_3$ production in the troposphere from the gas phase degradation of $NH_3$ is possible.

Sensitivity studies were made to get an insight in the influence of uncertain rate constants on the degradation pathway of $NH_3$. A variation of the rate constant for the isomerization of $NH_2O$ forming NHOH by 6 orders of magnitude leads to an influence on the rates of all reactions. However, the rate of the isomerization reaction itself is only slightly effected. A change in the $HO_x$ and $NO_x$ concentration is observed. Varying the experimentaly uncertain rate constant for the reaction of $NH_2$ and $O_3$ influences all reaction rates. A change of this rate constant by a factor of 1/3 and 3, respectively, leads to a change in the $HO_x$ and $NO_x$ concentration. Due to the substantial sensitivity to this rate constant the reaction deserves further kinetic studies. The isomerization of $NH_2O$ should also be investigated in order to provide further prove of the existence of this reaction and to improve the accuracy of rate constant.

## 7 References


[Atk92] R. Atkinson, D.L. Baulch, R.A. Cox, R.F. Hampson, Jr., J.A. Kerr, J. Troe, J. Phys. Chem. Ref. Data **21**(6) (1992)

[Bau92] D.L. Baulch, C.J. Cobos, R.A. Cox, C. Esser, P. Frank, Th. Just, J.R. Kerr, M.J. Pilling, J. Troe, R.W. Walker, J. Warnatz, J. Phys. Chem. Ref. Data **21** (1992)

[Böt78] A. Böttger, D.H. Ehhalt, G. Gravenhorst, Berichte Kernforschungsanlage Jülich, No. 1558, Jülich, 1978

[Bry93] M.G. Brykov, A.A. Kachanov, R. Timonnen. J. Seetula, J. Vandoren, O.M. Sarkisov, Chem. Phys Lett. **208**, 392 (1993)

[Bul80] V.P. Bulatov, A.A. Buloyan, S.G. Cheskis, M.Z. Kozliner, O.M. Sarkisov, A.I. Trostin, Chem. Phys. Lett. **74**, 288 (1980)

[Bul89] V.P. Bulatov, A.A. Ioffe, V.A. Lozovsky, O.M. Sarkisov, Chem. Phys. Lett. **159**, 171 (1991)

[Cic89] R.J. Cicerone, J. Geophys. Res. **94**(D15), 18265 (1989)

[Coh91] N. Cohen, K.R. Westberg, J. Phys. Chem. Ref. Data **20** (1991)

[DeM92] W.B. DeMore, S.P. Sander, S.P. Golden, R.F. Hampson, M.J. Kurylo, C.J. Howard, A.R. Ravishankara, C.E. Kolb, M.J. Molina, NASA/JPL Publication 92-10 (1992)

[DeM94] W.B. DeMore, S.P. Sander, R.F. Hampson, M.J. Kurylo, C.J. Howard, A.R. Ravishankara, C.E. Kolb, M.J. Molina, NASA/JPL Publication 94-26 (1994)

[Den94] F.J. Dentener, P.J. Crutzen, J. Atmos. Chem. **19**, 331 (1994)

[Dia90] E.W.-G. Diau, T.-L. Tso, Y.-P. Lee, J. Phys. Chem. **94**, 5261 (1990)

[Dia96] E.W.-G. Diau, S.C. Smith, J. Phys. Chem. **100**, 12349 (1996)

[Esp93] J. Espinosa-Garcia, J.C. Corchado, M. Sana, J. Chim. Phys **90**, 1181 (1993)

[Fer92] M. Ferm, Summary Document, in G. Ayers et al. (eds.), 2cnd IGAC CAAP Workshop (1992)

[Gar74] D. Garvin, R.F. Hampson, Chem. Kin. data survey, NBSIR 74-430, National Bureau of Standards, Washington D.C., 1974

[Gig76] P.A. Giguere, K. Herman, Chem. Phys. Lett. **44**, 273 (1976)

[Gme93] Gmelin Handbook of Inorganic and Organometallic Chemistry, N, Supp. Vol. B2, 8. Edit., Springerverlag Berlin, 1993

[Gor73] S. Gordon, W. Mulac, P. Nangia, J. Phys. Chem. **75**, 2087 (1971)

[Hac79] W. Hack, H. Schacke, M. Schröter, H.Gg. Wagner, 17th Symp. on Combust., 505 (1973)

[Hac81] W. Hack, O. Horie, H.Gg. Wagner, Ber. Bunges. Phys. Chem. **85**, 72 (1981)

[Hac82] W. Hack, O. Horie, H.Gg. Wagner, J. Phys. Chem. **86**, 765 (1982)

[Hal68] C.J. Halstead, D.R. Jenkins, Chem. Phys. Lett. **2**, 281 (1968)

[Han90] J.E. Hannsen, U. Pedderson, J. Schlaug, H. Dovland, J.M. Pacyna, A. Semb, J.E. Skjelmoen, EMEP/CCC-report 2/90 (1990)

[Har92] A. Hardwiger-Fangmeier, A. Fangmeier, H.-J. Jäger, Forschungsberichte zum Forschungsprogramm des Landes Nordrhein-Westfalen „Luftverunreinigungen und Waldschäden", Nr. 28, „Ammoniak in der bodennahen Atmosphäre - Emissionen, Immissionen und Auswirkungen auf terrestrische Ökosysteme, Düsseldorf 1992

[Iof89] A.A. Ioffe, V.P. Bulatov, V.A. Lozovsky, M.Ya. Goldenberg, O.M. Sarkisov, S.Ya. Umansky, Chem. Phys. Lett. **156**(5), 425 (1989)

[Jay76] R.K.M. Jayanty, R. Simonaitis, J. Heicklen, J. Phys. Chem. **80**(5), 433 (1976)

[Koh97] J.-P. Kohlmann, D. Poppe, to be published 1997

[Lan92] A.O. Langford, F.C. Fehsenfeld, J. Zachariassen, D.S. Schimel, Global Biogeochem. Cycl. **6**, 459 (1992)

[Lee97] D.S. Lee, I. Köhler, E. Grobler, F. Rohrer, R. Sausen. L. Gallardo-Klenner, J.J.G. Olivier, F.J. Dentener, Atmos. Environ. **31**(12), 1735 (1997)

[Lin92] M.C. Lin, Y. He, C.F. Melius, Int. J. Chem. Kinet. **24**, 489 (1992)

[Log83] J.A. Logan, J. Geophys. Res. 88(C15), 10785 (1983)

[Meb95] A.M. Mebel, C.-C. Hsu, M.C. Lin, K. Morokuma, J. Chem. Phys. **103**(13), 5640 (1995)

[Meb96] A.M. Mebel, E.W.G. Diau, M.C. Lin, K. Morokuma, J. Phys. Chem. **100**, 7517 (1996)

[Meu96] H. Meunier, P. Pagsberg, A. Sillesen, Chem. Phys. Lett. **261**, 277 (1996)

[Mic85] J.V. Michael, R.B. Klemm, W.D. Brobst, S.R. Bosco, D.F. Nava, J. Phys. Chem. **89**, 3335 (1985)

[Mil90] J.A. Miller, R.J. Kee, C.J. Westbook, Annu. Rev. Phys. Chem. **41**, 345 (1990)

[Mil92] J. Miller, C.F. Melius, Symp. Int. Combust. Proc. **24**, 719 (1992)

[Möl84] W. Möller, H.Gg. Wagner, Z. Naturforsch. **39 a**, 846 (1984)

[Oka94] S. Okada, A. Tezaki, A. Miyoshi, H. Matsui, J. Chem. Phys. **101**, 9582 (1994)

[Pag79] P.B. Pagsberg, J. Eriksen, H.C. Christensen, J. Phys. Chem. **83**, 582 (1979)

[Par96] J. Park, M.C. Lin, J. Phys. Chem. **100**, 3317 (1996)

[Par97] J. Park, M.C. Lin, J. Phys. Chem. **101**(A), 2643 (1997)

[Pat84] R. Patrick, D.M. Golden, J. Phys. Chem. **88**, 491 (1984)
[Pop94] D. Poppe, Jülich 1994
[Pra85] M.J. Prather, Nature **317**, 221 (1985)
[Qua95] R.W. Quandt, J.F. Hershberger, J. Phys. Chem. **99**, 16939 (1995)
[Qua96] R.W. Quandt, J.F. Hershberger, J. Phys. Chem. **100**, 9407 (1996)
[Quo94] M. Quotschalla, „Bericht zum Spezialpraktikum Atmosphärenchemie: Auswirkungen der Ammoniakemission auf die chemische Zusammensetzung der Atmosphäre", Jülich 1994
[Sar84] O.M. Sarkisov, S.G. Cheskis, V.A. Nadtochenko, E.A. Sviridenkov, V.I. Vendeneev, Arch. Combust **4**, 111 (1984)
[Sil82] J.A. Silver, C.E. Kolb, J. Phys. Chem. **86**, 3240 (1982)
[Sot91] M.R. Soto, M. Page, M.L. McKee, Chem. Phys. **153**, 415 (1991)
[Ste82] A.W. Stelson, J.H. Seinfeld, Atmos. Environ. **16**, 983 (1982)
[Sto90] W.R. Stockwell, P. Middelton, J.S. Chang, J. Geophys. Res. **95**(D10), 16343 (1990)
[Sum96a] R. Sumathi, S.D. Peyerimhoff, Chem. Phys. Lett. **263**, 742 (1996)
[Sum96b] R. Sumathi, B. Engels, S.D. Peyerimhoff, J. Chem. Phys. **105**(18), 8117 (1996)
[Tsa91] W. Tsang, J.T. Herron, J. Phys. Chem. Ref. Data **20** (1991)
[Tyn91] G.S. Tyndall, J.J. Orlando, K.E. Nickerson, C.A. Cantrell, J.G. Calvert, J. Geophys. Res. **96**(D11), 20761 (1991)
[Wal93] S.P. Walch, J. Chem. Phys. **99**, 5295 (1993)
[War88] P. Warneck, „Chemistry of Natural Atmosphere", Int. Geophys. Ser., Vol. 41, Academic Press, San Diego (1988)
[Wol94] M. Wolf, D.L. Yang, J.L. Durant, J. Photochem. Photobiol. A: Chem. **80**, 85 (1994)
[Wol97] M. Wolf, D.L. Yang, J.L. Durant, J. Chem. Phys. **101**(A), 6243 (1997)
[Yam91] K. Yamasaki, S. Okada, M. Koshi, H. Matsui, J. Chem. Phys. **95**, 5087 (1991)
[Zel74] R. Zellner, I.W.M. Smith, Chem. Phys. Lett. **26**, 72 (1974)

# Appendix A

### *File of chemistry of the RAD-NH3 for generating the Facsimile files*

The core of the RAD-NH3 mechanism is the RADM2 mechanism from Stockwell et al. [Sto89]. The added reactions of the gas-phase degradation of $NH_3$ can be found at the end of the mechanism.

List of species:

```
  2=NO2       3=NO        4=HONO      5=NO3       6=N2O5      7=HNO4
  8=HNO3      9=O3       10=H2O2     11=SO2      12=SULF     13=CO
 14=CO2      15=H2       16=O1D      17=O3P      18=HO       19=HO2
 20=O2       21=N2       22=H2O      23=CH4      24=ETH      25=HC3
 26=HC5      27=HC8      28=OL2      29=OLT      30=OLI      31=ISO
 32=TOL      33=CSL      34=XYL      35=HCHO     36=ALD      37=KET
 38=GLY      39=MGLY     40=DCB      41=PAN      42=TPAN     43=ONIT
 44=OP1      45=OP2      46=PAA      47=ORA1     48=ORA2     49=MO2
 50=ETHP     51=HC3P     52=HC5P     53=HC8P     54=OL2P     55=OLTP
 56=OLIP     57=TOLP     58=XYLP     59=ACO3     60=KETP     61=TCO3
 62=OLN      63=XNO2     64=XO2      65=TRA      66=NH3      67=NH2
 68=NH2O     69=HNO      70=N2O      71=NH       72=NHOH     73=NH3O
 74=NAC
```

Reactions 1 - 157 RADM2 from Stockwell et al. [Sto90]

```
  001  P1  NO2      -->  O3P + NO
      9.18e-3 * PHOT(0.256d0,zenith)
002  P2  O3       -->  O1D + O2
      3.18e-5 * PHOT(2.092d0,zenith)
003  P3  O3       -->  O3P + O2
      4.82e-4 * PHOT(1.00d0,zenith)
004  P4  HONO     -->  HO + NO
      1.66e-3 * PHOT(1.00d0,zenith)
005  P5  HNO3     -->  HO + NO2
      4.42e-7 * PHOT(1.00d0,zenith)
006  P6  HNO4     -->  HO2 + NO2
      6.58e-6 * PHOT(1.00d0,zenith)
007  P7  NO3      -->  NO + O2
      2.20e-2 * PHOT(0.0388d0,zenith)
008  P8  NO3      -->  NO2 + O3P
      1.80e-1 * PHOT(0.0388d0,zenith)
009  P9  H2O2     -->  2 HO
      7.56e-6 * PHOT(0.506d0,zenith)
010 P10  HCHO     -->  H2 + CO
      4.20e-5 * PHOT(0.393d0,zenith)
011 P11  HCHO     -->  2 HO2 + CO
      3.50e-5 * PHOT(0.601d0,zenith)
012 P12  ALD      -->  MO2 + HO2 + CO
      5.24e-6 * PHOT(1.00d0,zenith)
013 P13  OP1      --> HCHO + HO2 + HO
      7.36e-6 * PHOT(1.00d0,zenith)
014 P14  OP2      --> ALD + HO2 + HO
      7.36e-6 * PHOT(1.00d0,zenith)
015 P15  PAA      --> MO2 + CO2 + HO
      2.11e-6 * PHOT(1.00d0,zenith)
```

```
016 P16  KET      --> ACO3 + ETHP
      9.17e-7 * PHOT(1.00d0,zenith)
017 P17  GLY      --> 0.13 HCHO + 1.87 CO
      5.70e-5 * PHOT(1.00d0,zenith)
018 P18  GLY      --> 0.45 HCHO + 1.55 CO + 0.80 HO2
      6.76e-5 * PHOT(1.00d0,zenith)
019 P19  MGLY     --> ACO3 + HO2 + CO
      2.48e-4 * PHOT(1.00d0,zenith)
020 P20  DCB      --> 0.98 HO2 + TCO3 + 0.02 ACO3
      9.81e-5 * PHOT(1.00d0,zenith)
021 P21  ONIT     --> 0.20 ALD + 0.80 KET + HO2 + NO2
      1.21e-6 * PHOT(1.00d0,zenith)
022 T1   O3P + NO2 --> NO + O2
      6.50E-12 * EXP(   120. / T )
023   T2 O1D + N2 --> O3P + N2
      1.80E-11 * EXP(   110. / T )
024   T3 O1D + O2 --> O3P + O2
      3.20E-11 * EXP(    70. / T )
025   T4 O1D + H2O --> 2 HO
      2.20E-10
026   T5 O3 + NO --> NO2 + O2
      2.00E-12 * EXP( -1400. / T )
027   T6 O3 + HO --> HO2 + O2
      1.60E-12 * EXP(  -940. / T )
028   T7 O3 + HO2 --> HO + 2 O2
      1.10E-14 * EXP(  -500. / T )
029   T8 HO2 + NO --> NO2 + HO
      3.70E-12 * EXP(   240. / T )
030   T9 H2O2 + HO --> HO2 + H2O
      3.30E-12 * EXP(  -200. / T )
031  T10 NO + NO + O2 --> NO2 + NO2
      3.30E-39 * EXP(  530. / T )
032  T11 O3 + NO2 --> NO3
      1.40E-13 * EXP( -2500. / T )
033  T12 NO3 + NO --> NO2 + NO2
      1.70E-11 * EXP(   150. / T )
034  T13 NO3 + NO2 --> NO + NO2 + O2
      2.50E-14 * EXP( -1230. / T )
035  T14 NO3 + HO2 --> HNO3 + O2
      2.50E-12
036  T15 N2O5 + H2O --> 2 HNO3
      2.00E-21
037  T16 HO + HNO4 --> NO2 + H2O + O2
      1.30E-12 * EXP(  380. / T )
038  T17 HO + HO2 --> H2O + O2
      4.60E-11 * EXP(  230. / T )
039  T18 CH4 + HO --> MO2 + H2O
      T * T * 6.95E-18 * EXP( -1280. / T )
040  T19 ETH + HO --> ETHP + H2O
      T * T *1.37E-17 * EXP(  -444. /T )
041  T20 HC3 + HO --> 0.83 HC3P + 0.17 HO2 + 0.009 HCHO +
                --> 0.075 ALD + 0.025 KET + H2O
      1.59E-11 * EXP(  -540. / T )
042  T21 HC5 + HO --> HC5P + 0.25 XO2 + H2O
      1.73E-11 * EXP(  -380. / T )
043  T22 HC8 + HO --> HC8P + 0.75 XO2 + H2O
      3.64E-11 * EXP(  -380. / T )
044  T23 OL2 + HO --> OL2P
      2.15E-12 * EXP( 411. / T )
```

```
045  T24 OLT + HO --> OLTP
      5.32E-12 * EXP(   504. / T )
046  T25 OLI + HO --> OLIP
      1.07E-11 * EXP(  549. / T )
047  T26 TOL + HO --> 0.75 TOLP + 0.25 CSL + 0.25 HO2
      2.10E-12 * EXP(  322. / T )
048  T27 XYL + HO --> 0.83 XYLP + 0.17 CSL + 0.17 HO2
      1.89E-11 * EXP(  116. / T )
049  T28 CSL + HO --> 0.1 HO2 + 0.9 XO2 + 0.9 TCO3 + -0.9 HO
      4.00E-11
050  T29 HCHO + HO --> HO2 + CO + H2O
      9.00E-12
051  T30 ALD + HO --> ACO3 + H2O
      6.87E-12 * EXP(  256. / T )
052  T31 KET + HO --> KETP + H2O
      1.20E-11 * EXP(  -745. / T )
053  T32 GLY + HO --> HO2 + 2 CO + H2O
      1.15E-11
054  T33 MGLY + HO --> ACO3 + CO + H2O
      1.70E-11
055  T34 DCB + HO --> TCO3 + H2O
      2.8E-11
056  T35 OP1 + HO --> 0.5 MO2 + 0.5 HCHO + 0.5 HO
      1.00E-11
057  T36 OP2 + HO --> 0.5 HC3P + 0.5 ALD + 0.5 HO
      1.00E-11
058  T37 PAA + HO --> ACO3 + H2O
      1.00E-11
059  T38 PAN + HO --> HCHO + NO3 + XO2
      T * T * 6.85E-18 * EXP(  -444. / T )
060  T39 ONIT + HO --> HC3P + NO2
      1.55E-11 * EXP(  -540. / T )
061  T40 ISO + HO --> OLTP
      2.55E-11 * EXP(   409. / T )
062  T41 ACO3 + NO2 --> PAN
      2.80E-12 * EXP(  181. / T )
063  T42 PAN --> ACO3 + NO2
      1.95E+16 * EXP(-13543. / T )
064  T43 TCO3 + NO2 --> TPAN
      4.7E-12
065  T44 TPAN --> TCO3 + NO2
      1.95E16 * EXP(-13543. / T )
066  T45 MO2 + NO --> HCHO + HO2 + NO2
      4.20E-12 * EXP(  180. / T )
067  T46 HC3P + NO --> 0.75 ALD + 0.25 KET + 0.09 HCHO +
                --> 0.036 ONIT + 0.964 NO2 + 0.964 HO2
      4.20E-12 * EXP(  180. / T )
068  T47 HC5P + NO --> 0.38 ALD + 0.69 KET + 0.08 ONIT +
                --> 0.92 NO2 + 0.92 HO2
      4.20E-12 * EXP(  180. / T )
069  T48 HC8P + NO --> 0.35 ALD + 1.06 KET + 0.04 HCHO +
                --> 0.24 ONIT + 0.76 NO2 + 0.76 HO2
      4.20E-12 * EXP(  180. / T )
070  T49 OL2P + NO --> 1.6 HCHO + HO2 + NO2 + 0.2 ALD
      4.20E-12 * EXP(  180. / T )
071  T50 OLTP + NO --> ALD + HCHO + HO2 + NO2
      4.20E-12 * EXP(  180. / T )
072  T51 OLIP + NO --> HO2 + 1.45 ALD + 0.28 HCHO + 0.10 KET + NO2
      4.20E-12 * EXP(  180. / T )
```

```
073  T52 ACO3 + NO --> MO2 + NO2
      4.20E-12 * EXP(  180. / T )
074  T53 TCO3 + NO --> NO2 + 0.92 HO2 + 0.89 GLY + 0.11 MGLY +
                --> 0.05 ACO3 + 0.95 CO + 2 XO2
      4.20E-12 * EXP(  180. / T )
075  T54 TOLP + NO --> NO2 + HO2 + 0.17 MGLY + 0.16 GLY + 0.70 DCB
      4.20E-12 * EXP(  180. / T )
076  T55 XYLP + NO --> NO2 + HO2 + 0.45 MGLY + 0.806 DCB
      4.20E-12 * EXP(  180. / T )
077  T56 ETHP + NO --> ALD + HO2 + NO2
      4.20E-12 * EXP(  180. / T )
078  T57 KETP + NO --> MGLY + NO2 + HO2
      4.20E-12 * EXP(  180. / T )
079  T58 OLN  + NO --> HCHO + ALD + 2 NO2
      4.20E-12 * EXP(  180. / T )
080  T59 HCHO + NO3 --> HO2 + HNO3 + CO
      6.00E-13 * EXP( -2058. / T )
081  T60 ALD + NO3 --> ACO3 + HNO3
      1.40E-12 * EXP(  -1900. / T)
082  T61 GLY + NO3 --> HNO3 + HO2 + 2 CO
      6.00E-13 * EXP( -2058. / T )
083  T62 MGLY + NO3 --> HNO3 + ACO3 + CO
      1.40E-12 * EXP(  -1900. / T)
084  T63 DCB + NO3 --> HNO3 + TCO3
      1.40E-12 * EXP(  -1900. / T)
085  T64 CSL + NO3 --> HNO3 + XNO2 + 0.5 CSL
      2.20E-11
086  T65 OL2 + NO3 --> OLN
      2.00E-12 * EXP(  -2923. / T )
087  T66 OLT + NO3 --> OLN
      1.00E-11 * EXP( -1895. / T )
088  T67 OLI + NO3 --> OLN
      3.23E-11 * EXP( -975. / T )
089  T68 ISO + NO3 --> OLN
      5.81E-13
090  T69 OL2 + O3 --> HCHO + 0.42 CO + 0.4 ORA1 + 0.12 HO2
      1.20E-14 * EXP( -2633. / T )
091  T70 OLT + O3 --> 0.53 HCHO + 0.50 ALD + 0.33 CO + 0.20 ORA1 +
                --> 0.20 ORA2 + 0.23 HO2 + 0.22 MO2 + 0.10 HO +
                --> 0.06 CH4
      1.32E-14 * EXP( -2105. / T )
092  T71 OLI + O3 --> 0.18 HCHO + 0.72 ALD + 0.10 KET + 0.23 CO +
                --> 0.06 ORA1 + 0.29 ORA2 + 0.09 CH4 + 0.26 HO2 +
                --> 0.14 HO + 0.31 MO2
      7.29E-15 * EXP( -1136. / T )
093  T72 ISO + O3 --> 0.53 HCHO + 0.50 ALD + 0.33 CO + 0.20 ORA1 +
                --> 0.20 ORA2 + 0.23 HO2 + 0.22 MO2 + 0.10 HO
      1.23E-14 * EXP( -2013. / T )
094  T73 HO2 + MO2 --> OP1
      7.70E-14 * EXP( 1300. / T )
095  T74 HO2 + ETHP --> OP2
      7.70E-14 * EXP( 1300. / T )
096  T75 HO2 + HC3P --> OP2
       7.70E-14 * EXP( 1300. / T )
097  T76 HO2 + HC5P --> OP2
       7.70E-14 * EXP( 1300. / T )
098  T77 HO2 + HC8P --> OP2
       7.70E-14 * EXP( 1300. / T )
099  T78 HO2 + OL2P --> OP2
```

```
      7.70E-14 * EXP( 1300. / T )
100   T79 HO2 + OLTP --> OP2
      7.70E-14 * EXP( 1300. / T )
101   T80 HO2 + OLIP --> OP2
      7.70E-14 * EXP( 1300. / T )
102   T81 HO2 + KETP --> OP2
      7.70E-14 * EXP( 1300. / T )
103   T82 HO2 + ACO3 --> PAA
      7.70E-14 * EXP( 1300. / T )
104   T83 HO2 + TOLP --> OP2
      7.70E-14 * EXP( 1300. / T )
105   T84 HO2 + XYLP --> OP2
      7.70E-14 * EXP( 1300. / T )
106   T85 HO2 + TCO3 --> OP2
      7.70E-14 * EXP( 1300. / T )
107   T86 HO2 + OLN  --> ONIT
      7.70E-14 * EXP( 1300. / T )
108   T87 MO2 + MO2 --> 1.5 HCHO + HO2
      1.90E-13 * EXP(  220. / T )
109   T88 MO2 + ETHP --> 0.75 HCHO + HO2 + 0.75 ALD
      1.40E-13 * EXP(  220. / T )
110   T89 MO2 + HC3P --> 0.84 HCHO + HO2 + 0.77 ALD + 0.26 KET
      4.20E-14 * EXP(  220. / T )
111   T90 MO2 + HC5P --> 0.77 HCHO + HO2 + 0.41 ALD + 0.75 KET
      3.40E-14 * EXP(  220. / T )
112   T91 MO2 + HC8P --> 0.80 HCHO + HO2 + 0.46 ALD + 1.39 KET
      2.90E-14 * EXP(  220. / T )
113   T92 MO2 + OL2P --> 1.55 HCHO + HO2 + 0.35 ALD
      1.40E-13 * EXP(  220. / T )
114   T93 MO2 + OLTP --> 1.25 HCHO + HO2 + 0.75 ALD
      1.40E-13 * EXP(  220. / T )
115   T94 MO2 + OLIP --> 0.89 HCHO + HO2 + 0.725 ALD + 0.55 KET
      1.70E-14 * EXP(  220. / T )
116   T95 MO2 + KETP --> 0.75 HCHO + HO2 + 0.75 MGLY
      1.70E-14 * EXP(  220. / T )
117   T96 MO2 + ACO3 --> HCHO + 0.5 HO2 + 0.5 MO2 + 0.5 ORA2
      9.60E-13 * EXP(  220. / T )
118   T97 MO2 + TOLP --> HCHO + 2 HO2 + 0.17 MGLY + 0.16 GLY + 0.70 DCB
      1.70E-14 * EXP(  220. / T )
119   T98 MO2 + XYLP --> HCHO + 2 HO2 + 0.45 MGLY + 0.806 DCB
      1.70E-14 * EXP(  220. / T )
120   T99 MO2 + TCO3 --> 0.50 HCHO + 0.50 ORA2 + 0.460 HO2 + 0.445 GLY +
                  --> 0.055 MGLY + 0.025 ACO3 + 0.475 CO + XO2
      9.60E-13 * EXP( 220. / T )
121 T100 MO2 + OLN  --> 1.75 HCHO + 0.5 HO2 + ALD + NO2
      1.70E-14 * EXP(  220. / T )
122 T101 ETHP + ACO3 --> ALD + 0.5 HO2 + 0.5 MO2 + 0.5 ORA2
      3.40E-13 * EXP(  220. / T )
123 T102 HC3P + ACO3 --> 0.77 ALD + 0.26 KET + 0.5 HO2 + 0.5 MO2 +
                  --> 0.5 ORA2
      1.00E-13 * EXP(  220. / T )
124 T103 HC5P + ACO3 --> 0.41 ALD + 0.75 KET + 0.5 HO2 + 0.5 MO2 +
                  --> 0.5 ORA2
      8.40E-14 * EXP(  220. / T )
125 T104 HC8P + ACO3 --> 0.46 ALD + 1.39 KET + 0.5 HO2 + 0.5 MO2 +
                     0.5 ORA2
      7.20E-14 * EXP(  220. / T )
126 T105 OL2P + ACO3 --> 0.8 HCHO + 0.6 ALD + 0.5 HO2 + 0.5 MO2 +
                     0.5 ORA2
```

```
      3.40E-13 * EXP(  220. / T )
127 T106 OLTP + ACO3 --> ALD + 0.5 HCHO + 0.5 HO2 + 0.5 MO2 + 0.5 ORA2
      3.40E-13 * EXP(  220. / T )
128 T107 OLIP + ACO3 --> 0.725 ALD + 0.55 KET + 0.14 HCHO + 0.5 HO2 +
                  --> 0.50 MO2 + 0.50 ORA2
      4.20E-14 * EXP(  220. / T )
129 T108 KETP + ACO3 --> MGLY + 0.5 HO2 + 0.5 MO2 + 0.5 ORA2
      4.20E-14 * EXP(  220. / T )
130 T109 ACO3 + ACO3 --> 2 MO2
      1.19E-12 * EXP(  220. / T )
131 T110 ACO3 + TOLP --> MO2 + 0.17 MGLY + 0.16 GLY + 0.7 DCB + HO2
      4.20E-14 * EXP(  220. / T )
132 T111 ACO3 + XYLP --> MO2 + 0.45 MGLY + 0.806 DCB + HO2
      4.20E-14 * EXP(  220. / T )
133 T112 ACO3 + TCO3 --> MO2 + 0.92 HO2 + 0.89 GLY + 0.11 MGLY +
                  --> 0.05 ACO3 + 0.95 CO + 2 XO2
      1.19E-12 * EXP(  220. / T )
134 T113 ACO3 + OLN  --> HCHO + ALD + 0.5 ORA2 + NO2 + 0.5 MO2
      4.20E-14 * EXP(  220. / T )
135 T114 OLN + OLN --> 2 HCHO + 2 ALD + 2 NO2
      3.60E-16 * EXP(  220. / T )
136 T115 XO2 + HO2 --> OP2
      7.70E-14 * EXP( 1300. / T )
137 T116 XO2 + MO2 --> HCHO + HO2
      1.70E-14 * EXP(  220. / T )
138 T117 XO2 + ACO3 --> MO2
      4.20E-14 * EXP(  220. / T )
139 T118 XO2 + XO2 -->
      3.60E-16 * EXP(  220. / T )
140 T119 XO2 + NO --> NO2
      4.20E-12 * EXP(  180. / T )
141 T120 XNO2 + NO2 --> ONIT
      4.20E-12 * EXP(  180. / T )
142 T121 XNO2 + HO2 --> OP2
      7.70E-14 * EXP( 1300. / T )
143 T122 XNO2 + MO2 --> HCHO + HO2
      1.70E-14 * EXP(  220. / T )
144 T123 XNO2 + ACO3 --> MO2
      4.20E-14 * EXP(  220. / T )
145 T124 XNO2 + XNO2 -->
      3.60E-16 * EXP(  220. / T )
146 TR1  HO2 + NO2 --> HNO4
      TROE( 1.8D-31, 3.2d0, 4.7D-12, 1.4d0, M, T )
147 TR2  NO + HO --> HONO
      TROE( 7.0d-31, 2.6d0, 1.5d-11, 0.5d0, M, T )
148 TR3  NO3 + NO2 --> N2O5
      TROE( 2.2d-30, 4.3d0, 1.5d-12, 0.5d0, M, T )
149 TR4  HO + NO2 --> HNO3
      TROE( 2.6d-30, 3.2d0, 2.4d-11, 1.3d0, M, T )
150 TR5  HO + SO2 --> SULF + HO2
      TROE( 3.0d-31, 3.3d0, 1.5d-12, 0.0d0, M, T )
151  E1  HNO4 --> HO2 + NO2
      EQT(1.8d-31,3.2d0,4.7d-12,1.4d0,M,T,4.76d+26,10900.d0)
152  E2  N2O5 --> NO2 + NO3
      EQT(2.2d-30,4.3d0,1.5d-12,0.5d0,M,T,9.09d+26,11200.d0)
153  S1  O3P + O2 --> O3
      M * 6.0E-34 * (T/300.)**(-2.3)
154  S2  HO2 + HO2 --> H2O2
      2.2E-13 * EXP(620./T) + 1.9E-33 * M * EXP(980./T)
```

```
155  S3  HO2 + HO2 + H2O --> H2O2 + H2O
      3.08d-34*EXP(2820./T)+2.66d-54*M*EXP(3180./T)
156  S4  HO + HNO3 --> NO3 + H2O
      SPEZ(7.2d-15,785.d0,4.1d-16,1440.d0,1.9d-33,725.d0,M,T)
157  S5  CO + HO --> HO2 + CO2
      1.5E-13 * ( 1.0 + 2.439E-20 * M )
158      ISO-Source
      0
```

## Additional reactions 159 - 184 for the gas-phase degradation of $NH_3$

```
159  Z1   NH3 + HO --> H2O + NH2
      1.7E-12 * EXP(-710/T)
160  Z2   NH2 + O3 --> NH2O
      4.3E-12 * EXP(-930/T)
161  Z3   NH2 + HO2 --> NH2O + HO
      4.8E-7 * T**(-1.32)* EXP(-628/T)
162  Z4   NH2 + HO2 --> HNO + H2O
      9.4E-9 * T**(-1.12)* EXP(-356/T)
163  Z5   NH2 + HO2 --> NH3
      2.7E-20 * T**(1.55)* EXP(-1020/T)
164  Z6   NH2 + NO --> HO + HO2
      0.12 * 1.6E-11 * (T/298)**(-1.5)
165  Z7   NH2 + NO --> H2O
      0.88 * 1.6E-11 * (T/298)**(-1.5)
166  Z8   NH2 + NO2 --> N2O + H2O
      0.6 * 2.0E-11 * (T/298)**(-2.0)
167  Z9   NH2 + NO2 --> NH2O + NO
      0.4 * 2.0E-11 * (T/298)**(-2.0)
168 Z10  NH2 + HO --> H2O + NH
      7.7E-13 * (T/298)**1.5 * EXP(230/T)
169 Z11  NH2 + HO --> O3 + NH3
      3.31E-13 * (T/298)**0.41 * EXP(-250/T)
170 Z12  NH2O + O3 --> NH2
      1.2E-14
171 Z12  NH2O --> NHOH
      1.3E3
172 Z14  NH + O2 --> NO + HO
      1.09E-14 * (T/298)**1.5 * EXP(-50/T)
173 Z15  NH + NO --> HO
      4.9E-11
174 Z16  HNO + HO --> NO + H2O
      8E-11 * EXP(-500/T)
175 Z17  HNO + NHOH --> NH3O + NO
      1.66E-12 * EXP(-1500/T)
176 Z18  HNO + HNO --> N2O + H2O
      4.24E-17 * (T/298)**3.98 * EXP(-600/T)
177 Z19  HNO + HNO --> NAC
      6.64E-15 * EXP(-270/T)
178 Z20  HNO + HNO --> NAC
      3.02E-14 * (T/298)**(-2.4) * EXP(-590/T)
179 Z21  NAC --> N2O + H2O
      4.3E11 * EXP(-8250/T)
180 Z22  HNO + NO2 --> HONO + NO
      1.E-12 * EXP(-1000/T)
181 Z23  NHOH + HO --> HNO + H2O
      1.66E-12
182 Z24  HONO + HO --> NO2 + H2O
      1.8E-11 * EXP(-390/T)
```

```
183 Z25  NH3O + HO --> NHOH + H2O
      4.13E-11 * EXP(-2138/T)
184 Z26  HNO + O2 --> HO2 + NO
      3.65E-14 * EXP(-4600/T)
CEND OF MECHANISM
```

# Appendix B

## *Facsimile input file*

In the Facsimile file controls the calculations of the time dependence of the concentration. The calculation of the rate constants is done by the subroutine usubr4 which calls the subroutine *reak*. For the analysis the subroutine *usubr5* creates a file in the binary *LISTEN*-format.
The Facsimile file writes output to the following files:

- selected concentrations and rates to the file '*nh3.zeichn*' (format: *zeichn*) in the routine *table*
- selected concentrations, production and destruction rates as well as rates of selected reactions to the file '*nh3.um*'
- concentrations, rate constants as well as production and destruction rates of all reactions to the file '*nh3.LISTEN*' (format: *LISTEN*)

The logical end of each line is ';' in the Facsimile language. Lines containing comments start with '*'.

```
* INPUT FUER FAKSIMILE-PAKET FUER CHEMIE : nh3-nn
* mit Unterprogramm usubr4 zur Berechnung der k's;
* mit Einlesen der Anfangsbedingungen aus File inifac.con;
* in inifac.con stehen T, p, sowie Konzentrationen in Mischungsverhältnis
  sen;
* mit Unterprogramm usubr5 zur Erzeugung von binärem output;

 VARIABLE
  NO2   NO    HONO  NO3   N2O5  HNO4  HNO3  O3    H2O2  SO2   SULF  CO
  CO2   H2    O1D   O3P   HO    HO2   O2    N2    H2O   CH4   ETH   HC3
  HC5   HC8   OL2   OLT   OLI   ISO   TOL   CSL   XYL   HCHO  ALD   KET
  GLY   MGLY  DCB   PAN   TPAN  ONIT  OP1   OP2   PAA   ORA1  ORA2  MO2
  ETHP  HC3P  HC5P  HC8P  OL2P  OLTP  OLIP  TOLP  XYLP  ACO3  KETP  TCO3
  OLN   XNO2  XO2   TRA   NH3   NH2   NH2O  HNO   N2O   NH    NHOH  NH3O
  NAC;

 PARAMETER
V1 V2 V3 V4 V5 V6 V7 V8 V9 V10 V11 V12 V13 V14 V15 V16 V17 V18
V19 V20 V21 V22 V23 V24 V25 V26 V27 V28 V29 V30 V31 V32 V33
V34 V35 V36 V37 V38 V39 V40 V41 V42 V43 V44 V45 V46 V47 V48
V49 V50 V51 V52 V53 V54 V55 V56 V57 V58 V59 V60 V61 V62 V63
V64 V65 V66 V67 V68 V69 V70 V71 V72 V73 V74 V75 V76 V77 V78
V79 V80 V81 V82 V83 V84 V85 V86 V87 V88 V89 V90 V91 V92 V93
V94 V95 V96 V97 V98 V99 V100 V101 V102 V103 V104 V105 V106 V107
V108 V109 V110 V111 V112 V113 V114 V115 V116 V117 V118 V119
V120 V121 V122 V123 V124 V125 V126 V127 V128 V129 V130 V131
V132 V133 V134 V135 V136 V137 V138 V139 V140 V141 V142 V143
V144 V145 V146 V147 V148 V149 V150 V151 V152 V153 V154 V155
V156 V157 V158 V159 V160 V161 V162 V163 V164 V165 V166 V167
V168 V169 V170 V171 V172 V173 V174 V175 V176 V177 V178 V179
```

```
V180 V181 V182 V183 V184  ;

* nconc und nreak enthalten Zahl der Substanzen bzw. Reaktionen
 +1, da erstes Element 0 ist, erste Substanz aber Element 1,
 fuer Uebergabe an Unterprogramme usubr4 und 5;
integer #nconc 75 #nreak 185;
PARAMETER <#nconc> C P D;
PARAMETER <#nreak>  R;
parameter <12> con;
parameter <6> con1;

* in t_aufruf steht t [s] fuer Ausgabe in zeichn-Datei;
parameter t_aufruf 360;
* in t1_aufruf steht t [s] fuer Ausgabe in um-Datei;
parameter t1_aufruf 36000;
* in b_aufruf steht t [s] fuer Ausgabe in LISTEN-Datei;
parameter b_aufruf 36000;
* in laufzeit steht t [s] fuer gesamten Facsimilelauf;
parameter laufzeit 360000;
* in #X_mal steht die Zahl der Wiederholungen der Aufrufe;
integer #t_mal #t1_mal #b_mal #zaehler;
parameter zeitquotient z_kontroll;

parameter einleser dumm -12345 dumo -12345 jein -12345;
* parameter ablX als Zwischenablage, #umkanal ist Kanalnummer,
 auf der das file mit der Endung um geschrieben wird;
parameter abl1 abl2 abl3 abl4 abl5;
integer #umkanal;
PARAMETER MEDI TEMP M T CHI CHIGR RR PP NL PI HE 1.;
* Zum Einlesen der Startbedingungen aus Datei inifac.con;
* Zahl der Feldeintraege steht in inza;
integer #inza ;
* In Datei inifac.con ist M nicht enhalten, erstes benutztes
  Element ist 0;
exec #inza=73;
parameter <#inza> feld ;

compile instant;
* hier werden die im Programm verwendeten Ausgabefiles geoeffnet;
* inifac.con wird hier nicht geoeffnet, da es moeglicherweise mehrmals
  gelesen werden muss. Dies wird in der Routine Start erledigt
  in *.out steht zeichn-Format, in *.dat ist origin input;
open 8 "nh3.zeichn ";
open 10 "nh3.um";
* dieses File wird von usubr5 benoetigt, um die binaeren Daten zu
  speichern;
 open 11 "nh3.LISTEN" unformatted;
**;

compile instant;
hmax 6;
* Berechnung der Zeitschritte und Wiederholungen fuer die einzelnen
  Ausgaben;
zeitquotient = laufzeit/k_aufruf ;
zeitquotient = laufzeit/t_aufruf;
#t_mal=nint(zeitquotient);
zeitquotient =laufzeit/t1_aufruf ;
#t1_mal=nint(zeitquotient);
zeitquotient = laufzeit/b_aufruf;
```

```
#b_mal=nint(zeitquotient);
z_kontroll=laufzeit-k_aufruf;
**;

compile instant;
*Bestimmung von pi auf 15 Nachkommastellen;
PI = 4*artan(1);
* CHI in Teilen von PI, hier 30 grad;
CHI = (30/180)*PI;
RR = 8.314e4;
NL = 6.022e23;
**;

 COMPILE START;
* Einlesen von T, p und der Startkonzentrationen aus File ;
open 3 "inifac.con";
read 3 einleser;
T = einleser;
read 3 einleser;
PP = einleser;
 M = (PP * NL) / (RR * T);
* Nach T und p stehen die Mischungsverhaeltnisse im File;
do 1 for #1 = 0 (1) #inza;
 read 3 einleser;
 feld <#1> = einleser;
label 1;
close 3;
 In feld liegen die Mischungsverhaeltnisse der Substanzen;
 NO2  =  feld <0> * M;
 NO   =  feld <1> * M;
 HONO =  feld <2> * M;
 NO3  =  feld <3> * M;
 N2O5 =  feld <4> * M;
 HNO4 =  feld <5> * M;
 HNO3 =  feld <6> * M;
 O3   =  feld <7> * M;
 H2O2 =  feld <8> * M;
 SO2  =  feld <9> * M;
 SULF =  feld <10> * M;
 CO   =  feld <11> * M;
 CO2  =  feld <12> * M;
 H2   =  feld <13> * M;
 TRA  =  feld <14> * M;
 HC   =  feld <15> * M;
 HO   =  feld <16> * M;
 HO2  =  feld <17> * M;
 O2   =  feld <18> * M;
 N2   =  feld <19> * M;
 H2O  =  feld <20> * M;
 CH4  =  feld <21> * M;
 ETH  =  feld <22> * M;
 HC3  =  feld <23> * M;
 HC5  =  feld <24> * M;
 HC8  =  feld <25> * M;
 OL2  =  feld <26> * M;
 OLT  =  feld <27> * M;
 OLI  =  feld <28> * M;
 ISO  =  feld <29> * M;
 TOL  =  feld <30> * M;
```

```
 CSL   =  feld <31> * M;
 XYL   =  feld <32> * M;
 HCHO  =  feld <33> * M;
 ALD   =  feld <34> * M;
 KET   =  feld <35> * M;
 GLY   =  feld <36> * M;
 MGLY  =  feld <37> * M;
 DCB   =  feld <38> * M;
 PAN   =  feld <39> * M;
 TPAN  =  feld <40> * M;
 ONIT  =  feld <41> * M;
 OP1   =  feld <42> * M;
 OP2   =  feld <43> * M;
 PAA   =  feld <44> * M;
 ORA1  =  feld <45> * M;
 ORA2  =  feld <46> * M;
 MO2   =  feld <47> * M;
 ETHP  =  feld <48> * M;
 HC3P  =  feld <49> * M;
 HC5P  =  feld <50> * M;
 HC8P  =  feld <51> * M;
 OL2P  =  feld <52> * M;
 OLTP  =  feld <53> * M;
 OLIP  =  feld <54> * M;
 TOLP  =  feld <55> * M;
 XYLP  =  feld <56> * M;
 ACO3  =  feld <57> * M;
 KETP  =  feld <58> * M;
 TCO3  =  feld <59> * M;
 OLN   =  feld <60> * M;
 XNO2  =  feld <61> * M;
 XO2   =  feld <62> * M;
 NH3   =  feld <63> * M;
 NH2   =  feld <64> * M;
 NH2O  =  feld <65> * M;
 HNO   =  feld <66> * M;
 N2O   =  feld <67> * M;
 NH    =  feld <68> * M;
 NHOH  =  feld <69> * M;
 NH3O  =  feld <70> * M;
 NAC   =  feld <71> * M;
 O3P   =  feld <72> * M;
 O1D   =  feld <73> * M;
**;

 COMPILE REAKTIONSKONSTANTEN;
* Verzweigung in Unterroutine usubr4 zur Berechnung
  der Geschwindigkeitskonstanten abhaengig von T, Chi
  und time
  in con werden T, P, CHI und time uebergeben, sowie Konzentrationen
  einiger Stoffe (H2O, NO2, NO3, O3, O2, N2, M), die zur Berechnung
  benoetigt werden, und die Zahl der Reaktionen nreak und Konzentrationen
  nconc;
con<0> = T;
con<1> = PP;
con<2> = CHI;
con<3> = time;
con<4> = H2O;
con<5> = NO2;
```

```
con<6> = NO3;
con<7> = O3;
con<8> = M;
con<9> = O2;
con<10> = N2;
con<11> = float(#nconc)-1;
con<12> = float(#nreak)-1;
* hier kommt die Verzweigung ins Unterprogramm;
enter R con dumm dumo;
* Nach Rueckkehr aus USUBR4 geaenderte CON uebernehmen;
T = con<0> ;
PP = con<1> ;
CHI = con<2> ;
* Neuberechnung von [M], [O2] und [N2];
M = (PP * NL) / (RR * T);
* Errechnen von [O2] und [N2] aus [M];
O2=0.2095*M;
N2=0.7809*M;
**;

compile bi_naer;
* Hier werden die Ergebnisse binaer abgespeichert, z.B. als Input
  fuer Programme wie Diag.;
 C<1>  = M  ;
 C<2> =NO2  ;
 C<3> =NO   ;
 C<4> =HONO ;
 C<5> =NO3  ;
 C<6> =N2O5 ;
 C<7> =HNO4 ;
 C<8> =HNO3 ;
 C<9> =O3   ;
 C<10> =H2O2 ;
 C<11> =SO2  ;
 C<12> =SULF ;
 C<13> =CO   ;
 C<14> =CO2  ;
 C<15> =H2   ;
 C<16> =O1D  ;
 C<17> =O3P  ;
 C<18> =HO   ;
 C<19> =HO2  ;
 C<20> =O2   ;
 C<21> =N2   ;
 C<22> =H2O  ;
 C<23> =CH4  ;
 C<24> =ETH  ;
 C<25> =HC3  ;
 C<26> =HC5  ;
 C<27> =HC8  ;
 C<28> =OL2  ;
 C<29> =OLT  ;
 C<30> =OLI  ;
 C<31> =ISO  ;
 C<32> =TOL  ;
 C<33> =CSL  ;
 C<34> =XYL  ;
 C<35> =HCHO ;
 C<36> =ALD  ;
```

```
 C<37> =KET  ;
 C<38> =GLY  ;
 C<39> =MGLY ;
 C<40> =DCB  ;
 C<41> =PAN  ;
 C<42> =TPAN ;
 C<43> =ONIT ;
 C<44> =OP1  ;
 C<45> =OP2  ;
 C<46> =PAA  ;
 C<47> =ORA1 ;
 C<48> =ORA2 ;
 C<49> =MO2  ;
 C<50> =ETHP ;
 C<51> =HC3P ;
 C<52> =HC5P ;
 C<53> =HC8P ;
 C<54> =OL2P ;
 C<55> =OLTP ;
 C<56> =OLIP ;
 C<57> =TOLP ;
 C<58> =XYLP ;
 C<59> =ACO3 ;
 C<60> =KETP ;
 C<61> =TCO3 ;
 C<62> =OLN  ;
 C<63> =XNO2 ;
 C<64> =XO2  ;
 C<65> =TRA  ;
 C<66> =NH3  ;
 C<67> =NH2  ;
 C<68> =NH2O ;
 C<69> =HNO  ;
 C<70> =N2O  ;
 C<71> =NH   ;
 C<72> =NHOH ;
 C<73> =NH3O ;
 C<74> =NAC  ;
* in con1 stehen fuer Ausgabe benoetigte Bedingungen;
con1<0>=time;
con1<1>=CHIGR;
con1<2>=T;
con1<3>=HE;
con1<4>=jein;
con1<5> = float(#nconc)-1;
con1<6> = float(#nreak)-1;
* P- und D-Term fuer Stoff 1 (Luft) sind 0;
P<1>=0.;
D<1>=0.;
open 3 "inifac.con";
rewind 3;
* in usubr5 wird binaer geschrieben;
enter con1 C R P D;
* jein dient zur Ueberpruefung, ob schon binaer geschrieben wurde, da
  Kopf des Files nur einmal benoetigt wird (nicht: jein=-12345,
  geschrieben: jein=12345);
jein=12345;
close 3;
**;
```

```
 COMPILE EQUATIONS;

V1 =R<1>*NO2;
V2 =R<2>*O3;
V3 =R<3>*O3;
V4 =R<4>*HONO;
V5 =R<5>*HNO3;
V6 =R<6>*HNO4;
V7 =R<7>*NO3;
V8 =R<8>*NO3;
V9 =R<9>*H2O2;
V10 =R<10>*HCHO;
V11 =R<11>*HCHO;
V12 =R<12>*ALD;
V13 =R<13>*OP1;
V14 =R<14>*OP2;
V15 =R<15>*PAA;
V16 =R<16>*KET;
V17 =R<17>*GLY;
V18 =R<18>*GLY;
V19 =R<19>*MGLY;
V20 =R<20>*DCB;
V21 =R<21>*ONIT;
V22 =R<22>*O3P*NO2;
V23 =R<23>*O1D*N2;
V24 =R<24>*O1D*O2;
V25 =R<25>*O1D*H2O;
V26 =R<26>*O3*NO;
V27 =R<27>*O3*HO;
V28 =R<28>*O3*HO2;
V29 =R<29>*HO2*NO;
V30 =R<30>*H2O2*HO;
V31 =R<31>*NO*NO*O2;
V32 =R<32>*O3*NO2;
V33 =R<33>*NO3*NO;
V34 =R<34>*NO3*NO2;
V35 =R<35>*NO3*HO2;
V36 =R<36>*N2O5*H2O;
V37 =R<37>*HO*HNO4;
V38 =R<38>*HO*HO2;
V39 =R<39>*CH4*HO;
V40 =R<40>*ETH*HO;
V41 =R<41>*HC3*HO;
V42 =R<42>*HC5*HO;
V43 =R<43>*HC8*HO;
V44 =R<44>*OL2*HO;
V45 =R<45>*OLT*HO;
V46 =R<46>*OLI*HO;
V47 =R<47>*TOL*HO;
V48 =R<48>*XYL*HO;
V49 =R<49>*CSL*HO;
V50 =R<50>*HCHO*HO;
V51 =R<51>*ALD*HO;
V52 =R<52>*KET*HO;
V53 =R<53>*GLY*HO;
V54 =R<54>*MGLY*HO;
V55 =R<55>*DCB*HO;
V56 =R<56>*OP1*HO;
V57 =R<57>*OP2*HO;
```

```
V58 =R<58>*PAA*HO;
V59 =R<59>*PAN*HO;
V60 =R<60>*ONIT*HO;
V61 =R<61>*ISO*HO;
V62 =R<62>*ACO3*NO2;
V63 =R<63>*PAN;
V64 =R<64>*TCO3*NO2;
V65 =R<65>*TPAN;
V66 =R<66>*MO2*NO;
V67 =R<67>*HC3P*NO;
V68 =R<68>*HC5P*NO;
V69 =R<69>*HC8P*NO;
V70 =R<70>*OL2P*NO;
V71 =R<71>*OLTP*NO;
V72 =R<72>*OLIP*NO;
V73 =R<73>*ACO3*NO;
V74 =R<74>*TCO3*NO;
V75 =R<75>*TOLP*NO;
V76 =R<76>*XYLP*NO;
V77 =R<77>*ETHP*NO;
V78 =R<78>*KETP*NO;
V79 =R<79>*OLN*NO;
V80 =R<80>*HCHO*NO3;
V81 =R<81>*ALD*NO3;
V82 =R<82>*GLY*NO3;
V83 =R<83>*MGLY*NO3;
V84 =R<84>*DCB*NO3;
V85 =R<85>*CSL*NO3;
V86 =R<86>*OL2*NO3;
V87 =R<87>*OLT*NO3;
V88 =R<88>*OLI*NO3;
V89 =R<89>*ISO*NO3;
V90 =R<90>*OL2*O3;
V91 =R<91>*OLT*O3;
V92 =R<92>*OLI*O3;
V93 =R<93>*ISO*O3;
V94 =R<94>*HO2*MO2;
V95 =R<95>*HO2*ETHP;
V96 =R<96>*HO2*HC3P;
V97 =R<97>*HO2*HC5P;
V98 =R<98>*HO2*HC8P;
V99 =R<99>*HO2*OL2P;
V100 =R<100>*HO2*OLTP;
V101 =R<101>*HO2*OLIP;
V102 =R<102>*HO2*KETP;
V103 =R<103>*HO2*ACO3;
V104 =R<104>*HO2*TOLP;
V105 =R<105>*HO2*XYLP;
V106 =R<106>*HO2*TCO3;
V107 =R<107>*HO2*OLN;
V108 =R<108>*MO2*MO2;
V109 =R<109>*MO2*ETHP;
V110 =R<110>*MO2*HC3P;
V111 =R<111>*MO2*HC5P;
V112 =R<112>*MO2*HC8P;
V113 =R<113>*MO2*OL2P;
V114 =R<114>*MO2*OLTP;
V115 =R<115>*MO2*OLIP;
V116 =R<116>*MO2*KETP;
```

```
V117 =R<117>*MO2*ACO3;
V118 =R<118>*MO2*TOLP;
V119 =R<119>*MO2*XYLP;
V120 =R<120>*MO2*TCO3;
V121 =R<121>*MO2*OLN;
V122 =R<122>*ETHP*ACO3;
V123 =R<123>*HC3P*ACO3;
V124 =R<124>*HC5P*ACO3;
V125 =R<125>*HC8P*ACO3;
V126 =R<126>*OL2P*ACO3;
V127 =R<127>*OLTP*ACO3;
V128 =R<128>*OLIP*ACO3;
V129 =R<129>*KETP*ACO3;
V130 =R<130>*ACO3*ACO3;
V131 =R<131>*ACO3*TOLP;
V132 =R<132>*ACO3*XYLP;
V133 =R<133>*ACO3*TCO3;
V134 =R<134>*ACO3*OLN;
V135 =R<135>*OLN*OLN;
V136 =R<136>*XO2*HO2;
V137 =R<137>*XO2*MO2;
V138 =R<138>*XO2*ACO3;
V139 =R<139>*XO2*XO2;
V140 =R<140>*XO2*NO;
V141 =R<141>*XNO2*NO2;
V142 =R<142>*XNO2*HO2;
V143 =R<143>*XNO2*MO2;
V144 =R<144>*XNO2*ACO3;
V145 =R<145>*XNO2*XNO2;
V146 =R<146>*HO2*NO2;
V147 =R<147>*NO*HO;
V148 =R<148>*NO3*NO2;
V149 =R<149>*HO*NO2;
V150 =R<150>*HO*SO2;
V151 =R<151>*HNO4;
V152 =R<152>*N2O5;
V153 =R<153>*O3P*O2;
V154 =R<154>*HO2*HO2;
V155 =R<155>*HO2*HO2*H2O;
V156 =R<156>*HO*HNO3;
V157 =R<157>*CO*HO;
V158 =R<158>*MEDI;
V159 =R<159>*NH3*HO;
V160 =R<160>*NH2*O3;
V161 =R<161>*NH2*HO2;
V162 =R<162>*NH2*HO2;
V163 =R<163>*NH2*HO2;
V164 =R<164>*NH2*NO;
V165 =R<165>*NH2*NO;
V166 =R<166>*NH2*NO2;
V167 =R<167>*NH2*NO2;
V168 =R<168>*NH2*HO;
V169 =R<169>*NH2*HO;
V170 =R<170>*NH2O*O3;
V171 =R<171>*NH2O;
V172 =R<172>*NH*O2;
V173 =R<173>*NH*NO;
V174 =R<174>*HNO*HO;
V175 =R<175>*HNO*NHOH;
```

```
V176 =R<176>*HNO*HNO;
V177 =R<177>*HNO*HNO;
V178 =R<178>*HNO*HNO;
V179 =R<179>*NAC;
V180 =R<180>*HNO*NO2;
V181 =R<181>*NHOH*HO;
V182 =R<182>*HONO*HO;
V183 =R<183>*NH3O*HO;
V184 =R<184>*HNO*O2;
P<2>= V5+V6+V8+V21+V26+V29+V31+V31+V33+V33+V34+V37+V60+V63+V65+V66+.964*V67
      +.920*V68+.760*V69+V70+V71+V72+V73+V74+V75+V76+V77+V78+2.000*V79+V121
      +V134+2.000*V135+V140+V151+V152+V182;
D<2>= V1+V22+V32+V34+V62+V64+V141+V146+V148+V149+V166+V167+V180;
P<3>= V1+V4+V7+V22+V34+V167+V172+V174+V175+V180+V184;
D<3>= V26+V29+V31+V31+V33+V66+V67+V68+V69+V70+V71+V72+V73+V74+V75+V76+V77
      +V78+V79+V140+V147+V164+V165+V173;
P<4>= V147+V180;
D<4>= V4+V182;
P<5>= V32+V59+V152+V156;
D<5>= V7+V8+V33+V34+V35+V80+V81+V82+V83+V84+V85+V86+V87+V88+V89+V148;
P<6>= V148;
D<6>= V36+V152;
P<7>= V146;
D<7>= V6+V37+V151;
P<8>= V35+2.*V36+V80+V81+V82+V83+V84+V85+V149;
D<8>= V5+V156;
P<9>= V153+V169;
D<9>= V2+V3+V26+V27+V28+V32+V90+V91+V92+V93+V160+V170;
P<10>= V154+V155;
D<10>= V9+V30;
P<11>=0.;
D<11>= V150;
P<12>= V150;
D<12>=0.;
P<13>= V10+V11+V12+1.870*V17+1.550*V18+V19+V50+2.000*V53+V54+.950*V74+V80
       +2.000*V82+V83+.420*V90+.330*V91+.230*V92+.330*V93+.475*V120
       +.950*V133;
D<13>= V157;
P<14>= V15+V157;
D<14>=0.;
P<15>= V10;
D<15>=0.;
P<16>= V2;
D<16>= V23+V24+V25;
P<17>= V1+V3+V8+V23+V24;
D<17>= V22+V153;
P<18>= V4+V5+2.000*V9+V13+V14+V15+2.000*V25+V28+V29-.900*V49+.500*V56
       +.500*V57+.100*V91+.140*V92+.100*V93+V161+V164+V172+V173;
D<18>= V27+V30+V37+V38+V39+V40+V41+V42+V43+V44+V45+V46+V47+V48+V49+V50+V51
       +V52+V53+V54+V55+V56+V57+V58+V59+V60+V61+V147+V149+V150+V156+V157
       +V159+V168+V169+V174+V181+V182+V183;
P<19>= V6+2.000*V11+V12+V13+V14+.800*V18+V19+.980*V20+V21+V27+V30+.170*V41
       +.250*V47+.170*V48+.100*V49+V50+V53+V66+.964*V67+.920*V68+.760*V69
       +V70+V71+V72+.920*V74+V75+V76+V77+V78+V80+V82+.120*V90+.230*V91
       +.260*V92+.230*V93+V108+V109+V110+V111+V112+V113+V114+V115+V116
       +.500*V117+2.000*V118+2.000*V119+.460*V120+.500*V121+.500*V122
       +.500*V123+.500*V124+.500*V125+.500*V126+.500*V127+.500*V128
       +.500*V129+V131+V132+.920*V133+V137+V143+V150+V151+V157+V164+V184;
D<19>= V28+V29+V35+V38+V94+V95+V96+V97+V98+V99+V100+V101+V102+V103+V104
```

```
        +V105+V106+V107+V136+V142+V146+V154+V154+V155+V155+V161+V162+V163;
P<20>= V2+V3+V7+V22+V24+V26+V27+2.*V28+V34+V35+V37+V38;
D<20>= V24+V31+V153+V172+V184;
P<21>= V23;
D<21>= V23;
P<22>= V30+V37+V38+V39+V40+V41+V42+V43+V50+V51+V52+V53+V54+V55+V58+V155
        +V156+V159+V162+V165+V166+V168+V174+V176+V179+V181+V182+V183;
D<22>= V25+V36+V155;
P<23>= .060*V91+.090*V92;
D<23>= V39;
P<24>=0.;
D<24>= V40;
P<25>=0.;
D<25>= V41;
P<26>=0.;
D<26>= V42;
P<27>=0.;
D<27>= V43;
P<28>=0.;
D<28>= V44+V86+V90;
P<29>=0.;
D<29>= V45+V87+V91;
P<30>=0.;
D<30>= V46+V88+V92;
P<31>= V158;
D<31>= V61+V89+V93;
P<32>=0.;
D<32>= V47;
P<33>= .250*V47+.170*V48+.500*V85;
D<33>= V49+V85;
P<34>=0.;
D<34>= V48;
P<35>= V13+.130*V17+.450*V18+.009*V41+.500*V56+V59+V66+.090*V67+.040*V69
        +1.600*V70+V71+.280*V72+V79+V90+.530*V91+.180*V92+.530*V93
        +1.500*V108+.750*V109+.840*V110+.770*V111+.800*V112+1.550*V113
        +1.250*V114+.890*V115+.750*V116+V117+V118+V119+.500*V120+1.750*V121
        +.800*V126+.500*V127+.140*V128+V134+2.000*V135+V137+V143;
D<35>= V10+V11+V50+V80;
P<36>= V14+.200*V21+.075*V41+.500*V57+.750*V67+.380*V68+.350*V69+.200*V70
        +V71+1.450*V72+V77+V79+.500*V91+.720*V92+.500*V93+.750*V109
        +.770*V110+.410*V111+.460*V112+.350*V113+.750*V114+.725*V115+V121
        +V122+.770*V123+.410*V124+.460*V125+.600*V126+V127+.725*V128+V134
        +2.000*V135;
D<36>= V12+V51+V81;
P<37>= .800*V21+.025*V41+.250*V67+.690*V68+1.060*V69+.100*V72+.100*V92
        +.260*V110+.750*V111+1.390*V112+.550*V115+.260*V123+.750*V124
        +1.390*V125+.550*V128;
D<37>= V16+V52;
P<38>= .890*V74+.160*V75+.160*V118+.445*V120+.160*V131+.890*V133;
D<38>= V17+V18+V53+V82;
P<39>= .110*V74+.170*V75+.450*V76+V78+.750*V116+.170*V118+.450*V119
        +.055*V120+V129+.170*V131+.450*V132+.110*V133;
D<39>= V19+V54+V83;
P<40>=  .700*V75+.806*V76+.700*V118+.806*V119+.700*V131+.806*V132;
D<40>= V20+V55+V84;
P<41>= V62;
D<41>= V59+V63;
P<42>= V64;
D<42>= V65;
```

```
P<43>= .036*V67+.080*V68+.240*V69+V107+V141;
D<43>= V21+V60;
P<44>= V94;
D<44>= V13+V56;
P<45>= V95+V96+V97+V98+V99+V100+V101+V102+V104+V105+V106+V136+V142;
D<45>= V14+V57;
P<46>= V103;
D<46>= V15+V58;
P<47>= .400*V90+.200*V91+.060*V92+.200*V93;
D<47>=0.;
P<48>= .200*V91+.290*V92+.200*V93+.500*V117+.500*V120+.500*V122+.500*V123
       +.500*V124+.500*V127+.500*V128+.500*V129+.500*V134;
D<48>=0.;
P<49> = V12+V15+V39+.500*V56+V73+.220*V91+.310*V92+.220*V93+.500*V117
        +.500*V122+.500*V123+.500*V124+.500*V125+.500*V126+.500*V127
        +.500*V128+.500*V129+2.000*V130+V131+V132+V133+.500*V134+V138+V144;
D<49>= V66+V94+V108+V108+V109+V110+V111+V112+V113+V114+V115+V116+V117+V118
       +V119+V120+V121+V137+V143;
P<50>= V16+V40;
D<50>= V77+V95+V109+V122;
P<51>= .830*V41+.500*V57+V60;
D<51>= V67+V96+V110+V123;
P<52>= V42;
D<52>= V68+V97+V111+V124;
P<53>= V43;
D<53>= V69+V98+V112+V125;
P<54>= V44;
D<54>= V70+V99+V113+V126;
P<55>= V45+V61;
D<55>= V71+V100+V114+V127;
P<56>= V46;
D<56>= V72+V101+V115+V128;
P<57>= .750*V47;
D<57>= V75+V104+V118+V131;
P<58>= .830*V48;
D<58>= V76+V105+V119+V132;
P<59>= V16+V19+.020*V20+V51+V54+V58+V63+.050*V74+V81+V83+.025*V120
       +.050*V133;
D<59>= V62+V73+V103+V117+V122+V123+V124+V125+V126+V127+V128+V129+V130+V130
       +V131+V132+V133+V134+V138+V144;
P<60>= V52;
D<60>= V78+V102+V116+V129;
P<61>= V20+.900*V49+V55+V65+V84;
D<61>= V64+V74+V106+V120+V133;
P<62>= V86+V87+V88+V89;
D<62>= V79+V107+V121+V134+V135+V135;
P<63>= V85;
D<63>= V141+V142+V143+V144+V145+V145;
P<64>= .250*V42+.750*V43+.900*V49+V59+2.000*V74+V120+2.000*V133;
D<64>= V136+V137+V138+V139+V139+V140;
P<65>=0.;
D<65>=0.;
P<66>= V163+V169;
D<66>= V159;
P<67>= V159+V170;
D<67>= V160+V161+V162+V163+V164+V165+V166+V167+V168+V169;
P<68>= V160+V161+V167;
D<68>= V170+V171;
P<69>= V162+V181;
```

```
D<69>= V174+V175+V176+V176+V177+V177+V178+V178+V180+V184;
P<70>= V166+V176+V179;
D<70>=0.;
P<71>= V168;
D<71>= V172+V173;
P<72>= V171+V183;
D<72>= V175+V181;
P<73>= V175;
D<73>= V183;
P<74>= V177+V178;
D<74>= V179;
'NO2 =P<2>-D<2>;
'NO =P<3>-D<3>;
'HONO =P<4>-D<4>;
'NO3 =P<5>-D<5>;
'N2O5 =P<6>-D<6>;
'HNO4 =P<7>-D<7>;
'HNO3 =P<8>-D<8>;
'O3 =P<9>-D<9>;
'H2O2 =P<10>-D<10>;
'SO2 =P<11>-D<11>;
'SULF =P<12>-D<12>;
'CO =P<13>-D<13>;
'CO2 =P<14>-D<14>;
'H2 =P<15>-D<15>;
'O1D =P<16>-D<16>;
'O3P =P<17>-D<17>;
'HO =P<18>-D<18>;
'HO2 =P<19>-D<19>;
'O2 =P<20>-D<20>;
'N2 =P<21>-D<21>;
'H2O =P<22>-D<22>;
'CH4 =P<23>-D<23>;
'ETH =P<24>-D<24>;
'HC3 =P<25>-D<25>;
'HC5 =P<26>-D<26>;
'HC8 =P<27>-D<27>;
'OL2 =P<28>-D<28>;
'OLT =P<29>-D<29>;
'OLI =P<30>-D<30>;
'ISO =P<31>-D<31>;
'TOL =P<32>-D<32>;
'CSL =P<33>-D<33>;
'XYL =P<34>-D<34>;
'HCHO =P<35>-D<35>;
'ALD =P<36>-D<36>;
'KET =P<37>-D<37>;
'GLY =P<38>-D<38>;
'MGLY =P<39>-D<39>;
'DCB =P<40>-D<40>;
'PAN =P<41>-D<41>;
'TPAN =P<42>-D<42>;
'ONIT =P<43>-D<43>;
'OP1 =P<44>-D<44>;
'OP2 =P<45>-D<45>;
'PAA =P<46>-D<46>;
'ORA1 =P<47>-D<47>;
'ORA2 =P<48>-D<48>;
'MO2 =P<49>-D<49>;
```

```
'ETHP =P<50>-D<50>;
'HC3P =P<51>-D<51>;
'HC5P =P<52>-D<52>;
'HC8P =P<53>-D<53>;
'OL2P =P<54>-D<54>;
'OLTP =P<55>-D<55>;
'OLIP =P<56>-D<56>;
'TOLP =P<57>-D<57>;
'XYLP =P<58>-D<58>;
'ACO3 =P<59>-D<59>;
'KETP =P<60>-D<60>;
'TCO3 =P<61>-D<61>;
'OLN =P<62>-D<62>;
'XNO2 =P<63>-D<63>;
'XO2 =P<64>-D<64>;
'TRA =P<65>-D<65>;
'NH3 =P<66>-D<66>;
'NH2 =P<67>-D<67>;
'NH2O =P<68>-D<68>;
'HNO =P<69>-D<69>;
'N2O =P<70>-D<70>;
'NH =P<71>-D<71>;
'NHOH =P<72>-D<72>;
'NH3O =P<73>-D<73>;
'NAC =P<74>-D<74>;
* Fuer speichern in outputfile werden einige Zusatzergebnisse
  in ablX gespeichert;
* P(O~3)-D(O~3);
abl1=P<9>-D<9>;
* P(NO~x)-D(NO~x) nur aus NH3-Chemie;
abl2=V172+V174+V175+V182+V184-V164-V165-V166-V173;
* (P(NO~x)-D(NO~x))/D(NH~3);
abl3=abl2/D<66>;
* P(N~2O)/D(NH~3);
abl4=P<70>/D<66>;
* P(NO~x)-D(NO~x);
abl5=P<3>+P<2>-D<2>-D<3>;
**;

compile instant;
* Initialisierung der Startkonzentrationen;
call START;
**;

compile instant;
write 1=8,"[M] = ", (E10,3), M %;
write 1=8,"Zahl der reak/ultra-Aufrufe", #k_mal %;
write 1=8,"SPALTE 1=t [s]" %;
* write 1=8,"SPALTE 2=T [K]" %;
write 1=8,"SPALTE 2=[O~3] [cm${-3}]" %;
*write 1=8,"SPALTE 3=chi [$o]" %;
write 1=8,"SPALTE 3=[NH~3] [cm${-3}]" %;
write 1=8,"SPALTE 4=[OH] [cm${-3}]" %;
write 1=8,"SPALTE 5=P(O~3)-D(O~3)" %;
write 1=8,"SPALTE 6=P(N~2O)/D(NH~3)" %;
write 1=8,"SPALTE 7=[HNO] [cm${-3}]" %;
write 1=8,"SPALTE 8=Y(NO~x)/D(NH~3)" %;
write 1=8,"SPALTE 9=P(NO~x)-D(NO~x)" %;
write 1=8,"SPALTE 10=[HO~2] [cm${-3}]" %;
```

```
write 1=8,"SPALTE 11=[NO~2] [cm${-3}]" %;
write 1=8,"SPALTE 12=[NO] [cm${-3}]" %;
write 1=8,"ZAHL DER SPALTEN=12" %;
write 1=8,"&&&&&&&&&&&&" %;
**;

compile table;
write 1=8, (E9,2), time,((E10,2)), O3,
           NH3, HO, abl1, abl4, HNO,
            abl3, abl5, HO2, NO2, NO %;
**;

compile tab1;
* write 1=10,"k(NH2O->NHOH)=1E-03 /s" %;
* Ausgabe von Umsaetzen ausgewaehlter Reaktionen;
write 1=10,"++++++++++++++++++++++++++++++++++++++++" %;
dumo = time/3600;
write 1=10,"t [s,h]    = ", (E10,2), time,(F10,2), dumo %;
dumo=P<13>-D<13>;
write 1=10,"[CO],P(CO),D(CO),P-D       = ",((E10,2))
 ,CO,P<13>,D<13>,dumo %;
dumo=P<18>-D<18>;
write 1=10,"[OH],P(OH),D(OH),P-D       = ",((E10,2))
 ,HO,P<18>,D<18>,dumo %;
dumo=P<19>-D<19>;
write 1=10,"[HO2],P(HO2),D(HO2),P-D    = ",((E10,2))
 ,HO2,P<19>,D<19>,dumo %;
dumo=P<3>-D<3>;
write 1=10,"[NO],P(NO),D(NO),P-D       = ",((E10,2))
 ,NO,P<3>,D<3>,dumo %;
dumo=P<2>-D<2>;
write 1=10,"[NO2],P(NO2),D(NO2),P-D    = ",((E10,2))
 ,NO2,P<2>,D<2>,dumo %;
dumo=P<9>-D<9>;
write 1=10,"[O3],P(O3),D(O3),P-D       = ",((E10,2))
 ,O3,P<9>,D<9>,dumo %;
dumo=P<66>-D<66>;
write 1=10,"[NH3],P(NH3),D(NH3),P-D    = ",((E10,2))
 ,NH3,P<66>,D<66>,dumo %;
dumo=P<67>-D<67>;
write 1=10,"[NH2],P(NH2),D(NH2),P-D    = ",((E10,2))
 ,NH2,P<67>,D<67>,dumo %;
dumo=P<68>-D<68>;
write 1=10,"[NH2O],P(NH2O),D(NH2O),P-D = ",((E10,2))
 ,NH2O,P<68>,D<68>,dumo %;
dumo=P<72>-D<72>;
write 1=10,"[NHOH],P(NHOH),D(NHOH),P-D = ",((E10,2))
 ,NHOH,P<72>,D<72>,dumo %;
dumo=P<71>-D<71>;
write 1=10,"[NH],P(NH),D(NH),P-D       = ",((E10,2))
 ,NH,P<71>,D<71>,dumo %;
dumo=P<69>-D<69>;
write 1=10,"[HNO],P(HNO),D(HNO),P-D    = ",((E10,2))
 ,HNO,P<69>,D<69>,dumo %;
dumo=P<73>-D<73>;
write 1=10,"[NH3O],P(NH3O),D(NH3O),P-D = ",((E10,2))
 ,NH3O,P<73>,D<73>,dumo %;
dumo=P<74>-D<74>;
write 1=10,"[NAC],P(NAC),D(NAC),P-D    = ",((E10,2))
```

```
 ,NAC,P<74>,D<74>,dumo %;
dumo=P<70>-D<70>;
write 1=10,"[N2O],P(N2O),D(N2O),P-D    = ",((E10,2))
 ,N2O,P<70>,D<70>,dumo %;
write 1=10,"----------------------------------------" %;
write 1=10,"CO+OH      = ", (E10,3), V157 %;
write 1=10,"CH4 + OH   = ", (E10,3), V39 %;
write 1=10,"O3 + OH    = ", (E10,3), V27 %;
write 1=10,"O3 + NO    = ", (E10,3), V26 %;
write 1=10,"NH3 + OH   = ", (E10,3), V159 %;
write 1=10,"NH2 + O3   = ", (E10,3), V160 %;
dumo = V161 + V162 +V163;
write 1=10,"NH2 + HO2 = ", ((E10,3)), dumo, V161, V162,
   V163 %;
dumo = V164 + V165;
write 1=10,"NH2 + NO   = ", ((E10,3)), dumo, V164, V165 %;
dumo = V166 + V167;
write 1=10,"NH2 + NO2 = ", ((E10,3)), dumo, V166, V167 %;
dumo = V168 + V169;
write 1=10,"NH2 + OH   = ", ((E10,3)), dumo, V168, V169 %;
write 1=10,"NH2O + O3 = ", (E10,3), V170 %;
write 1=10,"NH2O       = ", (E10,3), V171 %;
write 1=10,"NH + O2    = ", (E10,3), V172 %;
write 1=10,"NH + NO    = ", (E10,3), V173 %;
write 1=10,"HNO + OH   = ", (E10,3), V174 %;
write 1=10,"HNO +NHOH = ", (E10,3), V175 %;
dumo = V176 + V177 + V178;
write 1=10,"HNO + HNO = ", ((E10,3)), dumo, V176, V177,
      V178 %;
write 1=10,"HNO + NO2 = ", (E10,3), V180 %;
write 1=10,"HNO + O2   = ", (E10,3), V184 %;
write 1=10,"NHOH + OH = ", (E10,3), V181 %;
write 1=10,"NH3O + OH = ", (E10,3), V183 %;
write 1=10,"P(N2O)/D(NH3) = ", (E10,3), abl4 %;
write 1=10,"P(NOx)-D(NOx) = ", (E10,3), abl5 %;
write 1=10,"Y(NOx)/D(NH3) = ",(E10,3),abl3 %;
**;

whenever time=  0  call
             reaktionskonstanten restart;
         time= #t1_mal* (+t1_aufruf) 0  call tab1;
         time= #t_mal* (+t_aufruf) 0  call bi_naer;
         time= #t_mal* (+t_aufruf) 0  call table;
         time= laufzeit %;
**;

begin;
* Programm;
stop;
```

### *Subroutines usubr4 und usubr5 called by Facsimile*

The subroutine *usubr4* is the interface between Facsimile and the subroutine *reak that* determine the rate constants. The rate constants are transfered between Facsimile and the subroutine *usubr4* using the array *R*. The transfer between usubr4 and reak is managed using the array RK. The elements of the array *con* contain the temperature, pressure, solar zenith angle, time, and selected concentrations (for

example density of air and gaseous water) needed for the calculation of the rate constants. The transfer to the subroutine reak is done using the variables *TIME*, *TEMP* and *DRUCK* as well as the array *C*.

```
C###USUBR4   USER SUBROUTINE, CALLED BY ENTER FOLLOWED BY 4 NAMES
C###USUBR4   wird z.b. von nh3-er.fac und kammXX.fac aufgerufen,
C     solange die Reaktionen 1-157 aus RADM2 nicht veraendert werden
C     selbes gilt fuer NH3-Chemie (Reaktionen 158-183)
      SUBROUTINE USUBR4 (IND,R,CON,DUMM,DUMO)
      implicit none
      DOUBLE PRECISION TEMP, DRUCK, TIME, ZENITH, DUMM,DUMO
      DOUBLE PRECISION R, CON, C, RK
      INTEGER IND(99)
      INTEGER I, ICEND, IREND
      DIMENSION CON(0:12)
c     von facsimile wird nreak und nconc in con(12)
C     und con(11) uebergeben
      INTEGER NREAK , NCONC
      DIMENSION R(0:INT(CON(12))),C(INT(CON(11))),RK(INT(CON(12)))
      NCONC=INT(CON(11))
      NREAK=INT(CON(12))
      TEMP = CON(0)
      DRUCK= CON(1)          ! DRUCK IN MILLIB
      C(22)= CON(4)          ! WASSER IN CM-3
      TIME = CON(3)          ! ZEIT IN SEC
      ZENITH=DCOS(CON(2))    ! COS(ZENITH)
      C(2)= CON(5)           ! NO2 IN CM-3
      C(5)= CON(6)           ! NO3 IN CM-3
      C(9)= CON(7)           ! O3 IN CM-3
      C(1)= CON(8)           ! M IN CM-3
      C(20) = CON(9)         ! O2 IN CM-3
      C(21) = CON(10)        ! N2 IN CM-3
      CALL REAK(RK,NREAK,IREND,C,NCONC,ICEND,TEMP,
     A    ZENITH)
      CON(0)=TEMP
      CON(1)=DRUCK
      CON(4)=C(22)            ! WASSER IN CM-3
      CON(3)=TIME             ! ZEIT IN SEC
      CON(2)=DACOS(ZENITH)    ! COS(ZENITH)
      DO I=1, NREAK
        R (I)=RK(I)
      END DO
      RETURN
      END
```

The subroutine *usubr5* is used for the binary output in *LISTEN* format. The file is opened by the Facsimile prior to the first entry of *usubr5* and connected to unit number 11.

```
C###USUBR5   USER SUBROUTINE, CALLED BY ENTER FOLLOWED BY 5 NAMES
C###USUBR5   wird z.b. von nh3-er.fac aufgerufen, um
C###USUBR5   binaerausgabe zu erzeugen
      SUBROUTINE USUBR5(IND,CON1,C,R,P,D)
      implicit none
      INTEGER K, NREAK, NCONC
      DOUBLE PRECISION TEMP, DRUCK, TIME, ZENITH
      DOUBLE PRECISION R, CON1, C, P, D, H
      INTEGER I, ICEND, IREND, IP, IP1, III, JJJ
```

```
      REAL*4 ZR, ZCON, ZC, ZP, ZD
      INTEGER IND(99)
      DIMENSION CON1(0:6),ZCON(0:4)
c     von facsimile wird nreak und nconc in con1(6)
C     und con1(5) uebergeben
      DIMENSION R(0:INT(CON1(6))),C(0:INT(CON1(5)))
      DIMENSION P(0:INT(CON1(5))), D(0:INT(CON1(5)))
      DIMENSION ZR(0:INT(CON1(6))),ZC(0:INT(CON1(5)))
      DIMENSION ZP(0:INT(CON1(5))), ZD(0:INT(CON1(5)))
      CHARACTER*8 TEXT(INT(CON1(5)))
      NCONC=INT(CON1(5))
      NREAK=INT(CON1(6))
      ICEND=NCONC
      IREND=NREAK
      IP1=-1
      IP=-1
      IF (CON1(4).LT.0) THEN
      WRITE (11) ICEND,IREND,IP1,IP
      call namen(text,nconc,icend,irend,6)
      WRITE (11) (TEXT(K),K=1,ICEND)
      ENDIF
      DO I = 1, ICEND
         ZC(I) = REAL(C(I))
         ZD(I) = REAL(D(I))
         ZP(I) = REAL(P(I))
      END DO
      DO I = 1, IREND
         ZR(I) = REAL(R(I))
      END DO
      ZCON(0) = REAL(CON1(0))
      ZCON(1) = REAL(CON1(1))
      ZCON(2) = REAL(CON1(2))
      ZCON(3) = REAL(CON1(3))
      WRITE(11) ZCON(0),ZCON(1),ZCON(2),ZCON(3),
     A     (ZC(III),III=1,ICEND),(ZR(JJJ),JJJ=1,IREND),
     A     (ZP(III),III=1,ICEND),( ZD(JJJ),JJJ=1,ICEND)
      RETURN
      END
```

### *Subroutine reak called by usubr4*

The subroutine *reak* calculates the rate constants of the reactions. The values of the rate constants are transfered to the subroutine *usubr4* using the array *RK*.

```
SUBROUTINE REAK(RK,NREAK,IREND,C,NCONC,
     A                ICEND,TEMP,ZENITH)
      PARAMETER (MREAK=200)
      IMPLICIT REAL*8(A-H,O-Z)
      REAL*8 RK(NREAK),C(NCONC),M,MEDIUM,CHI
      SAVE
      M=C(1)
      RK(   1)=9.18e-3*PHOT(0.256d0,zenith)
      RK(   2)=3.18e-5*PHOT(2.092d0,zenith)
      RK(   3)=4.82e-4*PHOT(1.00d0,zenith)
      RK(   4)=1.66e-3*PHOT(1.00d0,zenith)
      RK(   5)=4.42e-7*PHOT(1.00d0,zenith)
      RK(   6)=6.58e-6*PHOT(1.00d0,zenith)
```

```
RK(   7)=2.20e-2*PHOT(0.0388d0,zenith)
RK(   8)=1.80e-1*PHOT(0.0388d0,zenith)
RK(   9)=7.56e-6*PHOT(0.506d0,zenith)
RK(  10)=4.20e-5*PHOT(0.393d0,zenith)
RK(  11)=3.50e-5*PHOT(0.601d0,zenith)
RK(  12)=5.24e-6*PHOT(1.00d0,zenith)
RK(  13)=7.36e-6*PHOT(1.00d0,zenith)
RK(  14)=7.36e-6*PHOT(1.00d0,zenith)
RK(  15)=2.11e-6*PHOT(1.00d0,zenith)
RK(  16)=9.17e-7*PHOT(1.00d0,zenith)
RK(  17)=5.70e-5*PHOT(1.00d0,zenith)
RK(  18)=6.76e-5*PHOT(1.00d0,zenith)
RK(  19)=2.48e-4*PHOT(1.00d0,zenith)
RK(  20)=9.81e-5*PHOT(1.00d0,zenith)
RK(  21)=1.21e-6*PHOT(1.00d0,zenith)
RK(  22)=6.50E-12*EXP(120./T)
RK(  23)=1.80E-11*EXP(110./T)
RK(  24)=3.20E-11*EXP(70./T)
RK(  25)=2.20E-10
RK(  26)=2.00E-12*EXP(-1400./T)
RK(  27)=1.60E-12*EXP(-940./T)
RK(  28)=1.10E-14*EXP(-500./T)
RK(  29)=3.70E-12*EXP(240./T)
RK(  30)=3.30E-12*EXP(-200./T)
RK(  31)=3.30E-39*EXP(530./T)
RK(  32)=1.40E-13*EXP(-2500./T)
RK(  33)=1.70E-11*EXP(150./T)
RK(  34)=2.50E-14*EXP(-1230./T)
RK(  35)=2.50E-12
RK(  36)=2.00E-21
RK(  37)=1.30E-12*EXP(380./T)
RK(  38)=4.60E-11*EXP(230./T)
RK(  39)=T*T*6.95E-18*EXP(-1280./T)
RK(  40)=T*T*1.37E-17*EXP(-444./T)
RK(  41)=1.59E-11*EXP(-540./T)
RK(  42)=1.73E-11*EXP(-380./T)
RK(  43)=3.64E-11*EXP(-380./T)
RK(  44)=2.15E-12*EXP(411./T)
RK(  45)=5.32E-12*EXP(504./T)
RK(  46)=1.07E-11*EXP(549./T)
RK(  47)=2.10E-12*EXP(322./T)
RK(  48)=1.89E-11*EXP(116./T)
RK(  49)=4.00E-11
RK(  50)=9.00E-12
RK(  51)=6.87E-12*EXP(256./T)
RK(  52)=1.20E-11*EXP(-745./T)
RK(  53)=1.15E-11
RK(  54)=1.70E-11
RK(  55)=2.8E-11
RK(  56)=1.00E-11
RK(  57)=1.00E-11
RK(  58)=1.00E-11
RK(  59)=T*T*6.85E-18*EXP(-444./T)
RK(  60)=1.55E-11*EXP(-540./T)
RK(  61)=2.55E-11*EXP(409./T)
RK(  62)=2.80E-12*EXP(181./T)
RK(  63)=1.95E+16*EXP(-13543./T)
RK(  64)=4.7E-12
RK(  65)=1.95E16*EXP(-13543./T)
```

```
RK(  66)=4.20E-12*EXP(180./T)
RK(  67)=4.20E-12*EXP(180./T)
RK(  68)=4.20E-12*EXP(180./T)
RK(  69)=4.20E-12*EXP(180./T)
RK(  70)=4.20E-12*EXP(180./T)
RK(  71)=4.20E-12*EXP(180./T)
RK(  72)=4.20E-12*EXP(180./T)
RK(  73)=4.20E-12*EXP(180./T)
RK(  74)=4.20E-12*EXP(180./T)
RK(  75)=4.20E-12*EXP(180./T)
RK(  76)=4.20E-12*EXP(180./T)
RK(  77)=4.20E-12*EXP(180./T)
RK(  78)=4.20E-12*EXP(180./T)
RK(  79)=4.20E-12*EXP(180./T)
RK(  80)=6.00E-13*EXP(-2058./T)
RK(  81)=1.40E-12*EXP(-1900./T)
RK(  82)=6.00E-13*EXP(-2058./T)
RK(  83)=1.40E-12*EXP(-1900./T)
RK(  84)=1.40E-12*EXP(-1900./T)
RK(  85)=2.20E-11
RK(  86)=2.00E-12*EXP(-2923./T)
RK(  87)=1.00E-11*EXP(-1895./T)
RK(  88)=3.23E-11*EXP(-975./T)
RK(  89)=5.81E-13
RK(  90)=1.20E-14*EXP(-2633./T)
RK(  91)=1.32E-14*EXP(-2105./T)
RK(  92)=7.29E-15*EXP(-1136./T)
RK(  93)=1.23E-14*EXP(-2013./T)
RK(  94)=7.70E-14*EXP(1300./T)
RK(  95)=7.70E-14*EXP(1300./T)
RK(  96)=7.70E-14*EXP(1300./T)
RK(  97)=7.70E-14*EXP(1300./T)
RK(  98)=7.70E-14*EXP(1300./T)
RK(  99)=7.70E-14*EXP(1300./T)
RK( 100)=7.70E-14*EXP(1300./T)
RK( 101)=7.70E-14*EXP(1300./T)
RK( 102)=7.70E-14*EXP(1300./T)
RK( 103)=7.70E-14*EXP(1300./T)
RK( 104)=7.70E-14*EXP(1300./T)
RK( 105)=7.70E-14*EXP(1300./T)
RK( 106)=7.70E-14*EXP(1300./T)
RK( 107)=7.70E-14*EXP(1300./T)
RK( 108)=1.90E-13*EXP(220./T)
RK( 109)=1.40E-13*EXP(220./T)
RK( 110)=4.20E-14*EXP(220./T)
RK( 111)=3.40E-14*EXP(220./T)
RK( 112)=2.90E-14*EXP(220./T)
RK( 113)=1.40E-13*EXP(220./T)
RK( 114)=1.40E-13*EXP(220./T)
RK( 115)=1.70E-14*EXP(220./T)
RK( 116)=1.70E-14*EXP(220./T)
RK( 117)=9.60E-13*EXP(220./T)
RK( 118)=1.70E-14*EXP(220./T)
RK( 119)=1.70E-14*EXP(220./T)
RK( 120)=9.60E-13*EXP(220./T)
RK( 121)=1.70E-14*EXP(220./T)
RK( 122)=3.40E-13*EXP(220./T)
RK( 123)=1.00E-13*EXP(220./T)
RK( 124)=8.40E-14*EXP(220./T)
```

```
RK( 125)=7.20E-14*EXP(220./T)
RK( 126)=3.40E-13*EXP(220./T)
RK( 127)=3.40E-13*EXP(220./T)
RK( 128)=4.20E-14*EXP(220./T)
RK( 129)=4.20E-14*EXP(220./T)
RK( 130)=1.19E-12*EXP(220./T)
RK( 131)=4.20E-14*EXP(220./T)
RK( 132)=4.20E-14*EXP(220./T)
RK( 133)=1.19E-12*EXP(220./T)
RK( 134)=4.20E-14*EXP(220./T)
RK( 135)=3.60E-16*EXP(220./T)
RK( 136)=7.70E-14*EXP(1300./T)
RK( 137)=1.70E-14*EXP(220./T)
RK( 138)=4.20E-14*EXP(220./T)
RK( 139)=3.60E-16*EXP(220./T)
RK( 140)=4.20E-12*EXP(180./T)
RK( 141)=4.20E-12*EXP(180./T)
RK( 142)=7.70E-14*EXP(1300./T)
RK( 143)=1.70E-14*EXP(220./T)
RK( 144)=4.20E-14*EXP(220./T)
RK( 145)=3.60E-16*EXP(220./T)
RK( 146)=TROE(1.8D-31,3.2d0,4.7D-12,1.4d0,M,T)
RK( 147)=TROE(7.0d-31,2.6d0,1.5d-11,0.5d0,M,T)
RK( 148)=TROE(2.2d-30,4.3d0,1.5d-12,0.5d0,M,T)
RK( 149)=TROE(2.6d-30,3.2d0,2.4d-11,1.3d0,M,T)
RK( 150)=TROE(3.0d-31,3.3d0,1.5d-12,0.0d0,M,T)
RK( 151)=EQT(1.8d-31,3.2d0,4.7d-12,1.4d0,M,T,4.76d+26,10900.d0)
RK( 152)=EQT(2.2d-30,4.3d0,1.5d-12,0.5d0,M,T,9.09d+26,11200.d0)
RK( 153)=M*6.0E-34*(T/300.)**(-2.3)
RK( 154)=2.2E-13*EXP(620./T)+1.9E-33*M*EXP(980./T)
RK( 155)=3.08d-34*EXP(2820./T)+2.66d-54*M*EXP(3180./T)
RK( 156)=SPEZ(7.2d-15,785.d0,4.1d-16,1440.d0,1.9d-33,725.d0,M,T)
RK( 157)=1.5E-13*(1.0+2.439E-20*M)
RK( 158)=0
RK( 159)=1.7E-12*EXP(-710/T)
RK( 160)=4.3E-12*EXP(-930/T)
RK( 161)=4.8E-7*T**(-1.32)*EXP(-628/T)
RK( 162)=9.4E-9*T**(-1.12)*EXP(-356/T)
RK( 163)=2.7E-20*T**(1.55)*EXP(-1020/T)
RK( 164)=0.12*1.6E-11*(T/298)**(-1.5)
RK( 165)=0.88*1.6E-11*(T/298)**(-1.5)
RK( 166)=0.6*2.0E-11*(T/298)**(-2.0)
RK( 167)=0.4*2.0E-11*(T/298)**(-2.0)
RK( 168)=7.7E-13*(T/298)**1.5*EXP(230/T)
RK( 169)=3.31E-13*(T/298)**0.41*EXP(-250/T)
RK( 170)=1.2E-14
RK( 171)=1.3E3
RK( 172)=1.09E-14*(T/298)**1.5*EXP(-50/T)
RK( 173)=4.9E-11
RK( 174)=8E-11*EXP(-500/T)
RK( 175)=1.66E-12*EXP(-1500/T)
RK( 176)=4.24E-17*(T/298)**3.98*EXP(-600/T)
RK( 177)=6.64E-15*EXP(-270/T)
RK( 178)=3.02E-14*(T/298)**(-2.4)*EXP(-590/T)
RK( 179)=4.3E11*EXP(-8250/T)
RK( 180)=1.E-12*EXP(-1000/T)
RK( 181)=1.66E-12
RK( 182)=1.8E-11*EXP(-390/T)
RK( 183)=4.13E-11*EXP(-2138/T)
```

```
      RK( 184)=3.65E-14*EXP(-4600/T)
      RETURN
      END
      FUNCTION PHOT(ALP,ZENITH)
C*************************************************************
C****** ZENITHWINKELABH DER PHOTOLYSERATE **********************
C****** Z0=1/COS(REFERENZ-ZENITHWINKEL) ************************
C******          REFERENZ-ZENITHWINKEL = 21 GRAD ****************
C****** CHI-REF = 21.0 GRAD WIE BEI TRAINER ET AL. ANGEGEBEN *****
C*************************************************************
      IMPLICIT REAL*8(A-H,O-Z)
      DATA Z0,EMAX/1.0711D0,60.D0/
      YY=EMAX/ALP+Z0
      YY=DMAX1(ZENITH,1./YY)
      PHOT= DEXP(-ALP/YY+ALP*Z0)
      RETURN
      END
C
C-----------------------------------------------------------------------
      FUNCTION TROE( K0300, Q, KU300, R, M, T )
C     CALCULATION OF RATE CONSTANTS FOR TROE REACTIONS
      IMPLICIT REAL*8 (A-Z)
      TT= T / 3.D2
      K0= K0300 / TT**Q
      KU= KU300 / TT**R
      K0M= K0 * M
      KK= K0M / KU
      LGKK=0.434294481D0 * LOG(KK)
      E=1.D0 / ( 1.D0 + LGKK*LGKK )
      F=0.6D0 ** E
      TROE= F * K0M / ( 1.D0 + KK )
      RETURN
      END
C
C-----------------------------------------------------------------------
      FUNCTION EQT( K0300, Q, KU300, R, M, T, A, B )
      IMPLICIT REAL*8 (A-Z)
      KH= TROE( K0300, Q, KU300, R, M, T )
      EQT= KH * A *DEXP( -B / T )
      RETURN
      END
C
C-----------------------------------------------------------------------
      FUNCTION SPEZ(A0,B0,A2,B2,A3,B3,M,T)
C     SPECIAL RATE CONSTANTS
      IMPLICIT REAL*8 (A-Z)
      K0=A0*DEXP(B0/T)
      K2=A2*DEXP(B2/T)
      K3=A3*M*DEXP(B3/T)
      SPEZ= K0 + K3 / ( 1 + K3/K2 )
      RETURN
      END
```

Forschungszentrum Jülich

Jül-3473
December 1997
ISSN 0944-2952